Student Poster Session

2020 IEEE PES General Meeting
Montreal, Canada (Held Remotely)
August 2020

Poster Categories:

- Advanced Computational Methods for Power System Planning, Operation, and Control
- Asset Management
- Communication & Control in Energy Systems
- Cyber & Physical Security of the Smart Grid
- Dynamic Performance and Control of Power Systems
- Emerging Software Needs for the Restructured Grid
- Integrating Renewable Energy into the Grid
- Intelligent Monitoring & Outage Management
- Market Interactions in Power Systems
- Operation & Control
- Power Electronics
- Power System Modeling & Simulation
- Smart Cities
- Smart Grid Technology
- Smart Sensors
- Substation and Distribution Automation
- System-Wide Events and Analysis Methods

IEEE PES Student Activities Subcommittee
Valentina Cecchi, Ph.D., Sridhar Chouhan, Ph.D., Anthony Deese, Ph.D., Paras Mandal, Ph.D., and Luke Dosiek, Ph.D.

Last Name (Alphabetical Order)	First Name	Paper Title	UG/Grad	Research Area
Abdelmalak	Michael	Deep Learning Approach for Power System Stability Assessment	Grad	Power System Modeling & Simulation
Abdollahi	Roghieh	A Hybrid Control Framework for Large- Scale Battery Integration to the Power System for Stability Analysis	Grad	Operation & Control
Abdollahi	Roghieh	Frequency Control Using Tariff Regulation (A Comparison Between the MPC Feedback Control and Tariff Modification)	Grad	Market Interactions in Power Systems
Afrasiabi	Shahabodin	Wide-Area Measurement based Faulty Line Detection using Robust Deep Learning Network	Grad	
Akeyo,	Oluwaseun	Study of Large Solar PV Penetration on a Proposed Generation and Transmission Benchmark System	Grad	Integrating Renewable Energy into the Grid
Akter	Homeyra	Are Electric Transportation, Big Data and Machine Learning Transforming the Grid?	Grad	Smart Grid Technology
AlAshery	Mohamed	Risk Management via Second-Order Stochastic Dominance Constraints: Benchmark Selection Approaches	Grad	
Alden	Rosemary	Tradeoffs in Forecasting of Residential Electric Loads with Data from Smart Meters and Intelligent Circuit Breakers	UG	Emerging Software Needs for the Restructured Grid
Amoateng	David	A Deep Unsupervised Learning Approach to PMU Event Detection in an Active Distribution Network	Grad	Intelligent Monitoring & Outage Management
Bhusal	Narayan	Sizing of Movable Energy Resources for Service Restoration and Reliability Enhancement	Grad	Power System Modeling & Simulation
Bossart	Matthew	The Effect of Power Electronic Loads on Western Interconnection Stability	Grad	Power System Modeling & Simulation

Chaulagain	Asim	Integration of Renewable Energy Systems to Reduce Greenhouse Gas Emissions	Grad	Integrating Renewable Energy into the Grid
Chen	Yize	Learning to Solve Optimal Power Flow via Neural Decoding	Grad	Operation & Control
Chen	Haotian	Developing Bidding Strategy for Day- Ahead Electricity Markets Using Reinforcement Learning Methods	Grad	Market Interactions in Power Systems
da Cunha	Vinicius	Assessment of Capacitor Banks Control Practices in Distribution Systems with High PV Penetration	Grad	Integrating Renewable Energy into the Grid
Das	Ronit	Cross-Market Price Difference Forecast Using Deep Learning for Electricity Markets	Grad	Advanced Computational Methods for Power System Planning
Doubleday	Kate	Benchmarks and Improvements in Probabilistic Solar Forecasting	Grad	Integrating Renewable Energy into the Grid
Fan	He	A Dynamic Nonlinear Model of Once- Through Boiler- Turbine Units with Superheated Steam Temperature	Grad	Integrating Renewable Energy into the Grid
Fernandes	Arnold	Distributed Dynamic State Estimation in Power Systems under Cyber Attacks	Grad	Cyber & Physical Security of the Smart Grid
Fouad	Fouad	Real- Time Overload Detection Algorithm with Combined Learning and Analytical Model	Grad	Advanced Computational Methods for Power System Planning
Fu	Linbo	Distribution Market- Clearing and Pricing Considering Coordination of DSO and ISO: An MPEC Approach	Grad	Market Interactions in Power Systems
Gangopadhyay	Soumyajit	Trading of Smart Grid Data: Advantages and Challenges	Grad	Market Interactions in Power Systems
Gautam,	Mukesh	A Sensitivity- based Approach to Adaptive Under-Frequency Load Shedding	Grad	Power System Modeling & Simulation
Ghaljehei	Mohammad	A data- driven policy design for addressing the ramping product nodal deliverability issue in real-time markets	Grad	Market Interactions in Power Systems

Ghorai	Anwesha	A comprehensive method to analyze power system resilience to extreme weather	Grad	Power System Modeling & Simulation
Gupta	Pooja	Coordinated Wide- Area Control of Multiple Controllers in a Power System Embedded with HVDC Lines	Grad	Communication & Control in Energy Systems
Guruwacharya	Nischal	Development and Validation of Models to Assess Dynamic Response of Converter- Dominated Power Systems Across Multiple Spatiotemporal Scales	Grad	Dynamic Performance and Control of Power Systems
Hasan	Fouad	Real- Time Overload Detection Algorithm with Combined Learning and Analytical Model	Grad	Advanced Computational Methods for Power System Planning
He	Mingyue	Socially- aware Day- ahead Distributed Energy Resources Scheduling by Chance- constrained AC Optimal Power Flow	Grad	Power System Modeling & Simulation
Herre	Lars	Impact of Imbalance Settlement System Design on a Risk- Adverse Aggregator of Flexible Demand Side Resources	Grad	
Jan	Westman	Over Frequency Curtailment of PV Generation in Low Inertia, Islanded Microgrids	Grad	Dynamic Performance and Control of Power Systems
Johns	William	A Multi- function AAA Algorithm Applied to Frequency Dependent Line Modeling	Grad	Power System Modeling & Simulation
Kamel	Mariana	A Reinforcement Learning Approach for Branch Overload Relief in Power Systems	Grad	Operation & Control
Kaymanesh	Amirabbas	Industrial Smart Load Using Five- Level Packed U-Cell Converter	Grad	Power Electronics
Kenyon	Rick Wallace	Operating the Maui Power System with 100% Inverter Based Resources	Grad	Dynamic Performance and Control of Power Systems
Khan	Mohammad A I	Efficient Hosting Capacity Computation for Distribution Circuit	Grad	Communication & Control in Energy Systems
Kim	Taehyung	PMU-Based Evaluation of Transmission Bus Strength through Angle Sensitivity Metrics	Grad	

Konstantinopoulos	Stavros	WTG Active Power Control for Transient Stability Enhancement	Grad	Dynamic Performance and Control of Power Systems
Kumar	Avinash	Lissajous Parameters based Islanding Detection of Multiple DGs in Microgrid	Grad	Integrating Renewable Energy into the Grid
Ling	Xiejin	Reinforcement Learning for Optimal Allocation of Superconducting Fault Current Limiters	UG	Advanced Computational Methods for Power System Planning
Liu	Lu	SALSA-Based Method for Identifying Critical Component and Critical Component Outage Causality with Cascading Failure Data	Grad	
Majidi	Majid	Integrating Small Pumped-Storage Hydropower in the Operation of Power and Water Distribution Systems	Grad	
Mamun	M Al	Efficient Algorithm for Solving Combined T & D Power Flow and Dynamic Simulation	Grad	Dynamic Performance and Control of Power Systems
Martins,	Daniella	Probabilistic short- circuit analysis: a new approach integrating intermittent power injection	Grad	Power System Modeling & Simulation
Mehdipourpicha	Hossein	Risk- constrained Bi- level Optimization for Virtual Bidder Bidding Strategy in Day- Ahead Electricity Markets	Grad	Power System Modeling & Simulation
Mohammad	Mohammad	Computationally Efficient Formulations for Fault Isolation and Service Restoration in Distribution Systems	Grad	Power System Modeling & Simulation
Mohiuddin	Sheik M	A Unified Droop- Free Distributed Secondary Control for Grid- Following and Grid- Forming Inverters in AC Microgrids	Grad	Integrating Renewable Energy into the Grid
Mohseni	Soheil	A Game- Theoretic Approach to Model Interruptible Loads: Application to Micro- Grid Planning	Grad	Advanced Computational Methods for Power System Planning
Muhammad	Muhammad	Overcurrent Protection Scheme for the IEEE 13-Node Benchmark Test Feeder with Improved Selectivity	Grad	Intelligent Monitoring & Outage Management

Muthukaruppan	Valliappan	AMI Based Communication Scheme for Decentralized Volt/VAR Control	Grad	Smart Grid Technology
Nguyen	Bang	Distributed Dynamic State Estimation for Microgrids	Grad	System Wide Events & Analysis Methods
Patel	Shyamal	Efficient Operation of Distribution Grids with High Penetration of DER through Cluster Control	Grad	Operation & Control
Paudel	Amrit	Peer- to- Peer Energy Trading in Smart Grids Considering Network Utilization Fees	Grad	Market Interactions in Power Systems
Paul	Subho	Impact Assessment of Real Time Demand Control on Active AC/DC Hybrid Distribution Networks	Grad	Operation & Control
Peralta Moarry	Dario	Ground Source Heat Pump Modeling and Aggregation for Services Provision in Electricity Markets	Grad	Market Interactions in Power Systems
Pfeifer	Nils	Coupling Effects and Impact of EHV AC Cable Circuits on LV AC Systems within a Tunnel	Grad	Power System Modeling & Simulation
Pinceti	Andrea	Generation of Synthetic Multi- Resolution Time Series Load Data via Generative Adversarial Networks	Grad	Power System Modeling & Simulation
Poudel	Bikash	A Dynamic Model of Small Modular Reactor Based Nuclear Plant for Power System Studies	Grad	Power System Modeling & Simulation
Puvvada	Naha Yasasvi	Optimal Transmission Switching with Injection Uncertainties	Grad	Operation & Control
Ramesh	Arun V	Security Constrained Unit Commitment with Corrective Demand Response	Grad	Smart Grid Technology
Rehman	Waqas Ur	Deadband Voltage Control and Power Buffering to Enable Extreme Fast Charging of Electric Vehicles	Grad	Operation & Control
Ren	Junyu	A Method for Power System Transient Stability Assessment Based on Transfer Learning	UG	

Rong	Shuaiang	Impact of Photovoltaic Generation Integration on Protection of Distribution Systems	Grad	Integrating Renewable Energy into the Grid
Rosa de Jesus	Dan	Deep Learning Ensemble Based New Approach for Very Short- Term Wind Power Forecasting	Grad	
Saida	Masaru	Signal Dispatching Method for Secondary Frequency Control Based on Area Requirement Change and Merit- Order	Grad	
Sang	Linwei	A Scenario- adaptive Online Learning Algorithm for Demand Response	Grad	Smart Grid Technology
Savasci	Alper	Computational Efficiency Comparison of UC- OPF Formulations	Grad	Advanced Computational Methods for Power System Planning
Shirsat	Ashwin	Sensitivity Analysis of Time- of- Use Rates on Operations of Home Energy Management Systems	Grad	Operation & Control
Soltani,	Zahra	Real- Time Topology Detection in Unbalanced Distribution System Using Micro- PMU And Smart Meter Data: A MIQP Approach	Grad	Power System Modeling & Simulation
Souto	Laiz	Comparison of Principal Component Analysis Techniques for PMU Data Event Detection	Grad	System Wide Events & Analysis Methods
Subedi	Sunil	Model Predictive Voltage Support in Microgrids	Grad	Dynamic Performance and Control of Power Systems
Sun	Tingkai	N-k Security Assessment and Screening for Large-Scale Random Equipment Faults in Bulk Power Grid under Extreme Weather	Grad	
Tang	Zefan	Quantum- Secure Microgrid	Grad	Power System Modeling & Simulation
Vakili	Ramin	Enhancing Situational Awareness: Prediction of Protection Relay Operations After a Contingency	Grad	Dynamic Performance and Control of Power Systems
Vedullapalli	Divya	MPC Based Battery and Thermostat set- point Scheduling for Demand Response Applications in a University Campus Building	Grad	Smart Grid Technology

Venzke	Andreas	Verification of Physics- Informed Neural Networks: Formal Guarantees for Power System Applications	Grad	Operation & Control
Wang	Guofeng	An Online Energy Flow Control Strategy for Regional Integrated Energy System	Grad	Integrating Renewable Energy into the Grid
Wang	Wenyu	Diversity Factor Prediction for Distribution Feeders with Interpretable Machine Learning Algorithms	Grad	Advanced Computational Methods for Power System Planning
Wu	Chutian	Nonparametric Joint Chance Constraint for Spinning Reserve Requirements	Grad	Power System Modeling & Simulation
Xu	Chengsi	Analysis of Radial Constraint Representation Methods for Distribution Networks	Grad	Smart Grid Technology
Yan	Rong	Fast Transient Stability Batch Assessment using Cascaded Convolutional Neural Networks	Grad	Dynamic Performance and Control of Power Systems
Yang	Zhengwen	Virtual Synchronous Generator Control of Variable Speed Pumped Storage Hydropower with Full-size Converter	Grad	Integrating Renewable Energy into the Grid
Yousaf	Muhammad	Hidden Protection Challenges of Unbalanced Distributed Networks for Higher Concentration of Distributed Energy Resources	Grad	Integrating Renewable Energy into the Grid
Yu	Yanghao	Estimating the Flexibility Benefit of Concentrating Solar Plants in Electricity Markets	UG	Integrating Renewable Energy into the Grid
Zhihao	Hua	Distributed Optimal Scheduling of Multi- region Integrated Energy Systems Considering Regional Heating Network	Grad	Operation & Control

Deep Learning Approach for Power System Stability Assessment

Michael Abdelmalak, *Student Member, IEEE*, Bahram Parvin, *Member, IEEE*,
and Mohammed Benidris, *Member, IEEE*,

***Abstract*—The criticality to maintain the stability of power systems has increased significantly as a result of introducing various stochastic behaviors. The process to assess the dynamic performance of power systems has become more important to maintain reliability of the grid. Although time domain simulation approach provide the most accurate results, its computational time is relatively large especially for very large systems whereas direct methods, which usually consume less time, lacks the observability of system states in some cases. In this paper, a convolutional neural network approach is implemented to monitor and assess the system stability performance via time domain simulation. In the proposed approach, the concept of heatmap is proposed to be used as the input to the neural network. The heatmap is a graphical representation for three main parameters of stability assessment; voltage profile, rotor angle, and rotor angle deviation. Extensive simulations are carried for various loading conditions, fault locations, fault scenarios, and system topology. The integration of deep learning approach with time domain simulation has the ability to provide faster means to forecast the state of power system dynamics.**

***Index Terms*—Convolutional Neural Network, heatmap, time domain simulation, transient stability.**

I. Introduction

Power system stability is one of the crucial characteristics to maintain reliable operation, better performance, and maximum utilization [1]. Rotor angle stability has been studied using three main approaches; Time domain simulation (TED), Transient-energy function (TEF), and Equal Area Criteria (EAC). Time Domain simulation is based on solving nonlinear differential algebraic equations (DAE) that models the dynamic performance of power systems. Several mathematical approaches are implemented on TDS to enhance the results as well as obtain solutions in a faster way. In Transient-energy function method, the potential and kinetic energy margins are compared with threshold value to determine the system state. TEF approaches require the observability of system state pre- and during failure in order to provide good results. The implementation of Equal Area Criteria with TDS has provided a less computationally involved simulation but less accurate results. Thus, developing a method to determine the state of rotor angle stability in a faster way with high accuracy level is important to enhance power system stability.

Machine learning techniques have been applied in many power system problems to provide faster, more efficient, and less computation methods. Although several neural network methods have been studied in fault detection, classification, and rotor angle stability, most of them require the prior knowledge to the system state before, during, and after fault occurrence. Authors of [2] have proposed a support vector machine (SVM) approach to transient stability prediction, whereas in [3] another approaches based on decision tree and multilayer perceptrons have been analyzed and compared with SVM. Most of these approaches have low accuracy when implemented on larger systems and under noise measurements. A more robust method that does not reply fully on fault information can be integrated to enhance the methods of machine learning in rotor angle stability.

The authors are with the Department of Electrical and Biomedical Engineering, University of Nevada-Reno, Reno, NV, 89557 USA e-mail: (mabdelmalak@nevada.unr.edu and mbenidris@unr.edu).

II. Focus of this Work

In this work, a convolutional neural network (CNN) approach to assess the rotor angle stability is introduced. Several system parameters are used to generate heatmap representation of the power system time simulation profiles. Time domain simulations integrated on real-time simulators on dynamic simulators are used to extract the needed information under various conditions. The extracted data is converted to an RGB image representing the heatmap which will be used as an input for CNN. The proposed method is demonstrated on the Western Electricity Coordinating Council (WECC) 9-bus transmission system as well as the IEEE-39 bus system.

In order to generate the heatmap, time domain simulation is used to measure voltage magnitude, rotor angle, and rotor angle deviation. Each parameter represents one layer of the RGB heatmap image. To capture the dynamic system performance, heatmaps are generated based on varying loading condition, fault locations, and system topology. The loading condition is generated randomly based on statistical analysis of the load profile of IEEE RTS-24 system. The clearing time is modeled to have a Normal distribution with mean equal the contingency's critical clearing time and 5% standard deviation. Fault location is determined by selecting the impacted component (generator or transmission line) randomly. Two different architectures for CNN are selected to be tested based on the size of the system. Larger systems provide larger heatmap and as a result deeper and wider convolution can be applied. Finally, the trained CNN is tested with accurate real-time time domain simulation for validation and comparison.

References

[1] A. Gupta, G. Gurrala, and P. S. Sastry, "An online power system stability monitoring system using convolutional neural networks," *IEEE Transactions on Power Systems*, vol. 34, no. 2, pp. 864–872, March 2019.

[2] F. R. Gomez, A. D. Rajapakse, U. D. Annakkage, and I. T. Fernando, "Support vector machine-based algorithm for post-fault transient stability status prediction using synchronized measurements," *IEEE Transactions on Power Systems*, vol. 26, no. 3, pp. 1474–1483, Aug 2011.

[3] A. Gupta, G. Gurrala, and P. S. Sastry, "Instability prediction in power systems using recurrent neural networks," in *Proceedings of the Twenty-Sixth International Joint Conference on Artificial Intelligence, IJCAI-17*, 2017, pp. 1795–1801.

Wide-Area Measurement based Faulty Line Detection using Robust Deep Leraning Network

Shahabodin Afrasiabi
Department of Power and Control Engineering
Shiraz University

Shiraz, Iran
shpower77@yahoo.com

Mousa Afrasiabi
Department of Power and Control Engineering)
Shiraz University

Shiraz, Iran
musa.afra@shirazu.ac.ir

Mohammad Mohammadi
Department of Power and Control Engineering
Shiraz University

Shiraz, Iran
m.mohammadi@shirazu.ac.ir

***Abstract*— In this study, we aim to develop a real-time faulty line detection in the transmission networks in wide-area power systems. For this purpose, we design a robust deep Gabor filter convolutional neural network (RDGCNN) to understand the features of the complex and nonlinear signals during fault occurrence directly from the raw measured signals by the phasor measurement units (PMUs), on the basis of which a structure for fault detection, faulty line classification, and fault location estimation in the noisy condition. The performance of the proposed RDGCNN is examined in the IEEE 68-bus system.**

Keywords—component, formatting, style, styling, insert (*key words****)***

I. INTRODUCTION (*HEADING 1*)

In this paper, we propose a robust Gabor filter based deep CNN network, namely RDGCNN. The proposed method is one module-based network, which benefits from Gabor filter with less parameter in comparison with the standard CNN and is able to handle the temporal features by the capacity to transformation with convolutional layer redesigning. In contrast with hybrid methods that add additional feature extraction to only generate features, RDGCNN benefits from Gabor functions to modulate convolutional layers based Gabor filter and promote understanding ability from the raw signal. Furthermore, to improve the performance and robustness of the proposed method in noisy conditions, we modified the conventional cross-entropy loss function and reformulate a new loss function. The proposed method uses only half-cycle of the data measured by the PMUs and then is able to detect fault, determine the faulty line, and estimate fault location with high level of accuracy and reliability. Numerical studies in a large IEEE 68-bus network show the high level of the accuracy in high noisy conditions compared with combinational shallow-based methods and the standard CNN in the fault detection, faulty line classification, and fault location less than 4 ms. We can summarize the contribution of the paper as follows:

- In this paper a comprehensive wide-area fault detection and localization is proposed, where it only requires half-cycle of the raw data and does not need any additional feature extraction.
- The proposed method is highly robust in the noisy condition due to the reformulation of a new loss function and the inherent characteristics of the modulated Gabor filter and CNN.
- The proposed method is applicable in real-time application with fewer parameters than CNN.

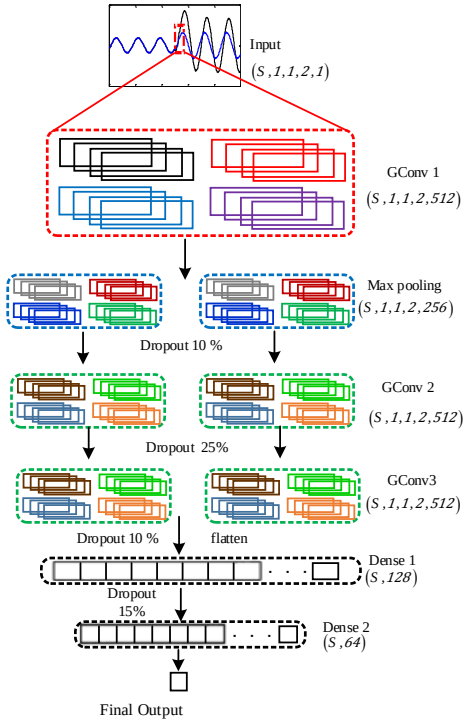

II. THE PROPOSED DEEP NETWORK

The designed RDGCNN network is visualized in Fig 1. To implement, RDGCNN for the transmission lines fault detection/localization the following procedure is used: The experimental data is firstly normalized, then converted from 1D- raw data measured by the set of PMUs, into 2D- signals and formed as a set of tensors with size $(S,1,1,2,1)$. As shown in Fig 1, the raw signals measured by the PMUs are considered as the input for the first Gabor filter, namely GConv 1 in Fig 1. This layer converts the input dataset into the feature vector with size $(S,1,1,2,512)$.Max pooling pools the maximum over each time interval as its output feature map. Thus, the length of max pooling outputs are smaller than convolution layer, the feature vectors are formed with $(S,1,1,2,256)$ and 10% dropout probability. The output of pooling layers is the input of the second and third Gabor based convolutional layer, namely GConv 2 & 3,

respectively, with 10% and 25% dropout probability and then both of them generate the output with $(S,1,1,2,512)$.The output of the GConv 2 should be converted from 2D-signals to 1D- signals. To this end, the output of max-pooling layers are flattened by a flatten layer and dropped out with 15% probability. Two different dense layers have been considered, which have outputs as a set of signals with $(S,128)$ and $(S,64)$ sizes, respectively. In the second dense layer, the outputs are dropped out with 15% probability. In the final step, the fault detection (fault/normal) conditions or faulty line, and fault location on the faulty line is determined.

III. Results

Overall, 43,000 different faulty conditions are generated. In addition, 1,000 normal condition based on stochastic characterization of the loads are produces. From the 44,000 different conditions, we devoted 70% of the dataset to the training of the proposed RDGCNN network and the rest of the dataset is used to test the performance of the proposed method and comparison with other methods. We evaluated the proposed method based on indices based confusion matrix, the accuracy (Ac), specificity (Sp), and positive predictivity (Pp). In the fault detection, we encounter with binary classification method, while the class number is 87 (86 lines and one non-fault condition) in faulty line classification problem in IEEE 68-bus. The obtained metrics from the proposed RDGCNN, CNN, ANN+SVM, and WT+SVM are given in Fig 2. The superiority of the proposed robust deep network in terms of accuracy and reliability is clear in this Fig.

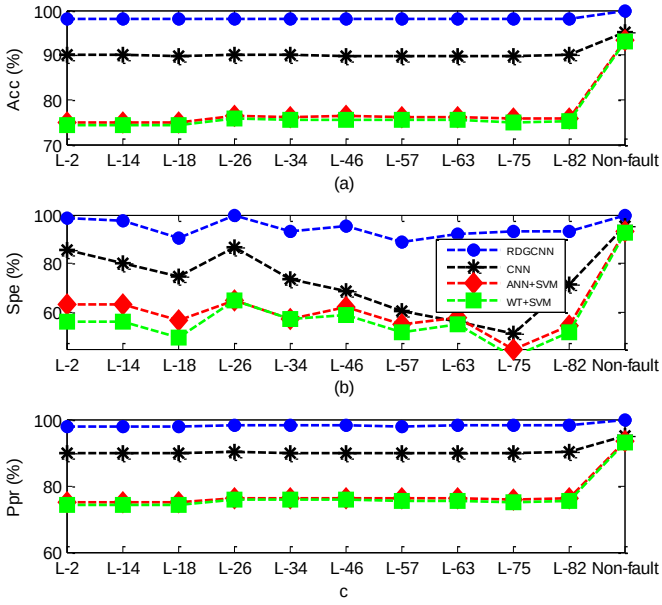

Fig. 2 – The results of faulty line detection of the proposed method, CNN, ANN+SVM, WT+SVM, (a) Ac, (b) Sp, (c) Pp

IV. Conculsion

In the faulty line classification, the results of an 87-class classification are assessed and show the superiority of the proposed method with more than 97% and more than 7% improvement in comparison with CNN and 13% improvement compared to the hybrid shallow-based networks. Consequently, the proposed method is at least 4, 11, and 14 times more accurate than CNN, ANN+SVM, and WT+SVM, respectively, in the fault location estimation. Furthermore, the proposed method is able to perform less than 3.84 ms and, therefore, validates its real-time application.

References

[1] W. Li, D. Deka, M. Chertkov, and M. Wang, "Real-Time Faulted Line Localization and PMU Placement in Power Systems ThroughConvolutional Neural Networks," IEEE Transactions on Power Systems, vol. 34, no. 6, pp. 4640-4651, 2019.

[2] S. Luan, C. Chen, B. Zhang, J. Han, and J. Liu, "Gabor Convolutional Networks," IEEE Transactions on Image Processing, vol. 27, no. 9, pp. 4357-4366, 2018.

Study of Large Solar PV Penetration on a Proposed Generation and Transmission Benchmark System

Oluwaseun Akeyo, *Student Member, IEEE*, Aron Patrick[1], and Dan M. Ionel, *Fellow, IEEE*

***Abstract*—A framework for estimating the maximum PV hosting capacity of a transmission network. Contrary to conventional approaches, in which the circuit maximum hosting capacity is evaluated for a fixed load level, the proposed scheme accounts for the possible load level variations that may affect the highest amount of PV system that can be connected to specified buses within the transmission circuit. The impact of high PV penetration was studied on a modified benchmark test system developed in PSS®E power system simulation software. The response of the circuit based on its bus voltages, branches power flow, PV points of interconnection and penetration were analyzed and used to evaluate the maximum PV hosting capacity of the system without a significant upgrade.**

***Index Terms*—Hosting capacity, photovoltaic, PSS/E, Transmission network, Voltage violations, Thermal limits, PV penetration**

I. Hosting Capacity for Modified Transmission Network

The modified benchmark transmission system analyzed in this work represents a small islanded power system network with 12 buses and four generating units (Fig. 1). At steady-state without renewable integration, the transmission network total system load is approximately 65% of the total generation capacity. The bus voltage voltages vary between 0.98pu to 1.03pu and the maximum loading for any of the transmission lines is 71%, which is the power flow between buses 6 and 4.

The study focuses on the maximum capacity of a PV system that may be connected to any one of the buses in the example transmission network without violating the bus voltages or the thermal limits of the circuit branches. Opposed to conventional approaches, the proposed framework accounts for the system load variation and employs an economic dispatch model to meet the demand at the cheapest operation cost. The mathematical model for the economic dispatch model is as follows:

$$minimize, \qquad C_T = \sum_{i=1}^{N} C_i(P_i), \qquad \epsilon = |P_T - L_c|, \quad (1)$$

where, C_T, represents the total operating cost at each specified time; P_T, combined generator output and L_c, the combined load. The generator ramp constraint is expressed as:

$$\max[P_i^{min}, P_i^{t-1} + R_i^{down}] \leq P_i^t \leq \min[P_i^{max}, P_i^{t-1} + R_i^{up}]. \quad (2)$$

where, P_i^t and P_i^t represents the generation units out power at time t and $t-1$, respectively; R_i^{up} and R_i^{down}, the generator rising and falling ramp rates, respectively.

Oluwaseun Akeyo and Dan M. Ionel are with the SPARK Laboratory, ECE Department, University of Kentucky, Lexington, KY. Aron Patrick is with LG&E and KU, Louisville, KY.

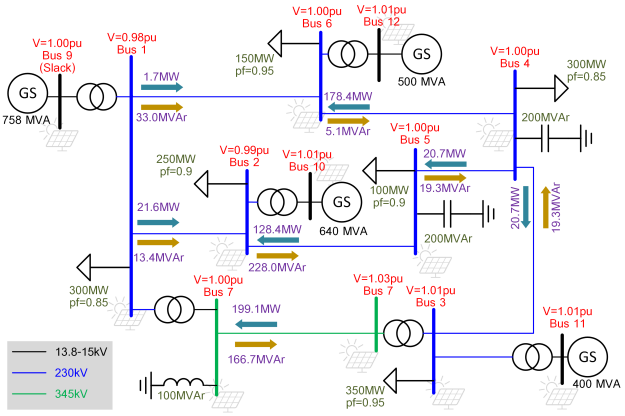

Figure 1. Single line diagram of the modified benchmark network, which has a load of approximately 65% of total generation capacity. The transmission circuit is completely assessed for PV connection at any of its buses.

II. Solar PV Penetration Impact Study

The network was analyzed at multiple load levels including the base network loading. The estimated PV hosting capacity for each bus at the base load level was compared with the evaluated values as the system load increases and the generators real power outputs are updated.

The results show that the maximum amount of renewable that may be connected to any of the system buses without violating any thermal or voltage limits depends on the selected bus and the total system load level.

For the example transmission network evaluated and PV hosting capacity estimation framework employed, at the baseload level, up to 200MW (approximately 10% of combined generation capacity) may be connected to any of the network buses without voltage or thermal violations (Fig. 2).

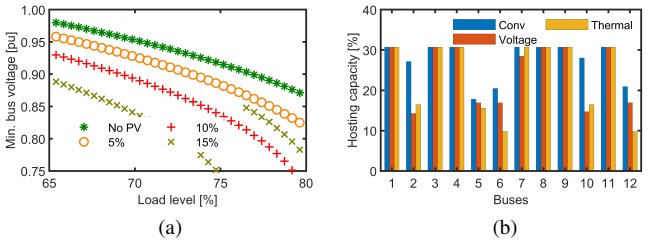

(a) (b)

Figure 2. (a) Minimum bus voltage at increasing network load levels. For this example network and the generator response algorithm employed, the minimum bus voltage reduces as the PV penetrations and load level increases. (b) Maximum PV hosting capacity with respect to the circuit solution convergence, voltage and thermal limits at 65% load level.

Are Electric Transportation, Big Data and Machine Learning Transforming the Grid?

Homeyra Akter
Department of Electrical and Electronics Engineering
University of the Ryukyus
Okinawa, Japan
homairaakter08@gmail.com

***Abstract*—The electrical power system is moving towards the next-generation smart grid system, including some advanced technologies such as power electronics, renewable energy sources, distributed generation, advanced monitoring and communication systems, etc. These enable bi-directional communication and power flow with enhancing security, reliability, and efficiency of the power system. These advanced technologies contradict the conventional power system. For example, renewable energy sources produce DC power instead of AC power, such as solar power. On the other hand, the AC power of renewable sources like wind energy varies greatly. Power electronics-based loads work separately, and electronic devices display constant power load characteristics that unstable the system. Bi-directional communication occurs in decentralized distributed systems, which opposed to conventional centralized systems. Connectivity and exchange of information are done by the Internet of things (IoT) devices, which enable the grid components to exchange data. By this time, a vast amount of data is generated, which can not be handled by the conventional system. So, carry out the advanced technologies in the traditional grid is challenging. That's why transforming the old power grid is attracted attention for moving on.**

Electric transport systems are introduced to reduce the oil dependency for transportation and to limit CO_2 emissions related to transportation. The integration of electric transport and renewable energy is reducing the world's dependence on fossil fuels and greenhouse gas emissions significantly. There are some barriers to implementing renewable energy generation. The output power of renewable generation depends on the weather, not on demand. Electronic vehicle (EV) storage batteries are an efficient solution to integrate the generation based on renewable energy. Vehicle to grid (V2G) concept is the most promising feature of the electric transport sector, which helps to store surplus energy and gives it back to the main grid during high demand for electricity. The widespread implementation of electric transportation could play a significant role in integrating renewable energy into transforming the existing power systems. On the other hand, big data analysis and machine learning techniques are very useful in transforming the grid. Big data contains a large amount of data from the smart grid that collects from monitoring transmission and distribution lines, generation units, smart metering, and smart home. This data should be stored in a cloud-based system for analyzing. Big data analysis is considered as the main functionality for supply and demand-side management for smart grids, control algorithms, and future energy market models. The management of dynamic energy through this kind of data analysis is also attracted attention. Dynamic energy management is necessary to process power flow optimization, the massive amount of data from the system monitoring, real-time operation, etc. Big data-based research strategies such as power generation, optimization techniques, and forecasting methodologies extend to renewable energy-based systems like wind power and solar power systems. The data in the grid comes from different sources. Different types of data generated in the grid contain confidential information of individual users. Such data needs to be protected following legal regulations. Besides, this data includes sensitive information of a country's organization or central grid. Manipulation of this data can affect the safe operation of the grid. So security and privacy is a critical issue with IoT integrated smart grid which is a cyber-physical system that makes it biased to cyber attacks. Another essential concern is to process and transfer of data within an acceptable range of time.

Machine learning is an effective solution that applies to big data processing and uses for security solutions. Machine learning techniques provide an efficient way of analyzing and making the appropriate decision for running the grid. It consists of a combination of different algorithms that analyze the available data through a set of instructions to generate data-driven predictions. Machine learning functionality can predict the energy consumption and generation, appropriate price, optimum schedule, and sizing of generators, fault detection, etc. In renewable energy-based grid systems, several machine learning methods are being introduced at different stages, creating entirely new possibilities for research. Support vector machines have provided many optimization and forecasting techniques in the grid for solving the problems of the renewable-based power system. Machine learning-based economic optimization, monitoring power quality, islanding detection are developed recently. Several algorithms are implemented for predicting the load data such as support vector regression, artificial neural network, deep neural network, etc. For solving the security problems of grid, machine learning can be considered as an effective solution.

Finally, we can say that the conventional electric grid is transforming to IoT based smart grid with the benefits of big data analysis, machine learning techniques, and integrated electric transportation with renewable energy.

Risk Management via Second-Order Stochastic Dominance Constraints: Benchmark Selection Approaches

Mohamed Kareem AlAshery, *Student Member, IEEE*, and Wei Qiao, *Fellow, IEEE*
Power and Energy Systems Laboratory
Department of Electrical and Computer Engineering
University of Nebraska–Lincoln
Lincoln, NE 68588-0511 USA
m.kareem@huskers.unl.edu; wqiao3@unl.edu

***Abstract*—This document includes the abstract for a poster submitted to the 2020 IEEE PES GM student poster contest.**

***Keywords*—Decision-making under uncertainty; risk management; stochastic dominance; stochastic programming.**

I. Poster's Abstract

Many decision-making problems, such as energy market operation and participation, are accompanied with various sources of uncertainty. A rational decision-making process should account for those uncertainties while making decisions. The stochastic programming technique has been applied to model such problems in three different ways [1]: expected utility maximization models, mean-risk models, and stochastic dominance models. The expected utility maximization models determine the optimal outcome based on the optimal expected value of the objective function, regardless of the objective function's variability. In contrast, the mean-risk models, firstly introduced by Harry Markowitz [2], account for the objective's variability by comparing the portfolios in two dimensions: expected (mean) value and risk, where the risk can be quantified via different risk measures, such as variance, value at risk (VaR), and conditional value at risk (CVaR).

The stochastic dominance models, which optimize the objective subject to stochastic dominance constraints that can be formed in different orders, have a solid theoretical basis for making choices under risk [1]. In a stochastic dominance model, the optimal solution dominates a predefined benchmark distribution (or simply called "benchmark") in the sense of the stochastic dominance concept. This benchmark ensures that the values and probabilities of the unfavorable outcome's scenarios are within the decision-maker's risk preference. The second-order stochastic dominance models proposed in [3] are the best to represent the risk preferences of rational risk-averse decision-makers [4]; and provide superior risk management performance compared to mean-CVaR models as demonstrated in [5]. Nevertheless, the stochastic dominance models underlay two major challenges. Firstly, they may be mathematically intractable for problems with large numbers of scenarios, as the number of a model's constraints is proportional to the product of the number of the problem's scenarios and the number of scenarios of the imposed benchmark. The second challenge is the difficulty in defining a benchmark distribution that best represents the decision-maker's risk preference while maintaining the feasibility of the model.

To overcome the obstacle of benchmark selection and unlock the potentials of the stochastic dominance models in different power and energy applications, this poster discusses two optimization-based benchmark selection approaches that are applicable to any optimization problems with second-order stochastic dominance constraints. The two approaches define a fixed effective feasible region and an adaptive feasible region, respectively, within which the benchmark distribution should be bounded to maintain the optimization problem's feasibility. These feasible regions of the benchmark distribution are determined by solving modified versions of the original optimization problem. The first approach defines a fixed effective feasible region for the whole benchmark distribution, while the second approach defines the feasible regions for benchmark's scenarios sequentially, starting from the worst to the best scenario. The approaches enable decision-makers to define benchmark distributions rigorously that best represent their risk preferences with the least number of scenarios, which is desirable from the computational tractability point of view. Compared to our work in [5], this poster discusses a new adaptive feasible region-based benchmark selection approach and the two benchmark selection approaches discussed in this poster do not need to solve a different optimization problem, i.e., the mean-risk model. A case study for the optimal bidding problem of a wind power producer in the electricity market is used to validate and demonstrate the proposed two approaches.

References

[1] D. Roman, K. Darby-Dowman, and G. Mitra, "Portfolio construction based on stochastic dominance and target return distributions," *Math. Program.*, vol. 108, no. 2–3, pp. 541–569, Sep. 2006.
[2] H. Markowitz, "Portfolio selection," *J. Finance*, vol. 7, no. 1, pp. 77–91, Mar. 1952.
[3] D. Dentcheva and A. Ruszczynski, "Risk-averse portfolio optimization via stochastic dominance constraints," in *Handbook of Financial Econometrics and Statistics*, New York, NY, USA: Springer, 2015, pp. 2281–2302.
[4] M. Kallio and N. Dehghan Hardoroudi, "Second-order stochastic dominance constrained portfolio optimization: Theory and computational tests," *Eur. J. Oper. Res.*, vol. 264, no. 2, pp. 675–685, Jan. 2018.
[5] M. K. AlAshery, D. Xiao, and W. Qiao, "Second-order stochastic dominance constraints for risk management of a wind power producer's optimal bidding strategy," *IEEE Trans. Sustain. Energy*, pp. 1–10, Jul., 2019.

Tradeoffs in Forecasting of Residential Electric Loads with Data from Smart Meters and Intelligent Circuit Breakers

Rosemary E. Alden, *Student Member, IEEE*, Cristinel Ababei, *Senior Member, IEEE* , Dan M. Ionel, *Fellow, IEEE*

***Abstract*—Major recent developments in the smart grid include the collection of large data sets through smart devices and energy management systems. The need for improved understanding of the current and future loads, motivated the emergence of machine learning (ML) techniques, such as artificial neural networks, to forecast electrical loads. These ML are at the forefront of research in the smart grids area and of interest to the industry. As devices become more sophisticated, with higher sampling frequencies and the IoT becomes more widespread, "big data" is facing renewed challenges related to interpretation and considering portions of data while maintaining accuracy for electric load forecasting. Our primary objective is studying data size and resolution needed to construct effective ML models for residential electric load forecasting. We are, specifically, interested in developing long short term memory (LSTM) models using energy consumption data from the most influential appliances and circuits such as HVAC, water heater, and electric mains. Moreover, we are interested in integrating these models with EnergyPlus to enable detailed building energy simulations and optimizations for horizons of 24 hours. Our investigations will inform the big data collection efforts in order to make it more focused and storage-conscious, thus more meaningful.**

***Index Terms*—Big data, EnergyPlus, variable loads, machine learning, residential**

I. Energy Monitoring Technologies and Big Data

Intelligent circuit breakers monitor the energy consumed by large power appliances, such as heating, ventilation, and air conditioning (HVAC) systems and electric water heaters (EWH) at fine resolutions. Smart meters can report the total energy measured on a residential main circuit every 15 minutes. These developments offer unprecedented opportunities to monitor residential loads at higher resolutions than ever before.

The natural consequence of closer monitoring is "big data" from these IoT devices resulting in new formatting and interpretation challenges. We are working to identify a minimal data set (a subset of the much larger data set) that provides enough information to build accurate energy consumption models in residencies. Our focus is on sampling frequency and selection of specific measurements. The resolution drastically changes the experimental data and thus, the quality and relevance of predictions as illustrated in Fig. 1. We will consider other aspects related to big data, such as the impact of variations in weather, occupancy, and high variability loads.

Rosemary E. Alden and Dan M. Ionel are with the SPARK Laboratory, Electrical and Computer Engineering Dept., University of Kentucky, Lexington, KY. Cristinel Ababei is with the Electrical and Computer Engineering Dept., Marquette University, Milwaukee, WI.

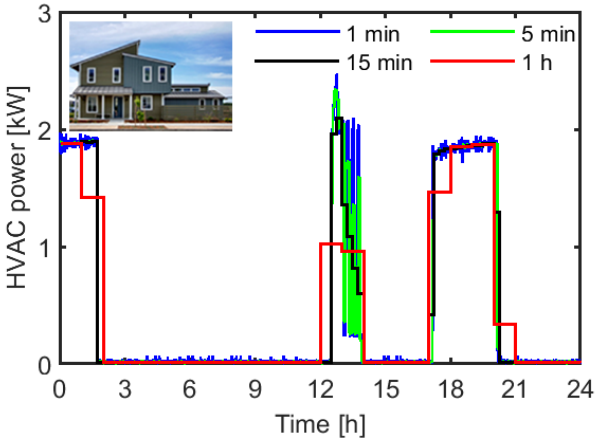

Figure 1. Power usage at different resolutions of the Honda Smart Home, on December 15, 2018.

II. Experimental Data and ML Techniques for Prediction of High Variability Loads

Our two primary data sets include TVA Robotic Houses located in Knoxville, TN and the publicly available Honda Smart Home (HSM) in Davis, CA. The HSM includes 230+ sensors collecting minutely data. We are producing 5-15 minute and hourly time resolutions using scripts in R. The importance of sampling frequency for high variability loads such as HVAC is shown in Fig. 2).

To handle such rapid changes a long short term memory (LSTM) model is under development for the 1 to 5 minute resolutions. We chose LSTM as an RNN model to predict a home's daily energy load because, among the ML techniques studied in literature, we find it one of the most promising.

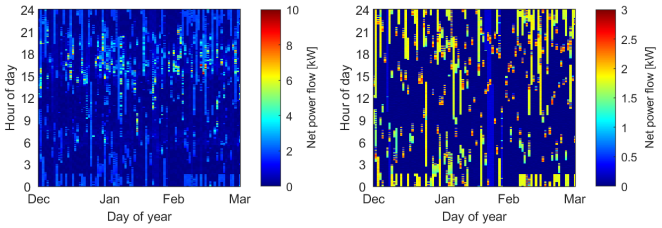

Figure 2. (a) Total electric and (b) HVAC load for HSM over Dec- Feb, 2019. HVAC is a large consumer in homes and requires effective forecasting.

A Deep Unsupervised Learning Approach to PMU Event Detection in an Active Distribution Network

David Ofosu Amoateng, *Student Member, IEEE*, Ruifeng Yan, *Member, IEEE*, Tapan Kumar Saha, *Fellow, IEEE*
School of ITEE, The University of Queensland, Australia

***Abstract*—The increased deployment of advanced metering devices such as PMUs in active distribution networks offers network operators the potential to develop applications which may help improve visibility regarding the operating state of their network. Considering the high reporting rates of PMUs, it is imperative to develop schemes capable of analysing PMU data in near real-time, which will enable system operators take timely actions. However, current methods used for situational awareness in active distribution grids are heavily dependent on data sample size or on detectors that require great effort in tuning. By training deep autoencoders with PMU data from a real active distribution network, we develop and validate a framework which automatically learns a representation of the network. With this approach, our framework can monitor the state of the network and also detect events in a fraction of a second, making it suitable for online analysis of PMU data from multiple streams or analysis of large amounts of historical PMU data. The performance of the proposed model is validated by comparison with a sample based statistical anomaly detector.**

I. Problem Formulation and Introduction

Let $X = [X_i, X_{i+1}, \ldots, X_{n_l}]^T$, $X \in \mathbb{R}^{n_l \times n_v}$ denote a vector sequence of PMU measurements for a fixed window size, where n_l and n_v are the window size and the number of variables being analysed by the event detector respectively. $X_i \in \mathbb{R}^{1 \times n_l}$, which is an observation in the above vector:

$$X_i = \left[\; V_1^{abc}, F_1, I_{11}^{abc}, V_{l1}^{abc}, \ldots, V_j^{abc}, F_j, I_{1j}^{abc}, V_{lj}^{abc} \; \right]$$

where j represents the number of PMU devices providing measurements. V^{abc}, F are the three phase voltages and frequency and I_l^{abc}, V_l^{abc}, F_l are the lag one difference of the current magnitude, voltage magnitude, and frequency respectively.

The input sample $X_i \in \mathbb{R}^{1 \times n_l}$ may contain data points that may either be a subset of $\{D_E\}$, the set of event data points or $\{D_{NE}\}$, the set of non-event data points. Using recorded PMU data, our goal is to construct a model using deep autoencoders that automatically learns a representation of the network, reconstructs PMU data and predicts which set an PMU data sample belongs to. To achieve this, we assume the PMU dataset for building the model is unbalanced set where the number of event data points $D_E \ll D_{NE}$, the number of non-event data points. As such we aim to build a model which is biased towards recognising and reconstructing normal data points, such that a non event data point will yield a high reconstruction error when presented as input.

This Activity received funding from the Australian Renewable Energy Agency (ARENA) as part of ARENA's advancing renewables programme.

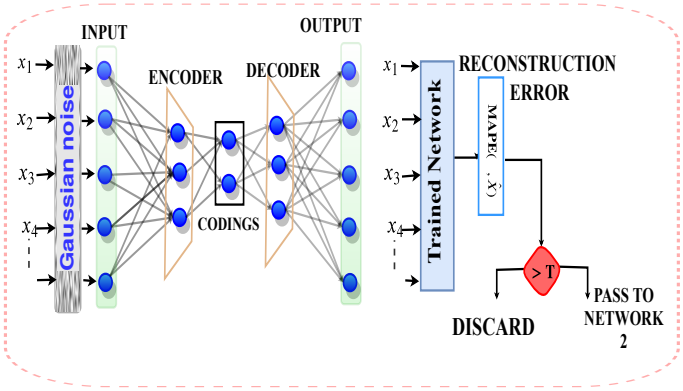

Fig. 1: a) Data Outlier Filter Framework for Event Detection

II. Model Performance

The figure below shows the performance of the proposed model in comparison with a statistical anomaly detector [1].

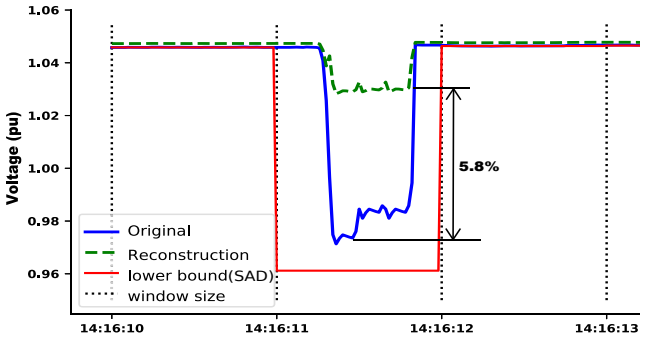

Fig. 2: Event II (Static window size) : Failed event detection by the statistical anomaly detector

III. Conclusion

This paper presents a framework for detecting events in distribution network in order to improve situational awareness. This would be instrumental in providing real time situation awareness using high streaming PMU data. Future work includes pairing this event detector with a machine learning classifier, to automatically predict the type of event detected.

References

[1] A. Shahsavari, M. Farajollahi, E. Stewart, E. Cortez, and H. Mohsenian-Rad, "Situational awareness in distribution grid using micro-pmu data: A machine learning approach," *IEEE Transactions on Smart Grid*, 2019.

Model Predictive Voltage Support in Microgrids

Niranjan Bhujel†, Ujjwol Tamrakar, Timothy M. Hansen, and Reinaldo Tonkoski
Department of Electrical Engineering and Computer Science
South Dakota State University
Brookings, South Dakota, USA 57007
Email: †niranjan.bhujel@jacks.sdstate.edu

***Abstract*—For the good performance and reliability of microgrids, voltage regulation is necessary. Since line resistance to reactance ratio is high in microgrids, it might be easier to regulate voltage with active power than reactive power but the cost of active power is higher. Thus, an optimal control method should be implemented. Model predictive control (MPC) is proposed for this purpose.**

***Index Terms*—Voltage support, model predictive control, optimal control, microgrid.**

I. Key Equations

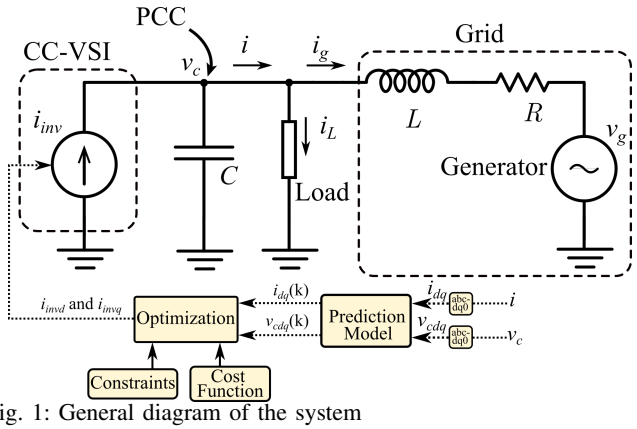

Fig. 1: General diagram of the system

For the system shown in the Fig. 1, state differential equations can be written as

$$x_{k+1} = Ax_k + Bu_k \tag{1}$$

Let N be the horizon length (in terms of sample instant). Our objective is to control the voltage at the PCC v_c within acceptable values. Then the objective of the controller is to support $v_{c,d}$ using the control inputs i_{invd} and i_{invq}. Next, let us assume $\Gamma = \{1, 2, ..., N\}$ represents the discrete sample time instants in the forward-time horizon. Let $y_k = \Delta v_{cdk}$ and $u_k = [i_{invd_k}\ i_{invq_k}]^\top$ be the measured output of and be the input respectively, then the proposed MPC formulation will take the following form:

$$\begin{aligned} \underset{i_{invd}, i_{invq}}{min} \quad & J_\Gamma = \sum_{k=1}^{N} (y_k^\top Q y_k + u_k^\top R u_k) \\ \text{s.t.} \quad & \boldsymbol{x}_{k+1} = Ax_k + Bu_k \ \forall\ k \in \Gamma, \\ & |i_{invd_k}| \leq i_{d,max} \ \forall\ k \in \Gamma, \\ & |i_{invq_k}| \leq i_{q,max} \ \forall\ k \in \Gamma, \\ & |i_{invd_{k+1}} - i_{invd_k}| \leq S_d \ \forall\ k \in \Gamma, \\ & |i_{invq_{k+1}} - i_{invq_k}| \leq S_q \ \forall\ k \in \Gamma \end{aligned} \tag{2}$$

where J is the cost function, Q and R are weighting matrices. $Q = Q_{11}$ is the weight for voltage, R_{11}, and R_{22} are the weight for d-component and q-component of the inverter current respectively. The MPC formulation was implemented in pyomo. The weighting parameters used were $Q_{11} = 1, R_{11} = 0.01, \text{and} R_{22} = 0.001$

II. Key Results

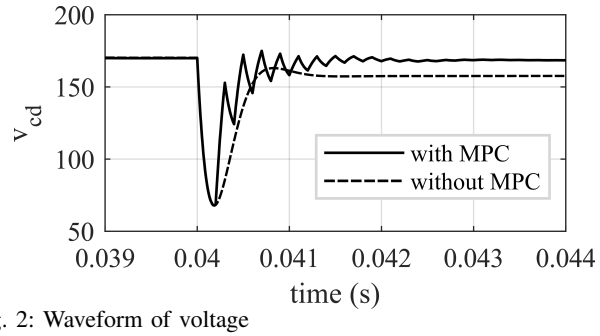

Fig. 2: Waveform of voltage

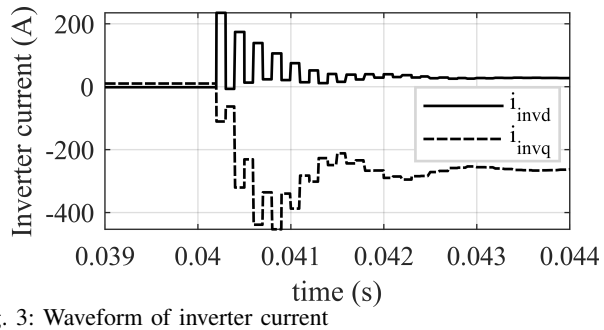

Fig. 3: Waveform of inverter current

Fig. 2 shows the plot of voltage when load changes by 0.75 pu. From the plot, we can see that the inverter is able to provide support for voltage. Since weight for i_{invd} is higher compared to that of i_{invq}, higher value of i_{invq} is used for voltage support.

III. Futute Work

The inverter was able to support voltage but there was still some oscillation that could be removed when PLL is improved. They are part of future work.

Sizing of Movable Energy Resources for Service Restoration and Reliability Enhancement

Narayan Bhusal, *Student Member, IEEE*, Mukesh Gautam, *Student Member, IEEE*,
and Mohammed Benidris, *Member, IEEE*
Department of Electrical and Biomedical Engineering
University of Nevada, Reno, NV 89557, USA
Emails: bhusalnarayan62@nevada.unr.edu, mukesh.gautam@nevada.unr.edu, and mbenidris@unr.edu

***Abstract*—The dramatic increase of extreme events (e.g. hurricanes, earthquake, cyber-attacks) have severely impacted power systems ranging from long outage times to major equipment destruction. Distribution system failures and outages are major contributors to power supply interruptions. This work proposes a two-stage strategy to determine the minimum sizes of MERs with network reconfiguration (NR) for distribution service restoration and supplying local and isolated loads. After a contingency, the first stage determines the NT based on the spanning tree search algorithm. In the second stage, if some system loads cannot be fed by NR, MERs are deployed and the optimal routes to reach isolated areas are determined based on the Dijkstra's shortest path algorithm (DSPA). The traveling time obtained from the DSPA is incorporated with the proposed sequential Monte Carlo simulation-based approach to determine the sizes of MERs. The results are demonstrated through case studies on IEEE-13 and IEEE-123 node test feeders.**

***Index Terms*—Distribution service restoration, extreme events, isolated loads, movable energy resources, network reconfiguration, and spanning tree search algorithm.**

I. INTRODUCTION

The dramatic increase of the extreme events (e.g. hurricanes, earthquakes, cyber-attacks) have led to large blackouts and major destructions of power grids resulting in economic losses and more importantly, long outage duration times. Therefore developing control and operation method and planning strategies to improve distribution service restoration (DSR) is very vital. Network reconfiguration (NR), microgrid (MG) formation, and splitting power grid into several smaller and reliable MG, Distributed Generations (DGs), and movable energy resources (MERs) to form dynamic MGs are considered as the most effective DSR approach. Mobile energy resources (MERs) are flexible and movable resources that can play an important role in DSR, specifically when there are no other means of power supply during contingencies.

II. SIZING OF MOVABLE ENERGY RESOURCES

This paper proposes a storchastic strategy to determine the size of MER for DSR considering NR, travel times, and outage duration of distribution components (DCs). Dijkstra's shortest path algorithm has been implemented to determine the optimal route for MERs, spanning tree search algorithm is used to determine the optimal NR, and sequential Monte-Carlo simulations are used to model the outages of DC. and

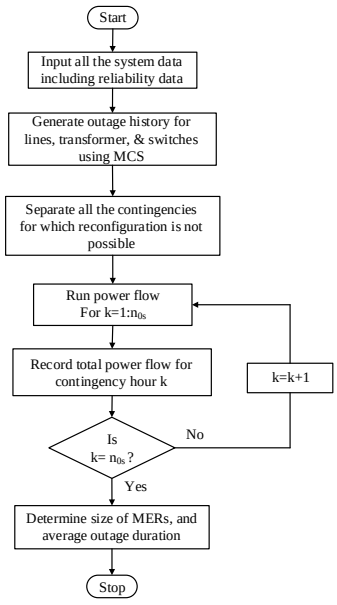

Fig. 1. Flow chart of proposed approach

all the simulations are performed in MATLAB and OpenDSS integrated environment. The procedure to determine the sizes of MERs is explained as follows and shown in Fig.1.

III. CASE STUDIES

The proposed approach is validated through case studies on IEEE 13- and IEEE 123-node test feeders. The MER sizes and interruption times of the IEEE 13-node test feeder are given in Table I. Even though both the feeders have same

TABLE I
RESULTS FOR ALL CASE STUDIES

	IEEE 13	IEEE 123
Average Size (kWh)	3998	810
Average Size (kW)	370	138.67
Maximum Size (kW)	590	198
Average Duration Time (hours)	10.8	5.84

level of loads, the average size of MERs in IEEE 13-node is significantly larger than that of the IEEE 123-node because of the fact that reconfiguration is not possible for the case of IEEE 13-node feeder.

The Effect of Power Electronic Loads on Western Interconnection Stability

Matthew Bossart[1,2], Rick Wallace Kenyon[1,2], Dragan Maksimovic[1], Bri-Mathias Hodge[1,2]
[1]*Electrical, Computer & Energy Engineering,* [2]*Renewable & Sustainable Energy Institute, University of Colorado Boulder*
Boulder, CO
{matthew.bossart, richard.kenyonjr, maksimov, brimathias.hodge}@colorado.edu

***Abstract*—The prevalence of power electronics in the bulk power system is increasing rapidly in both the generation and consumption of electricity. This work focuses on the effect of changing load composition - specifically the transition from single phase air conditioner motors to power electronics backed air conditioners - on power system stability. Various transmission and generation contingency events for the Western Interconnection were simulated using Positive Sequence Load Flow software and planning models from the Western Electricity Coordinating Council. In general, an increased proportion of power electronic load leads to more instability. For some specific faults resulting in fault-induced delayed voltage recovery, transitioning to higher proportions of power electronic loads helps expedite system recovery. These results demonstrate that load composition should be examined in conjunction with generation composition when evaluating system stability.**

I. Methods

This work focuses on the stability impact of one current trend in the changing electrical load: the replacement of single phase air conditioners with power electronics interfaced air conditioners and/or air source heat pumps. This study uses the 2023 Heavy Summer Planing Case (HS-Base) which was originally developed by the Western Electricity Coordinating Council and modified for use in the Western Wind and Solar Integration Study Phase 3 [1]. Two parameters, which determine the proportion of single phase air conditioner and power electronic load, were systematically adjusted to derive additional cases from the HS-Base case. Positive sequence type simulations of the entire Western Interconnection were run for a set of five contingencies, including one generation loss contingency and four transmission faults (Fig. 1).

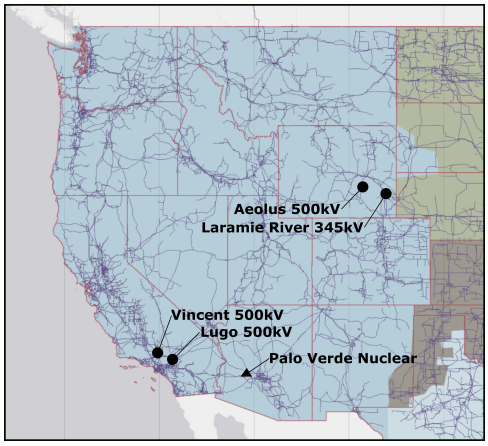

Fig. 1. The major transmission lines of the Western Interconnection with the location of the large disturbances considered. Circles indicate transmission faults and the triangle indicates a generation loss.

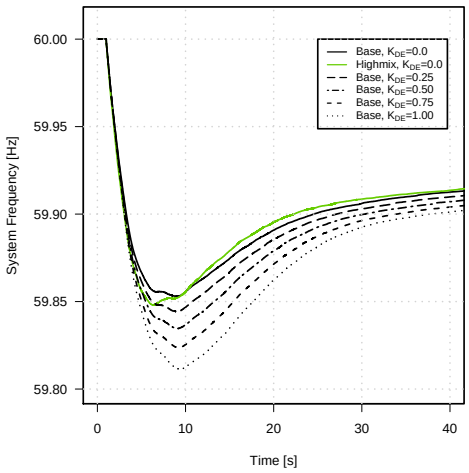

Fig. 2. System frequency after an N-2 contingency event: simultaneous loss of two Palo Verde generators. Larger values of K_{DE} indicate a more complete shift from single-phase air conditioning to power electronic air conditioning.

II. Main Results & Conclusions

Fig. 2 shows the frequency drop in the Western Interconnection due to an N-2 contingency event: simultaneous loss of two Palo Verde nuclear generators. The dotted lines show the frequency nadir dropping significantly as the single-phase air conditioning load is shifted to power electronic interfaced air conditioning load. Unlike single-phase air conditioners, power electronic load tends to consume constant power even as frequency and voltage drop, leading to a more extreme system response to a loss of real power.

The fundamental conclusion of this study is that load composition is important to the stability of the bulk power system and should be studied in conjunction with changes in generation.

References

[1] N. W. Miller, M. Shao, S. Pajic, and R. D'Aquila, "Western Wind and Solar Integration Study Phase 3: Frequency Response and Transient Stability," National Renewable Energy Laboratory, Tech. Rep. December, 2014.

Optimal Transmission Switching with Injection Uncertainties

Snehil Chandra, P. Naga Yasasvi, Abheejeet Mohapatra, and S. C. Srivastava
Department of Electrical Engineering, Indian Institute of Technology Kanpur, Kanpur, India 208016
Email: snehil0704@gmail.com; yasasvi@iitk.ac.in; abheem@iitk.ac.in; scs@iitk.ac.in

***Abstract*—This poster proposes a robust optimization model for the optimal transmission switching problem of the power networks to cater to the short-term uncertainties in the power injections of demands and renewable energy sources. The novelty of the proposed model is that the base-point generation of the conventional generators and the switching statuses of the transmission lines are considered as robust variables. The proposed approach uses the Benders Decomposition technique, with both feasibility and optimality cuts, to solve for the robust variables.**

***Index Terms*—Transmission Switching, Mixed-Integer Programming, Robust Optimization, Benders Decomposition.**

I. Introduction

Optimal Transmission Switching (OTS) is typically an operational problem. The real-time operation of the system is usually heavily influenced by various uncontrollable factors such as the uncertainty and variability in demand, uncertainty in transmission and generation parameters, equipment failures, weather, etc. Hence, it is important to develop a proficient approach for OTS that considers the multi-fold uncertainties in the power network, with base-point generation of conventional generators and switching statuses of lines considered as robust variables.

II. Proposed approach for robust OTS

The robust OTS model (1)-(7) with demand and output of RESs as major sources of uncertainty is considered. The proposed approach for robust OTS intends to find the robust values of the base-point generations ($P_{g_{base_i}} \forall i \in \mathbf{G}$) of the conventional generators and the transmission line switching statuses ($\alpha_{ij} \forall (i,j) \in \mathbf{L}$), which ensure feasible system operation for all load and RESs output scenarios (including the worst-case), as defined by the uncertainties.

$$\min \quad \sum_{i \in \mathbf{G}} C_i(P_{g_{base_i}} + \beta_i \sum_{j \in \mathbf{B}} \{\zeta_{dj} - \zeta_{rj}\}) \tag{1}$$

$$\text{s.t.} \quad -\alpha_{ij}\overline{P_{ij}} \leq P_{ij} \leq \alpha_{ij}\overline{P_{ij}}, \forall (i,j) \in \mathbf{L} \tag{2}$$

$$-2\overline{\theta}(1-\alpha_{ij}) \leq \theta_i - \theta_j - x_{ij}P_{ij} \leq 2\overline{\theta}(1-\alpha_{ij}), \forall (i,j) \in \mathbf{L} \tag{3}$$

$$\sum_{j \in \delta(i)} P_{ij} - P_{g_{base_i}} - \beta_i \sum_{j \in \mathbf{B}} (\zeta_{dj} - \zeta_{rj}) + P_{di} + \zeta_{di} - P_{ri} - \zeta_{ri} = 0, \forall i \in \mathbf{B} \tag{4}$$

$$\underline{P_{gi}} \leq P_{g_{base_i}} + \beta_i \sum_{j \in \mathbf{B}} (\zeta_{dj} - \zeta_{rj}) \leq \overline{P_{gi}}, \forall i \in \mathbf{G} \tag{5}$$

$$-\theta_\epsilon \leq \theta_i \leq \theta_\epsilon, \forall i \in \mathbf{B}, \theta_{ref} = 0 \tag{6}$$

$$\alpha_{ij} \in \{0,1\}, \forall (i,j) \in \mathbf{L} \tag{7}$$

To incorporate the injection uncertainties in loads and RESs outputs, the real power generation of a conventional generator is modified as $P_{gi} = P_{g_{base_i}} + \beta_i \sum_{j \in \mathbf{B}} (\zeta_{dj} - \zeta_{rj}) \forall i \in \mathbf{G}$.

A. Solution methodology

The proposed formulation is solved by the BD technique [1]. The primal master problem aids in determining the robust variables while the dual slave problem aids in worst-case realization of the injection uncertainties. It is observed that the dual slave problem becomes unbounded as the base-point generations of the conventional generators are chosen as robust variables. To circumvent this, both optimality and feasibility cuts are used in the proposed approach.

III. Numerical Results

Effect of load and RESs uncertainty is considered with respect to OTS operational problem for standard IEEE systems (Tables I, II). The robustness of the solution obtained is verified by MCS and is found to be feasible for all the realizations within the uncertainty set.

TABLE I
Deterministic OTS and Robust OTS with load uncertainty

System (Max. u%)		IEEE 14 (70%)	IEEE 30 (10%)	IEEE 57 (5%)
Cost of generation ($)	Deterministic	16025.9	1693.27	22815.125
	Robust	16044.277	1706.56	23165.823

TABLE II
Robust OTS with load and RESs uncertainty

System	Uncertainty (u%)		Generation cost ($)	Lines which are switched off
	Pd	Pr		
IEEE 14	70	0	16031.130	1-2, 1-5, 2-5, 3-4, 6-11, 6-13, 7-9, 9-14
		50	16035.6251	1-2, 1-5, 2-5, 3-4, 6-11, 6-12, 9-14
		100	16044.27697	1-5, 2-5, 4-9, 6-13, 12-13
IEEE 57	5	0	22616.6140	4-5, 9-10, 13-14, 3-15, 4-18, 21-20, 21-22, 24-25, 27-28, 30-31, 41-43, 48-49, 49-50, 44-45, 56-41, 56-42, 57-56, 9-55
		50	22761.0281	2-3, 13-15, 1-15, 1-17, 4-18, 5-6, 10-12, 12-13, 14-15, 19-20, 24-26, 26-27, 34-32, 34-35, 37-38, 36-40, 38-44, 53-54, 11-43, 40-56, 56-42, 38-48
		100	23165.8228	9-10, 9-13, 1-15, 3-15, 24-26, 41-43, 38-44, 56-42, 38-49

References

[1] R. A. Jabr, "Robust transmission network expansion planning with uncertain renewable generation and loads,"IEEE Trans. Power Syst.,vol. 28, no. 4, pp. 4558 – 4567, Nov. 2013.

Integration of Renewable Energy Systems to Reduce Greenhouse Gas Emissions

Asim Chaulagain, Muhammad Khalil, Sejuti Fatima, Raynier Leyeza, Maisha Nasim, Muntasir Sauvik, Jason Pannell, Ramakrishna Gokaraju
Electrical and Computer Engineering, University of Saskatchewan, Sasakatoon, Canada
Email: chaulagain.asim@usask.ca, ahsan.khalil@usask.ca, sef526@mail.usask.ca, rjl048@mail.usask.ca, mnn525@mail.usask.ca, sms804@mail.usask.ca, jason.pannell@usask.ca, rama.krishna@usask.ca

***Abstract*—With recent technological advancements in energy storage systems, power production using wind and solar-based renewable energy systems has become more viable. This poster presents the integration of renewable energy systems as a power source displacing GHG intensive electricity production in Saskatchewan. For this, Federated Co-operatives Limited (FCL) facilities, which are dispersed throughout Saskatchewan, are taken as a case system. Wind and solar data from diverse parts of the province are collected and analyzed for choosing the best renewable energy systems based on geographic location. Hosting Capacity Analysis is performed in selected individual sites to ensure that the current grid can accommodate the distributed energy resources (DER). Finally, the results from the Cost-Benefit Analysis reflects the viability of integrating renewable energies at a specific location.**

Keywords—Greenhouse Gas, Grid Integration, Distributed Energy Sources, Hosting Capacity, Cost Benefit Analysis

I. INTRODUCTION

In Saskatchewan, the power is produced mostly through coal plants (about 32%). SaskPower, which is Saskatchewan's primary utility company, is taking the initiative of reducing greenhouse gas emissions by 40% by the year 2030 [1]. The utility's plan to achieve this goal is by significantly increasing renewable generation and supporting independent power producers who can host renewables and modernizing the grid (adding energy storage, HVDC interconnections to Manitoba, etc.). During the past decade, several research papers and standards have appeared explaining the grid interconnection of renewable energy sources [2]-[3]. Countries such as Australia, Denmark, Germany, UK, and some states in the USA, such as California, have adopted large amounts of solar photovoltaic generation and wind generation. However, there is a very limited amount of solar photovoltaic and wind generation currently being used in Canada except for solar PVs in Ontario. A recent work from the research group analyzing the hosting capacity of photovoltaic (PV) for a remote community in the northern part of Saskatchewan has been described in [4]. Solar PVs would provide significantly reduced power during the winter months, which creates hurdles in terms of providing a cost-benefit to the IPPs. The challenge for the western Canadian provinces with these two renewables is the inter-provincial transmission connections are weak. So the utilities would need large amounts of energy storage to support more of these two renewables sources within its jurisdiction. Putting large amounts of electrical energy storage also adds significantly to the capital cost. Limited planning studies and research literature are dealing with this subject in the Canadian context. The overarching objectives of the proposed project are, therefore, to carry out an in-depth cost-benefit analysis, hosting capacity analysis, and grid integration studies with the renewables mentioned earlier and energy storage, with primary focus to reduce GHG emission. Various sites of Federated Co-operatives Limited (FCL) in Saskatchewan are used as case-studies.

II. KEY RESULTS

TABLE I. MONTHLY POWER BILL AND CARBON EMISSION DATA

Monthly power bill of FCL Facilities	FCL Total Carbon Footprint
$285,197	2.1 kilo tonnes CO_2 / year

TABLE II. COST BENEFIT ANALYSIS (SOLAR)

System	Total Cost ($)	Total Benefit ($ bill saved / year)	Break Even (years)
25 kWh with battery	126081.63	4874.43	25.87
25 kWh without battery	97536.51	4874.43	20.00
100 kWh with battery no PGPP	292420.17	19699.69	14.80
100 kWh no battery no PGPP	178844.67	19699.69	9.1
100 kWh with PGPP	197393.42	13452.22 gained from PGPP	14.7

TABLE III. REDUCTION IN GHG EMISSION

System	Power Generation (kW/year)	Projection of GHGE reduction in 20 years
25 kWh Solar	31098	560 tonnes
100 kWh Solar	124304	2240 tonnes

III. REFERENCES

[1] 2030 Emission Reduction Goal Progressing, July. 2018.

[2] R. K. Varma, M. Salama, R. Seethapathy and C. Champion, " large-Scale Photovoltaic Solar Power Integration in Transmission and Distribution Networks", 2009 IEEE PES General Meeting.

[3] S. Narasimalu and B. Chelliah, "Integration of Energy Storage System with Renewable Energy Source," 2018 Asian Conference on Energy, Power and Transportation Electrification (ACEPT), Singapore, 2018, pp. 1-7.

[4] K. Joshi and R. R. Gokaraju, "An Iterative Approach to Improve PV Hosting Capacity for a Remote Community," 2018 IEEE Power & Energy Society General Meeting (PESGM), Portland, OR, 2018, pp. 1-5.

Learning to Solve Optimal Power Flow via Neural Decoding

Yize Chen*
*Department of Electrical Engineering, University of Washington, Seattle, USA
yizechen@uw.edu

***Abstract*—Many decision-making problems in engineering applications such as transportation, power system and operations research require repeatedly solving large-scale linear programming problems with a large number of different inputs. For example, in energy systems with high levels of uncertain renewable resources, tens of thousands of scenarios may need to be solved every few minutes. Standard iterative algorithms for linear network flow problems, even though highly efficient, becomes a bottleneck in these applications. In this work, we propose a novel learning approach to accelerate the solving process. By leveraging the rich theory and economic interpretations of LP duality, we interpret the output of the neural network as a noisy codeword, where the codebook is given by the optimization problem's KKT conditions. We propose a feedforward decoding strategy that finds the optimal set of active constraints. This design is error correcting and can offer orders of magnitude speedup compared to current state-of-the-art iterative solvers, while providing much better solutions in terms of feasibility and optimality compared to end-to-end learning approaches.**

I. Introduction

In many engineering applications, optimization programs are solved repeatedly to find real-time decisions. Among them, network flow problems form an important class and have been studied for decades with wide-ranging applications. They arise naturally in the context of transportation, networking, communication and energy systems. In many of these settings, a network flow problem takes the form of a linear program (LP). Computational challenges exist in practice. Often these challenges are due to the increased stochasticity and the low-latency requirements of real-time applications. The resource allocation process in power systems is called the optimal power flow (OPF) problem, where it takes the form of a network flow problem that minimizes the cost of power generation to satisfy the loads, subject to all of the physical network constraints (e.g., generator limits and line capacities). Typically, a linear version called DCOPF–an LP problem–is often applied in practice and solved periodically (e.g., every 5 minutes) to find the optimal operating conditions. Because of the uncertainties brought on by the renewables on many of the nodes, the number of generation and load scenarios that need to be considered are starting to grow exponentially. Despite the inherent similarity between scenarios, the OPF problem needs to be resolved. Even if each one of the LPs takes 0.1 seconds using modern solvers, not all of them can be completed within the required time period. Therefore, using machine learning to learn the mapping between variable input load profiles and the corresponding optimal generation outputs has gained significant attention, since making inference via a trained architecture can offer orders of magnitude of computational speedup compared to an iterative solver.

In this poster, we answer the question of whether a (standard) neural network can learn the solution of LP problems in the affirmative. Instead of viewing it as an end-to-end learning task, we leverage the rich algorithmic understanding of LPs as well as the economic interpretation of the primal and dual variables to offer a new solution architecture. Our workflow is shown in Figure 1. Concretely, we construct a neural network that takes the net load at each node as the input and the optimal system costs as the output. However, we do not take these outputs as the solution of the LP. Rather, using the neural network, we compute the *gradient* of the cost with respect to the net loads. Identifying these as the dual variables, we use them to predict the binding nodal and line constraints. Once these constraints are found, the optimal solutions are given by solving a simple linear system of equations. The overall procedure can be seen as an efficient surrogate learning model for optimization solvers.

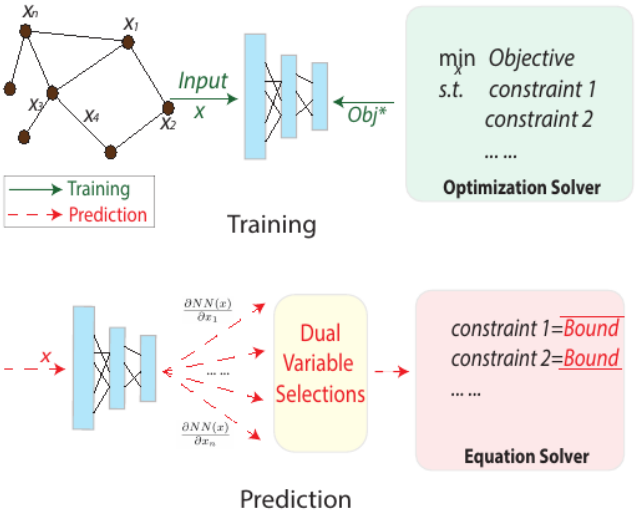

Fig. 1: The schematic of our proposed Neural Decoder for solving LP problems. During supervised training, a neural network (NN) is learned to predict the optimal objective value; during implementation for solving LP, we interpret the NN's gradient as a noisy codeword to find active constraints, and solve linear equations to get optimal solutions satisfying all constraints of original problems.

Developing Bidding Strategy for Day-Ahead Electricity Markets Using Reinforcement Learning Methods

Haotian Chen, *Student Member, IEEE* Rui Bo, *Senior Member, IEEE*
Missouri University of Science and Technology, Rolla, USA (rbo@mst.edu)

***Abstract*—This paper introduces the detailed process of applying reinforcement learning to solve market participant bidding strategy problem. The process includes the setup of market clearing environment, reinforcement learning structure. A comprehensive study demonstrates the reinforcement learning method can generate bidding strategies that achieve profits close to those from optimization methods. This study provides insights to the learning process and performance of reinforcement learning and demonstrates the performance varies with the changing condition of the environment, and tends to degrade with more complex patterns or random disturbances in the environment.**

I. INTRODUCTION

In electric markets, GENCOs submit offers to independent system operators (ISOs), and ISO clears day-ahead electricity markets by running Security Constrained Unit Commitment (SCUC), and Security Constrained Economic Dispatch (SCED). After the market clearing, ISO publishes the results to market participants including GENCOs. The results include energy clearing price and generation dispatch, which determines the revenue of the GENCOs. In fully competitive markets, GENCOs are expected to submit marginal cost as the offer price. However, in electricity markets with limited number of participants and with transmission congestions creating market power opportunities, it is possible for a GENCO to place strategic offer into the market, which may affect the cleared dispatch and/or market price and subsequently change the profits of the GENCO. GENCOs may have the incentive to develop bidding strategies in order to maximize their profit.

In the literature, optimization approaches have been developed to optimize bidding strategy based on electricity market model and forecasted information. In recent years, reinforcement learning based methods have been applied to tackle the bidding strategy problem. The advantage of this method is it does not require as much information of the market and other participants. However, it takes time to learn and it needs to have the environment to interact with ISO clearing process in order to create the learning process. Although studies have been reported on this topic, the details are lacking. This paper intends to provide a significant detail of the process for applying reinforcement learning to develop bidding strategy, and provides insightful discussion around how the performance of the reinforcement learning based method changes with the complexity of the domain problem, and the impact of different design on the performance.

II. METHODOLOGY

A. Day-ahead SCED Modelling

The goal of day-ahead SCED is to maximize hourly social welfare of the operating day, considering demand bids, generator offers and cost associated with constraint violations. This model is implemented by using C++ and CPLEX.

B. Bidding Strategy for Generators

Prior to day-ahead market clearing, market participants submit offers/bids to the market for each hour of the next operating day. Generator owners can apply bidding strategy on the offer price in the hope to influence market price, which subsequently impact the revenue and profit of the generator.

C. Reinforcement Learning Model Structure

The sequence of market clearing and reinforcement learning method for day *i* is:

1. The agent makes a decision on the offer price based on reinforcement learning method, and submit the offer to ISO;
2. ISO clears day-ahead SCED based on market participant offers and various constraints.
3. Participants compute their profit based on market clearing results;
4. The agent updates reinforcement learning model. Return to 1

III. RESULTS

In this section, episodic profits from three types of reinforcement learning methods, which are Q-Learning, Double Deep Q-Learning (DDQN) and Deep Deterministic Policy Gradient (DDPG), are compared with results from an optimization method. As shown in figure 1, the final profit from DDQN and DDPG can achieve the profit nearly as high as that from the optimization method, and significantly better than Q-learning.

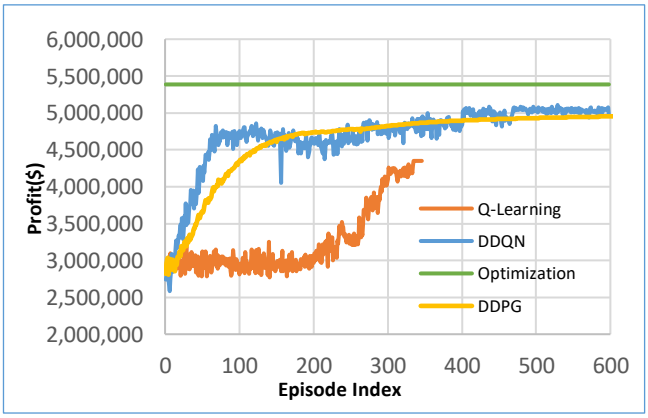

Figure 1. Episodic aggregated profit from reinforcement learning methods (Q-Learning, DDQN, DDPG) and an optimization method

Assessment of Capacitor Banks Control Practices in Distribution Systems with High PV Penetration

Vinicius C. Cunha, José Andrade, Tiago R. Ricciardi,
Fernanda C. L. Trindade, Walmir Freitas
Department of Systems and Energy
University of Campinas
Campinas, SP, Brazil
{vcunha, jcga, tiago, fernanda, walmir}@dsee.fee.unicamp.br

Rafael A. G. Rosolen, Heliton O. Vilibor
Engineering Division
CPFL Energia
Campinas, SP, Brazil
{rosolen, hdeoliveira}@cpfl.com.br

***Abstract*—This work evaluates the impact of photovoltaic (PV) generation on the operation of switched capacitor banks for an entire utility. The number of switching operations must not surpass four operations per day. In the simulations, the PV generators considered are small units installed at low voltage (LV) systems. More than 760 switched capacitor banks are assessed, where only the banks controlled by current and power factor experienced problems with the number of switching. The proposed solution for these cases is to update their control mode to reactive power, which, according to the simulation results, respects the imposed limit for all banks considering scenarios of high PV penetration. Therefore, such change in the control philosophy represents a plausible solution to counteract the effects of PV penetration increase.**

***Index Terms* — Capacitor banks, distribution systems, photovoltaic generation.**

I. Introduction

The penetration of photovoltaic generation (PV) into distribution energy systems has been increasing considerably worldwide. Although the PV generators provide several benefits, as more diversity of the energy matrix, the distribution utilities are concerned about how the presence of such generators will affect their established proceedings to plan and operate the distribution systems. Then, one topic to be evaluated refers to the switched capacitor banks operation. In this context, this work evaluates the impacts of distributed PV generation in the switched capacitor banks operation for all feeders from a Brazilian utility. The PV generators are considered to be installed at low voltage (LV) systems. The banks that experience operational problems (*i.e.*, excessive number of switching) have their control strategy altered as a simple solution to counteract the PV generation increase.

II. Capacitor Banks Characteristics

For a brief contextualization of the problem size, this utility provides energy for almost 4.5 million customers in 234 cities through 1,282 feeders. The number of capacitor banks installed by the utility corresponds to 2,037, with 60% being fixed. For the switched banks, the most common control mode is current, followed by time, power factor (PF) and reactive power (kvar). Fig. 1 presents the percentage of capacitor banks per control mode.

This work was supported in part by Sao Paulo Research Foundation (FAPESP) under Grants #2019/20186-8, #2017/10476-3, #2016/08645-9, and #2015/24448-6, in part by the National Council for Scientific and Technological Development (CNPq) under Grant #304783/2016-1 and in part by CPFL Energia under ANEEL P&D program, Grant PD-00063-3047/2018.

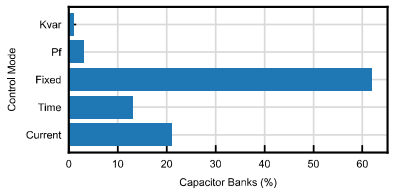

Fig. 1. Percentage of capacitor banks per control mode for all 2,037 banks from a Brazilian utility.

III. Description of the Studies and Results

The PV generators installed in the LV systems are designed to compensate the consumption of the customer, based on the net metering tariff system. The radiance curve is acquired from real measurements with 1-minute resolution. The number of generators installed is specified for each substation, ranging from 5% to 35% of the total number of customers from each substation evaluated.

The capacitor banks controlled by current and PF experienced unacceptable increase in their switching number. Fig. 2 (a) shows the statistical distribution of the number of switching operations per day in the form of boxplot for the current and PF control modes. After the change in the operational mode to reactive power, the number of switching respects the limit imposed, as shown in Fig. 2 (b).

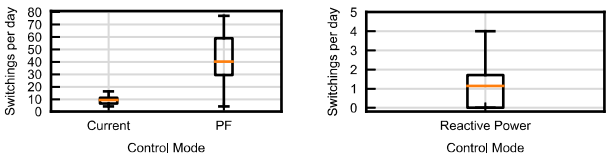

Fig. 2. Distribution of capacitor banks operations per day (a) before and (b) after the changes in the operational mode.

IV. Conclusions

This work presents an assessment of the potential impacts of PV generation in the switched capacitor banks. The results have shown that capacitor banks controlled by current and PF have surpassed the utility predefined switching limits. However, simply changing their operation mode for reactive power control guarantees the proper operation for the banks.

Cross-Market Price Difference Forecast Using Deep Learning for Electricity Markets

Ronit Das, Rui Bo, Waqas Ur Rehman, Haotian Chen, and Donald Wunsch
Department of Electrical and Computer Engineering
Missouri University of Science and Technology, Rolla USA (rbo@mst.edu)

***Abstract*—Price forecasting is in the center of decision making in electricity markets. Many researches have been done in forecasting energy prices while little research has been reported on forecasting price difference between day-ahead and real-time markets due to its high volatility, which however plays a critical role in virtual trading. To this end, this paper takes the first attempt to employ novel deep learning architecture with Bidirectional Long-Short Term Memory (LSTM) units to forecast the price difference between day-ahead and real-time markets for the same node. The raw data is collected from PJM market, processed and fed into the proposed network. The Root Mean Squared Error (RMSE) and customized performance metric are used to evaluate the performance of the proposed method. Case studies show that it outperforms the traditional statistical models like ARIMA, and machine learning models like XGBoost and SVR methods in both RMSE and the capability of forecasting the sign of price difference. In addition to cross-market price difference forecast, the proposed approach has the potential to be applied to solve other forecasting problems such as price spread forecast in DA market for Financial Transmission Right (FTR) trading purpose.**

***Index Terms*—DA/RT price difference, forecasting, Long-Short Term Memory, LSTM, electricity markets, deep learning**

I. Introduction

With the evolution of competitive deregulated power markets, forecasting of electricity prices has become a vital task for market participants: accurate prediction of short-term electricity prices is crucial for generation companies (GENCOs) to make optimal bidding strategies for participation in electricity market, and thereby get maximum profit.

II. Methodology

The data is collected from the PJM Market from 1st January till 31st December, 2016. The collected data is from both the DA and RT markets on an hourly basis. For our purpose, a generator node is chosen at random. Then price differences are calculated for the node across the DA and RT markets. In this paper, we stationarize the series by differencing [1].

The actual model used is the bi-directional variation of the Long-Short Term Memory, which is a kind of Recurrent Neural Network which can capture both long-term and short-term dependencies in the data, making is suitable for forecasting, speech recognition, etc. It was proposed by Hochreiter, et al. [2] in 1997. In a bidirectional LSTM, the input is fed in both forward and backward directions.

III. Results and Future Work

A. Results

The proposed model is compared against ARIMA, SVR and XGBoost.

TABLE I
Performance Comparison among different Forecasting Techniques

Model	RMSE ($/MWh)	Direction Accuracy (%)
ARIMA(5, 0, 1)	45.186	48.36
SVR	40.544	55.1
XGBoost	40.194	56.05
Bidirectional LSTM	32.209	57.82

Moreover, Fig.1 show in time series the cross-market price difference forecasting performance of the different models for different time windows in 2016.

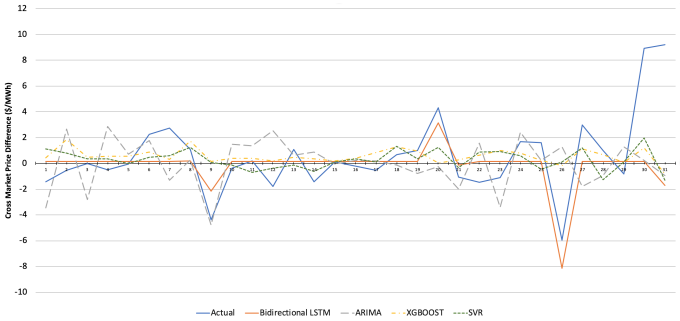

Fig. 1. Actual and forecasted cross-market price difference of different models from Oct. 26 to Oct. 27, 2016 in PJM Market

B. Future Work

This paper only deals with a univariate time series model, where one is looking at the price, or rather the price differences at different time intervals. Lastly, the proposed model currently only forecasts price difference for the next hour. It should be expanded to multi-hour (such as 24 hours in US electricity markets) to align with industry practices.

IV. Acknowledgment

This material is based upon work supported by DARPA under Grant D18AP00054, and by the U.S. Department of Energy's Office of Energy Efficiency and Renewable Energy (EERE) under the Water Power Technologies Office Award Number DE-EE0008781.

References

[1] D. A. Dickey and S. G. Pantula, "Determining the order of differencing in autoregressive processes," *Journal of Business & Economic Statistics*, vol. 5, no. 4, pp. 455–461, 1987.

[2] S. Hochreiter and J. Schmidhuber, "Long short-term memory," *Neural computation*, vol. 9, no. 8, pp. 1735–1780, 1997.

Benchmarks and Improvements in Probabilistic Solar Forecasting

Kate Doubleday, Stephen Jascourt, Vanessa Van Sycoc Hernandez, William Kleiber, and Bri-Mathias Hodge

I. Introduction

The field of probabilistic solar forecasting has grown significantly in the past few years as a variety of statistical, machine learning, and numerical weather prediction (NWP) post-processing methods have been proposed. These probabilistic forecasts can inform adaptive reserves and stochastic or robust unit commitment/economic dispatch models. However, the developing field does not yet have a consistent validation approach to compare novel methods to standard benchmark methods, which would allow easy comparison among papers. This poster shows standard implementations of common benchmark methods, then illustrates how advanced forecasting techniques outperform two of those benchmarks.

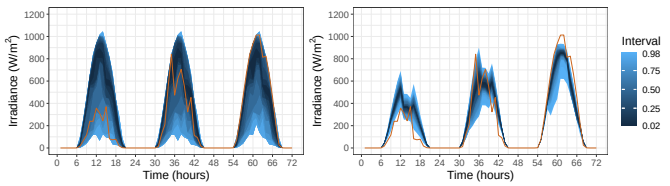

(a) (b)

Fig. 1. Example hourly-resolution benchmark forecasts for 3 spring days for the SURFRAD site in Boulder, CO using the (a) PeEn and (b) ECMWF NWP ensemble methods. The fan plots show the 1% to 99% prediction intervals of the probabilistic forecasts. The orange line shows the observed hourly average irradiance.

II. Forecast Benchmarking

A literature review of 31 probabilistic solar forecast papers showed that 8 did not include any benchmark method at all, which does not allow the reader to easily compare among papers. In the remaining papers, four common benchmark classes were used, of which two are shown in Fig. 1: (1) a persistence ensemble (PeEn) of observations from the past ∼20 days at the same time of day and (2) an NWP ensemble, shown here using the European Centre for Medium-Range Weather Forecasts (ECMWF) 51-member ensemble. These benchmarks have different characteristics: the PeEn has broad prediction intervals, while the ECMWF ensemble has very sharp intervals. The ECMWF ensemble, however, can be unreliable with the observation frequently falling outside the 98% confidence interval.

K. Doubleday, V. Van Sycoc Hernandez, W. Kleiber, and B.-M. Hodge are with the University of Colorado Boulder, Boulder, CO, 80309 USA and the National Renewable Energy Laboratory (NREL), Golden, CO 80401. S. Jascourt is with Maxar, Gaithersburg, MD 20878. This work was authored in part by NREL, operated by Alliance for Sustainable Energy, LLC, for the U.S. Department of Energy (DOE) under Contract No. DE-AC36-08GO28308. Funding provided by DOE's Office of Energy Efficiency and Renewable Energy under Solar Energy Technologies Office Agreement Number 33505. The views expressed in the article do not necessarily represent the views of the DOE or the U.S. Government.

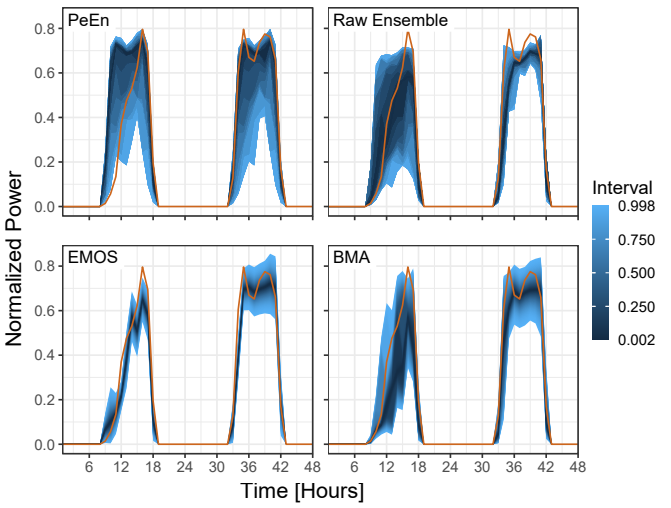

Fig. 2. 4-hour ahead power forecasts from the (clock-wise) PeEn, raw ensemble, EMOS, and BMA methods for a utility-scale (MW's) 1-axis tracking plant over two days with mixed cloudiness.

III. Advanced NWP Post-Processing

To improve upon these two benchmark approaches, two NWP ensemble post-processing methods were explored for forecasting power from utility-scale photovoltaic plants: an ensemble model output statistics (EMOS) method from the literature [1] and a novel Bayesian model averaging (BMA) [2] method tailored to solar power. EMOS fits a parametric truncated normal distribution to the ensemble, while BMA uses a mixture model that also accounts for inverter "clipping." For a utility-scale plant in Texas, Fig. 2 compares the results to the two benchmarks: EMOS and BMA are both sharper than a basic PeEn, but EMOS can err on the side of too sharp resulting in poorer reliability. BMA is can more flexibly capture uncertainty in the ensemble and can improve upon the reliability deficiencies of the raw ensemble.

[1] A. E. Raftery, T. Gneiting, F. Balabdaoui, and M. Polakowski, "Using Bayesian model averaging to calibrate forecast ensembles," *Monthly Weather Review*, 133(5): 1155–1174, 2005.

[2] Simone Sperati and Stefano Alessandrini and Luca Delle Monache, "An application of the ECMWF Ensemble Prediction System for short-term solar power forecasting," *Solar Energy*, 133: 437–450, 2016.

A Dynamic Nonlinear Model of Once-Through Boiler-Turbine Units with Superheated Steam Temperature

He Fan, *Student Member, IEEE,* Zhi-gang Su, Pei-hong Wang
School of Energy and Environment
Southeast University
Nanjing, China
phfan@seu.edu.cn, phwang@seu.edu.cn, zhigangsu@seu.edu.cn

Kwang Y. Lee, *Life fellow, IEEE*
Department of Electrical and Computer Engineering
Baylor University
Waco, TX, USA
Kwang_Y_Lee@baylor.edu

***Abstract*—With the rapid development of renewable energy in recent years, the once-through boiler-turbine (OTBT) units in China are required to improve operating flexibility in order to absorb more renewable energy integrated into the power grid. However, it is a challenge for control systems in OTBT units to provide load following capability while maintaining stable superheated steam temperature. To this end, this paper proposes a dynamic nonlinear model of the OTBT units by introducing superheated steam temperature into the model. Model structure is derived from mass and energy conservation laws by using a lumped parameter method, and parameters and functions in model structure are identified by combining optimization algorithm and running data. Validation results show that the model has acceptable dynamic accuracies as well as a clear physical structure, and, furthermore, it can be used for controller design to improve the performance of OTBT units.**

***Keywords*—Controller design, nonlinear model, once-through boiler-turbine, superheated steam temperature.**

I. INTRODUCTION

Nowadays, renewable energy in China has been developed rapidly due to its clean energy merits, but the intermittence and randomness of renewable energy pose a challenge to the stability of power grid. To reduce the negative influence, once-through boiler-turbine (OTBT) units are required to regulate the unit power frequently. However, frequent load change is not conductive to safe and economical operation of OTBT units, especially for superheated steam temperature (SST) system. To capture the essential characteristics of OTBT units, we propose a dynamic nonlinear model of OTBT units by incorporating SST into the model, where model has a clear physical structure derived from mass and energy conservation laws. Importantly, the model has satisfactory performances suitable for controller design to track load command while adjusting the SST.

II. MODEL OF OTBT UNITS

According to the mechanism analysis, model structure of OTBT units in the state-space form can be given as below:

$$\dot{x}_1 = -\frac{1}{c_0}x_1 + \frac{e^{-\tau s}}{c_0}u_1,$$

$$\dot{x}_2 = (\frac{h_{fw}-d_1}{c_1})(u_2-u_4) + (\frac{d_1-lx_3}{c_1})f(y_1,h_{st})u_3 + (\frac{lx_3-d_1}{c_1})x_5 + k_1\frac{x_1}{c_1},$$

$$\dot{x}_3 = (\frac{h_{fw}-d_2}{c_2})(u_2-u_4) + (\frac{d_2-lx_3}{c_2})f(y_1,h_{st})u_3 + (\frac{lx_3-d_2}{c_2})x_5 + k_1\frac{x_1}{c_2},$$

$$\dot{x}_4 = \frac{u_2-u_4}{c_3} - \frac{x_4}{c_3},$$

$$\dot{x}_5 = -\frac{1}{c_{sw}}x_5 + \frac{1}{c_{sw}}u_4,$$

$$\dot{x}_6 = \frac{k_2(h_{st}-h_{fw})f(y_1,h_{st})u_3}{c_5} - \frac{x_6}{c_5},$$

$$h_{fw} = h(x_2), h_{st} = lx_3 - \frac{(lx_3-h_{fw})x_5}{x_4+x_5}, c_{sw} = c_4\cdot c(u_2),$$

$$y_1 = x_2 - g(x_2),$$

$$y_2 = x_3,$$

$$y_3 = x_6,$$

$$y_4 = T(y_1,h_{st}),$$

where $[x_1, x_2, x_3, x_4, x_5, x_6]=[r_B, p_m, h_m, D_s, D_{swr}, N_e]$; $[u_1, u_2, u_3, u_4]=[u_B, D_{fw}, u_t, D_{sw}]$; $[y_1, y_2, y_3, y_4]=[p_{st}, h_m, N_e, T_{st}]$; and $h(.)$ and $T(.,.)$ are nonlinear functions.

III. VALIDATONS

TABLE I. MEAN RELATIVES ERRORS AND ROOT MEAN SQUARE ERRORS OF OUTPUT VARIABLES IN A WIDE LOAD RANGE

Index	Output variables			
	p_{st} (MPa)	h_m (kJ.kg^{-1})	N_e (MW)	T_{st} (^{o}C)
MRE(%)	0.66	0.62	0.76	0.36
RMSE	0.18	24.12	7.8	2.66

IV. CONCLUSION

The model proposed has a physical structure and is validated with a proper accuracy. The dynamic model can be used for controller design to track the load command and maintain stable superheated steam temperature.

This work is supported by National Natural Science Foundation of China (51676034).

Distributed Dynamic State Estimation in Power Systems under Cyber Attacks

Arnold Fernandes *Student Member, IEEE*, Rui Bo *Senior Member, IEEE*
Electrical and Computer Engineering Department
Missouri University of Science and Technology, Rolla MO, 65401

***Abstract*—A distributed dynamic framework for estimating the states of the power system has been presented. This framework employs distributed Kalman filters located at distributed control centers that obtain locally available measurements and state estimates from neighboring control centers. The Kalman filters then aggregate the information and obtain an estimate of the states. A linearized state-space dynamical model of a power system consisting of synchronous generators, buses and static loads has been considered along with linear measurement functions. It has been shown in the literature that Bayesian learning can be utilized to filter out Gaussian attack signals. A similar technique has been applied to secure the linearized power system.**

***Index Terms*—Distributed estimation, security, attack mitigation**

I. Introduction

With the increasing usage of phasor measurement units (PMUs) it is possible to obtain high resolution measurements. This measurement data could be given as input to the dynamic state estimator which combines the measurement information along with the power system dynamic model information to give a temporally consistent state estimate.

A distributed state estimation framework is advantageous as it reduces long distance communication, eliminates the need for a centralized state estimation algorithm, and allows for parallel computation. Attack detection and mitigation in a distributed estimation framework will be considered here.

II. Power System Dynamic Model

$$\begin{aligned}\dot{\delta}^i(t) =&\omega^i(t), \quad \dot{\omega}^i(t) = -\frac{D^i}{2H^i}\omega^i(t) + \frac{\omega_0^i}{2H^i}(P_m^i - P_e^i(t)),\\ \dot{E}_q^i(t) =& -\frac{1}{T^i}E_q^i(t) + b_0^i z_1^i(t) + b_1^i z_2^i(t) + \frac{X_q^i - X_d^i}{T^i}I_d^i(t),\\ \dot{z}_1^i(t) =&z_2^i(t), \quad \dot{z}_2^i(t) = -c_1^i z_2^i(t) - c_0^i z_1^i(t) + u^i(y^i, t)\end{aligned} \tag{1}$$

A linearized version of the aforementioned model is obtained in Equation (2) which is dicretized to give equation (3)

$$\dot{X} = AX + BU + W \tag{2}$$

$$X_k = A_d X_{k-1} + B_d U_{k-1} + W_{k-1}. \tag{3}$$

III. Distributed Kalman Filter

The measurement at the lth distributed control center (DCC) and the estimate are given by

$$Y_{k-1}^l = C^l X_{k-1}^l + V_{k-1}^l, \hat{Y}_{k-1}^l = C^l \hat{X}_{k-1}^l, \tag{4}$$

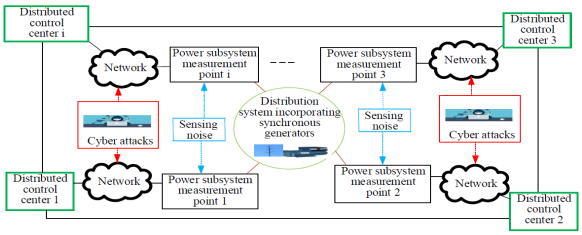

Fig. 1: Distributed Power System under Attacks

and the dynamical estimator is

$$\begin{aligned}\hat{X}_k^l =&A_d\hat{X}_{k-1}^l + B_d U_{k-1} + K_{k-1}^l\left(Y_{k-1}^l - \hat{Y}_{k-1}^l\right)\\ &+ L_{k-1}^l \sum_{m\in\mathcal{N}^l}\left(\hat{X}_{k-1}^m - \hat{X}_{k-1}^l\right).\end{aligned} \tag{5}$$

IV. Bayesian Learning

In the event that an attacker tries to inject a Gaussian attack signal $\overline{V}_k^l \sim \mathcal{N}(\mu^{al}, R^{al})$ at the lth DCC

$$Y_k^l = C^l X_k + V_k^l + \overline{V}_k^l, \tag{6}$$

variational Bayesian learning is used to estimate the attack mean $\hat{\mu}^{al}$ and attack co-variance $\hat{R}^{al}$ [1]. These values are provided to the Kalman Filter when attack is detected so that the attack is filtered out along with the noise.

V. Results and Discussion

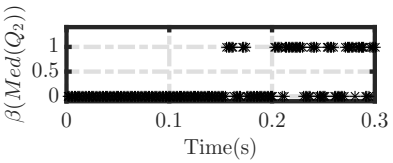

Fig. 2: Attack detection at $l = 2$

A median χ^2 detector is used to detect attacks at the DCC. Here the measurements available to DCC 2 are attacked. Once the attacks are detected Bayesian learning can be used to mitigate the attack.

References

[1] S. Zheng, T. Jiang, and J. S. Baras, "Robust state estimation under false data injection in distributed sensor networks," in *2010 IEEE Global Telecommunications Conference GLOBECOM 2010*, pp. 1–5, IEEE, 2010.

Distribution Market-Clearing and Pricing Considering Coordination of DSO and ISO: An MPEC Approach

Linbo Fu, Houhe Chen, Rufeng Zhang and Xue Li

Department of Electrical Engineering, Northeast Electric Power University, Jilin 132012, Jilin Province, China;

Email: 2201800164@neepu.edu.cn

***ABSTRACT*: Distribution-level electricity market provides a platform for trading energy and grid services from large-amount of small-scale distributed energy resources (DERs) located on distribution grids. The behavior of the DERs in the distribution electricity market may ultimately impact the market clearing and locational marginal prices (LMP) in the wholesale market. This work proposes a bi-level optimization model for distribution market clearing and distribution locational marginal pricing (DLMP) considering the interactions between distribution and transmission wholesale markets. In the proposed model, the upper-level model represents the distribution system operator (DSO) market clearing and the lower-level model represents the wholesale market-clearing by the independent system operator (ISO). The mathematical program with equilibrium constraints (MPEC) approach is applied to find the equilibria among DSO and ISO. Results show that the LMP at the substation will impact the DER dispatch, power demands of the DSO as well as the DLMP. In turn, the power demands of the DSO will further impact the ISO market and its LMPs. Using MPEC approach to clearing markets can improve the economic benefits of the distribution network.**

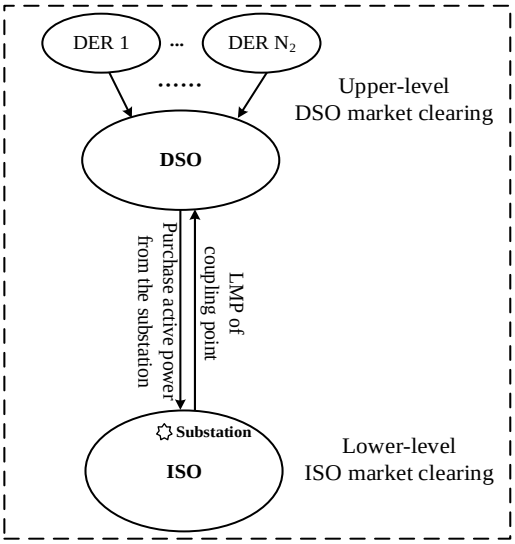

Fig.1 DSO-ISO market clearing framework

Key results:

Case 1: DSO market clearing without considering ISO market.

Case 2: DSO market clearing considering interactions with the ISO market based on the proposed MPEC model.

Figure 2 and Figure 3 verify the proposed method with the coupled PJM5 and IEEE 33 system. Table I compares the results of distribution market-clearing in Cases 1 and 2.

TABLE I DISTRIBUTION MARKET-CLEARING RESULTS OF ADN

	Case 1	*Case 2*
Power from Trans./MW	18.72	18.72
DER1/MW	24	24
DER2/MW	24	24
Total cost /$	1807.2	1732.32

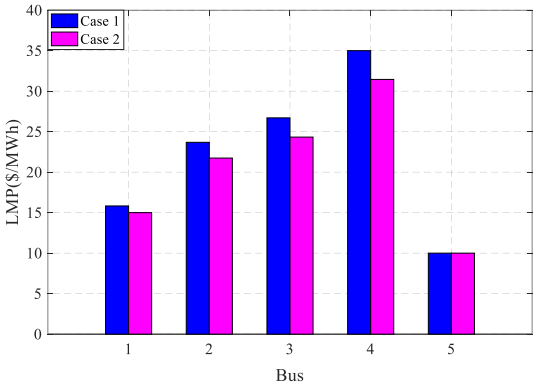

Fig.2 Comparison of LMPs in transmission system in Case 1 and Case 2

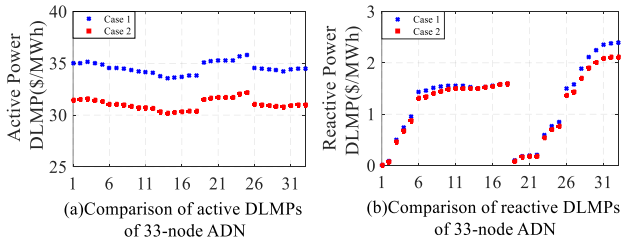

(a)Comparison of active DLMPs of 33-node ADN

(b)Comparison of reactive DLMPs of 33-node ADN

Fig.3 Comparison of DLMPs in 33-node ADN between Case 1 and Case 2

Trading of Smart Grid Data: Advantages and Challenges

Soumyajit Gangopadhyay, Sarasij Das
Department of Electrical Engineering
Indian Institute of Science
Bangalore, India
Email: soumyajitg@iisc.ac.in, sarasij@iisc.ac.in

***Abstract*—Smart grid data form the backbone of various data driven power system applications like identification of low frequency oscillation sources, instability prediction and post-mortem analysis of blackouts. Currently, the access of smart grid data is limited due to the lack of a data trading platform. Trading of smart grid data may enable proper data exchange across various entities of smart grids. This may help to exploit the beneficial uses of the data. Besides data access, trading of smart grid data has several other advantages. However, several challenges are also associated with trading of smart grid data. This paper discusses the advantages and the challenges involved in trading of smart grid data. Possible solutions are also discussed that may help to address some of the challenges.**

I. Introduction

Smart grid data mining can help in understanding the dynamics of the power system during power system disturbances along with identification of low frequency oscillation sources and instability prediction in power grids. The advantages gained from trading smart grid data are outlined below.

TABLE I
Smart Grid Data Types

Measurement data	Smart meters, EMS, DEMS, SCADA, PMU, power quality meters, disturbance recorders
Planning data	Network and generation expansion planning data
Operational data	Scheduling, congestion data
Meteorological data	Weather, GIS data
Financial data	Energy market data

II. Advantages gained

A. Increased accessibility of smart grid data

Trading of smart grid data can help to access the various types of smart grid data listed in Table I. This may help to exploit beneficial uses of the data. For example, PMU data may be used to identify the source generator responsible for low frequency oscillations in power grids. Weather forecasting data can be used along with historical energy consumption data to increase the accuracy of load forecasting.

B. Revenue generation

Trading of smart grid data shall lead to the generation of revenue. The obtained revenue can be used to install highly accurate sensors in substations. This may help in substation automation to a great extent.

C. Better data management practices

The revenue earned from trading of smart grid data can be used to improve the existing data management practices. This may in turn help to improve the quality of the data.

III. Challenges involved

A. Determining the price of data

Price of data may depend on various factors like data accuracy, completeness, measurement rate, cost of data collection, demand for the data and age of the data. Determining the influence of each of these factors on the price of data is one of the challenges associated with trading of smart grid data.

B. Balancing privacy concerns against the value of data

Privacy concerns of the data owners may limit the access of smart grid data. Addressing the privacy concerns during trading of smart grid data is a challenging task. Privacy preserving algorithms may be used to mitigate the loss of privacy. However, the value of data reduces with increasing privacy preservation. Therefore, balancing between protecting privacy of the data owners and maintaining the value of data is a tough issue. Privacy pricing may help to address this issue.

C. Ensuring security

Security is an important aspect during smart grid data trading. Proper record of the transactions need to be maintained within a secured database to increase the trust among the data buyers. Using the blockchain technology for data access control can help to ensure security.

IV. Conclusion

Advantages and challenges in smart grid data trading are outlined in this paper. Research is needed to address the challenges for successful trading of smart grid data.

A Sensitivity-based Approach to Adaptive Under-Frequency Load Shedding

Mukesh Gautam, *Student Member, IEEE*, Mohammed Benidris *Member, IEEE*,
Department of Electrical & Biomedical Engineering,
University of Nevada, Reno, Reno, NV 89557
(emails: mukesh.gautam@nevada.unr.edu, mbenidris@unr.edu)

***Abstract*—This paper proposes a Lagrange multipliers-based adaptive under-frequency load shedding (UFLS) method for frequency control in power systems. UFLS is one of key factors for frequency stability especially in stressed power grids with high penetration of renewable energy generation and deregulated electricity market. Conventional UFLS methods usually shed fixed amount of predetermined loads at predetermined locations which can lead to over or under load curtailment. This paper presents an adaptive method, based on Lagrange multipliers of power balance constraints, to determine not only the amount of the load-step to be shed but also the best locations for load shedding. This method applies a two-stage strategy for load-shedding. In the first stage, the deficit/disturbance power is computed based on the initial rate of change of frequency. In the second stage, the optimization analysis is performed so as to calculate Lagrange multipliers, which are used in the determination of the location and the amount of load-step to be shed. The proposed method is implemented on several test systems including the reduced 9-bus 3-machine Western Electricity Coordinating Council (WECC) system and the New England 39-bus 10-machine system. The results show that the proposed UFLS approach can effectively bring the system back to normal state after contingencies.**

***Index Terms*—Adaptive load shedding, frequency control, Lagrange multipliers.**

I. Introduction

Frequency stability is one the main concerns in modern power systems due to electricity market deregulation and high penetration of renewable energy sources. Frequency drop occurs usually when the generation deficit occurs in the power system. Load shedding is usually performed when the system frequency drops below predefined frequency setting. Since load shedding is performed as the last remedial action, it should be quick, able to protect system from danger state, and able to avoid unnecessary load curtailment. Conventionally, to retain the power balance in case of generation deficit, a fixed amount of predetermined load at predetermined locations is gradually shed based on frequency deviations. Semi-adaptive and adaptive approaches have been found more effective and efficient than fixed amount of predetermined load shedding at certain predetermined locations. Among these schemes, adaptive UFLS has advantage of optimizing the amount of load to be shed. Adaptive load shedding is basically performed in two steps: calculation of real deficit power in the system and distributing the deficit power on certain load-shedding steps. Therefore, a reliable and appropriate methodology that relates the sensitivity of frequency to loads to determine the size and location of load to be shed is crucial for developing an adaptive UFLS scheme.

Numerous methods have been proposed in the literature for the control of frequency instability resulting from generation deficit. Anderson and Mirheydar [1] have proposed a method for setting under-frequency relays based on the initial rate of change of frequency. An under-frequency load shedding scheme for islanded microgrids, which is not only independent of the microgrid parameters but also considers power generation variations during the process has been proposed in [2]. Although numerous adaptive UFLS schemes for determination of deficit/disturbance power have been documented in the literature, determination of the locations and sizes of load-shedding steps simultaneously using sensitivity based approach has not been given much attention. The work proposed in [3] determines the location and step size of load shedding based on the frequency sensitivity of the loads which does not count for the change in Lagrange multipliers of power balance constraints. This paper uses Lagrange multipliers to capture the impact of power balance constraints on the power balance.

This paper proposes an adaptive method for the frequency control of power system that sheds the optimal amount of loads at optimal locations. A two-stage strategy is implemented for the adaptive load shedding. In the first stage, the deficit/disturbance power is calculated based on the rate of change of frequency. In the second stage, deficit powers calculated in first stage are distributed based on Lagrange multipliers of the power balance constraints to determine the location and amount of load to be shed. Therefore, the proposed method simultaneously determines the locations and amounts of load-shedding steps. The proposed approach is applied on several systems including the reduced Western Electricity Coordinating Council (WECC) system and the New England 39 bus. The results show that the proposed UFLS approach can effectively bring the system back to normal state after contingencies.

References

[1] P. Anderson and M. Mirheydar, "An adaptive method for setting under-frequency load shedding relays," *IEEE Transactions on Power Systems*, vol. 7, no. 2, pp. 647–655, May 1992.

[2] A. Ketabi and M. Fini, "An underfrequency load shedding scheme for islanded microgrids," *International Journal of Electrical Power & Energy Systems*, vol. 64, pp. 599–607, November 2014.

[3] C. P. Reddy, S. Chakrabarti, and S. C. Srivastava, "A sensitivity-based method for under-frequency load-shedding," *IEEE Transactions on Power Systems*, vol. 29, no. 2, pp. 984–985, March 2014.

A data-driven policy design for addressing the ramping product nodal deliverability issue in real-time markets

Mohammad Ghaljehei, *Student Member,IEEE,* and Mojdeh Khorsand, *Member, IEEE*
School of Electrical, Computer, and Energy Engineering, Arizona State University, Tempe, AZ 85287, USA
Email: mghaljeh@asu.edu *and* mojdeh.khorsand@asu.edu

New resource mix, e.g. renewable resources, are imposing operational complexities to modern power systems by intensifying uncertainty and variability in the system net load. The intensified uncertainty and variability lead to a significant need for ramp capabilities as illustrated by the "duck curve" of the California independent system operator (CAISO) [1]. In the case of insufficient ramp capabilities in the system, the power balance violation will occur, which can not only jeopardize the system's reliability, but can also cause high penalty prices during the real-time (RT) market processes and consequently create market inefficiency in the long run [2]. To address this issue, some ISOs, e.g., CAISO and Midcontinent ISO (MISO), have been augmenting their operating markets with flexible ramping products (FRPs) in order attain higher responsiveness from the existing flexible resources to meet the net load's variability and uncertainty.

Since the FRP requirement policies proposed from industry are based on the proxy system wide or zonal requirements, there is no guarantee that FRPs, which are procured by the market, will actually be deliverable without violating transmission line limits. The reason can simply be associated with the fact that the deliverability for the post-deployment of FRPs within transmission limits is disregarded when making decision on the FRPs allocation.

More advanced techniques to deal with the uncertainty imposed to the power system include, but are not limited to, (i) stochastic programming, wherein the uncertainties are explicitly represented and simultaneously solved in the model [3] and (ii) robust optimization, which mitigates worst-case consequences [4]. The ISOs in U.S. do not utilize the stochastic programming and the robust optimization for the generation scheduling since (i) these approaches are complex and computationally challenging for the large-scale operational scheduling models [5], and (ii) pricing and market settlements of markets based on these approaches are not well-acceptable by stakeholders.

Therefore, an approach is desirable in this situation that can create a proper balance between decisions efficiency (i.e., deliverability of FRP awards) and complexity, while being practically implementable. As the system operation can be considerably improved by exploiting the statistical information of the scenarios, the focus of this paper is to integrate data-mining techniques and enhanced FRP requirement policies in a holistic way without disrupting the existing practices and compromising computational efficiency.

In this paper, in order to address the post-deployment deliverability of FRPs, a computationally tractable dynamic policy is proposed for FRPs awarded in fifteen-minute market (FMM), which improves upon the existing industry models (as shown in Fig. 1). The key idea is to allocate the FRPs to the flexible resources that can effectively deploy their ramping capabilities in the corresponding locations when needed without violating transmission line limits. To do so, the proposed approach uses data-mining algorithms to specify response factors for a set of generators that have higher responsiveness given a set of ramping events. Furthermore, the impacts of the FRPs post-deployment on the transmission line flows are predicated so that the ramp capabilities are allocated to the locations that are potentially deliverable. Finally, the performance of the enhanced FMM market model, modified to include the proposed FRP policy design, is compared against FMM market model with CAISO's FRP design through a validation methodology. This validation methodology mimics RT unit commitment (RTUC) of CAISO's FMM.

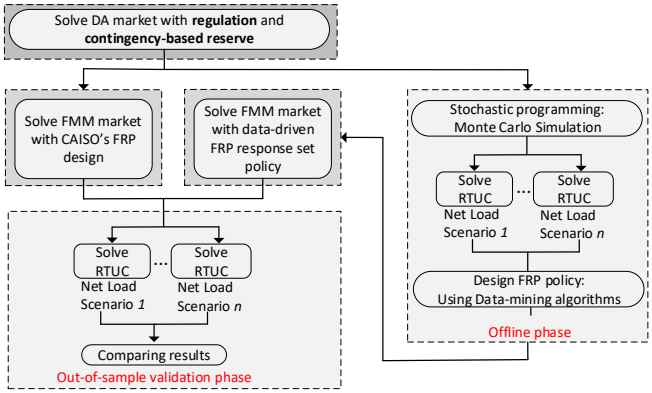

Fig. 1. Flowchart of the proposed data-driven FRP policy.

REFERENCES

[1] CAISO, "What the duck curve tells us about managing a green grid," 2016.www.caiso.com/Documents/FlexibleResourcesHelpRenewables_FastFacts.pdf.

[2] N. Navid and G. Rosenwald, "Market Solutions for Managing Ramp Flexibility With High Penetration of Renewable Resource," *IEEE Transactions on Sustainable Energy*, vol. 3, no. 4, pp. 784–790, Oct. 2012, doi: 10.1109/TSTE.2012.2203615.

[3] J. M. Morales, A. J. Conejo, and J. Perez-Ruiz, "Economic Valuation of Reserves in Power Systems With High Penetration of Wind Power," *IEEE Transactions on Power Systems*, vol. 24, no. 2, pp. 900–910, May 2009, doi: 10.1109/TPWRS.2009.2016598.

[4] C. Zhao, J. Wang, J.-P. Watson, and Y. Guan, "Multi-Stage Robust Unit Commitment Considering Wind and Demand Response Uncertainties," *IEEE Transactions on Power Systems*, vol. 28, no. 3, pp. 2708–2717, Aug. 2013, doi: 10.1109/TPWRS.2013.2244231.

[5] M. Doostizadeh, F. Aminifar, H. Ghasemi, and H. Lesani, "Energy and Reserve Scheduling Under Wind Power Uncertainty: An Adjustable Interval Approach," *IEEE Transactions on Smart Grid*, vol. 7, no. 6, pp. 2943–2952, Nov. 2016, doi: 10.1109/TSG.2016.2572639.

A comprehensive method to analyze power system resilience to extreme weather

Anwesha Ghorai, *Student Member, IEEE* and Mojdeh Khorsand, *Member, IEEE*
School of Electrical, Computer, and Energy Engineering, Arizona State University, Tempe, AZ 85287, USA
Email: aghorai1@asu.edu and mojdeh.khorsand@asu.edu

Severe weather is considered as the leading cause of power system outages in the United States. As per the reports from the Electric Power Research Institute (EPRI), Lawrence Berkeley National Laboratory (LBNL), and U.S. Department of Energy (DOE) [1], there is an estimated loss of $30 -$400 billion per year due to these events. The change in weather pattern as well as shift of energy resources from conventional fossil fuel units to intermittent renewable resources increase the necessity of quantifying system performance in response to extreme events. The concept of reliability in power systems has been extensively researched; however, the notion of power system resilience to low probability, high impact scenarios has not been explored extensively. The first definition of resilience was given by [2] as the system competency to sustain instabilities without itself deteriorating to it, has been perceived by different other disciplines like Economy, Social, Medical sciences [3-4]. A more formal explanation of a resilient power grid is given by Federal Energy Regulatory Committee (FERC) as the "the ability to withstand and reduce the magnitude and/or duration of disruptive events, which includes the capability to anticipate, absorb, adapt to, and/or rapidly recover from such events" [5]. Several methodologies have been proposed to measure the grid resilience in terms of discrete metrics. A critical dimension of the resilience, which is to quantify it based on a time dependent approach considering different phases of power system response to a severe weather, has been introduced in [6].

Majority of these prior work rely on steady state analysis of power to assess power system resilience to extreme events. However, power system response during extreme events need to be evaluated from its dynamic response perspective, which is governed by various control and protection assets responses. Adequate analysis of system behaviour during extreme events requires proper and simultaneous assessment of both protection scheme behaviour and dynamic characteristics. Analysis that is conducted with inadequate consideration of these two aspects may result in an inaccurate assessment of system behaviour. This work proposes a framework to evaluate system resilience while considering both transient stability as well as steady state response. An overview of the proposed method is shown in Figure 1.

The weather profile of the hurricane data is outlined with the fragility curve in order to obtain the failure probability as a function of weather intensity for each transmission line. Monte Carlo Simulation is used to identify the status of lines as a binary, i.e., '1' meaning the line is on and '0' meaning the line is tripped, based on the failure probability. After this, the system might become unstable due to line outages; thus, it is essential to evaluate stability of power system via TDS while including protection systems. The settings of protection devices are chosen according to the North American Electric Reliability Corporation (NERC) Protection and Control (PRC) standards. This paper considers distance relays, underfrequency load shedding (UFLS), undervoltage load shedding relays (UVLS), and under frequency generator tripping as the protection models. Moreover, steady state response of power system is evaluated using AC Optimal Power Flow (ACOPF). The objective function for ACOPF is minimizing amount of load shedding happening at each simulation step. In this paper, percentage of load shed for the operational resilience and number of online transmission lines for the infrastructure resilience are taken as the resilience indicators and resilience metrics are calculated based on the results of TDS and ACOPF. The proposed algorithm is tested on the IEEE 145 test system using PSSE Software tool.

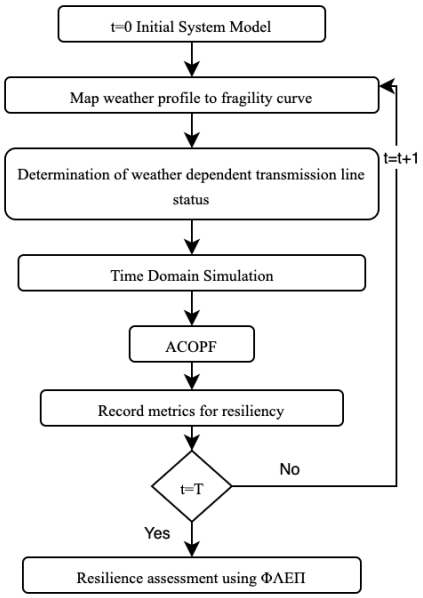

Fig.1. The proposed approach

REFERENCES

[1] Anya Castillo, "Risk analysis and management in power outage and restoration: A literature survey," *Electric Power Systems Research*, vol.107, pp 9-15, 2014.

[2] C. S. Holling, "Resilience and stability of ecological systems," *Annu. Rev. Ecol. Systematics*, vol. 4, pp. 1–23, 1973.

[3] W. Neil Adger, "Social and ecological resilience: Are they relate" *Progr. Human Geography*, vol. 24, pp. 347–364, 2000.

[4] A. Rose, "Economic resilience to natural and man-made disasters: Multi- disciplinary origins and contextual dimensions," *Environ. Hazards*, vol. 7, no. 4, pp. 383-398, 2007.

[5] Federal Energy Regulation Committee, *Grid Resilience in RTOs/ISOs*, June 2018.

[6] M. Panteli, P. Mancarella, D. N. Trakas, E. Kyriakides and N. D. Hatziargyriou, "Metrics and Quantification of Operational and Infrastructure Resilience in Power Systems," *IEEE Trans. Power Syst.*, vol. 32, no. 6, pp. 4732-4742, Nov. 2017.

Coordinated Wide-Area Control of Multiple Controllers in a Power System Embedded with HVDC Lines

Pooja Gupta
Arizona State University, USA

Anamitra Pal
Arizona State University, USA

Vijay Vittal
Arizona State University, USA

***Abstract*—This abstract assesses the stability improvements that can be achieved through the coordinated wide-area control of power system stabilizers (PSSs), static VAr compensators (SVCs) and supplementary damping controllers (SDCs) for damping low frequency oscillations (LFOs) in a power system embedded with multiple high voltage DC (HVDC) lines. The improved damping is achieved by designing a coordinated wide-area damping controller (CWADC) that employs partial state feedback. The design methodology uses a linear matrix inequality (LMI)-based mixed H_2/H_∞ control with regional pole-placement that is robust for multiple operating scenarios. To reduce the high computational burden, an enhanced version of selective modal analysis (SMA) is employed that reduces the number of required wide-area PMU feedback signals. The studies are performed on a 29 machine, 127 bus equivalent model of the Western Electricity Coordinating Council (WECC) system-embedded with two HVDC lines.**

***Index Terms*—Coordinated Wide-Area Damping Controller (CWADC), Linear Matrix Inequality (LMI), Polytopic Control.**

I. Introduction

Low frequency oscillations (LFOs) are recognized as one of the most challenging problems in electric grids, that can result into system instability and limit power transfer capability. Traditionally, LFO damping is provided by PSSs installed at generator units. But they have to be carefully coordinated to damp both local and inter-area modes. HVDC systems that are primarily used for power delivery, can rapidly alter their power flows to enhance the damping of these modes. Additionally, many other approaches have been attempted to improve the damping of inter-area modes using the coordinated wide-area controllers [1], [2], however, a thorough investigation using detailed control models was not performed.

Addressing some of the issues identified in [2], the key contributions of this work are: a) evaluation of the improvement in small-signal stability that HVDC based SDC (DC-SDC) can achieve, b) use of detailed dynamic models of control devices such as PSSs and SVCs to accurately determine the interactions between the controls and the network, c) development of a robust coordinated wide-area damping controller (CWADC) for a reduced-order polytopic system using LMI-based mixed H_2/H_∞ control with partial state feedback and regional pole placement constraints, d) systematic study of the impact of communication delays on the proposed approach and, e) identification of alternate feedback signals for CWADC.

II. Development of Coordinated Control

The state-space model of the system corresponding to an operating condition (OC) posed with polytopic H_2/H_∞ formulation is:

$$\begin{aligned} \dot{x} &= Ax + B_1 w + B_2 u \\ z_\infty &= C_1 x + D_{11} w + D_{12} u \\ z_2 &= C_2 x + D_{22} u \\ y &= C_y x + D_{y1} w + D_{y2} u \end{aligned} \tag{1}$$

where x is the state of system, u is the control, w is the disturbance, y is the output, z_2 and z_∞ are control signals for H_2 and H_∞ optimizations, respectively. The control law for the LMI polytopic controller with gain matrix, $K_{LMI-poly}$, is given by $u = K_{LMI-poly} x_l$, where

$$K_{LMI-poly} = \begin{bmatrix} K_{11} & K_{12} & K_{13} & .. & K_{1l} \\ K_{21} & K_{22} & K_{23} & .. & K_{2l} \\ .. & .. & .. & .. & .. \\ K_{i1} & K_{i2} & K_{i3} & .. & K_{il} \end{bmatrix} \tag{2}$$

where x_l denotes the reduced number of states obtained using the enhanced SMA, while i signifies the number of controls present in the system.

III. Preliminary Results

To investigate the impact of proposed controller, a set of three different OCs for a 29 machine, 127 bus WECC system (with multiple controllers) is created: a) base case, b) increase in load at bus 6 by 25 MW and, c) increase in load at bus 55 by 50 MW. Modal analysis of the system at each of the three vertices (OCs) of polytope reveals multiple modes with poor damping ($< 5\%$). Fig. 1, provides the result of the application of the LMI control designed for a single polytopic system. All modes have attained minimum damping of more than 15%.

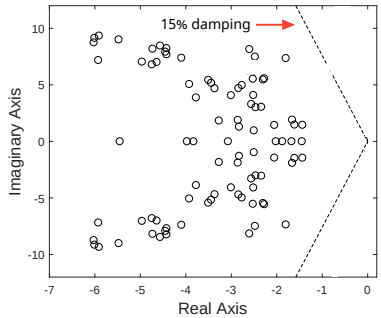

Fig. 1. LMI control for 29 machine,127 bus system.

References

[1] T. Wang, A. Pal, J. S. Thorp, and Y. Yang, "Use of polytopic convexity in developing an adaptive interarea oscillation damping scheme," *IEEE Trans. Power Syst.*, vol. 32, no. 4, pp. 2509–2520, 2017.

[2] P. Gupta, A. Pal, C. Mishra, and T. Wang, "Design of a coordinated wide area damping controller by employing partial state feedback," in *PES General Meeting (Atlanta)*, pp. 1–5, IEEE, 2019.

Development and Validation of Models to Assess Dynamic Response of Converter-Dominated Power Systems Across Multiple Spatiotemporal Scales

Nischal Guruwacharya†, Ujjwol Tamrakar, Timothy M. Hansen, and Reinaldo Tonkoski
Department of Electrical Engineering and Computer Science
South Dakota State University
Brookings, South Dakota, USA 57007

***Abstract*—In order to satisfy future electricity demand from renewable energy sources such as wind and photovoltaics, a significant amount of converter-based generation is being integrated into a bulk power grid. The dynamics of such converter systems can no longer be ignored as before. So, a data-driven, black-box approach is used to model the dynamics of a power electronic converter. System identification tools are used to identify the dynamic models. The different linear transfer function models thus obtained are combined through a statistical approach to derive a generalized non-linear model that captures the most significant inverter dynamics.**

I. Introduction

With a growing interest in renewable energy and batteries, power electronic converters are becoming a crucial part of power distribution networks [1]. As the future energy demand is met by converter-based generation, models that accurately represent the interaction between the grid and the converters are essential. To accurately model power electronic converters, one needs to have detailed knowledge of various aspects of a converter such as its physical topology, the complex models of the various voltage/current control loops, the models of the phase-locked-loop, the protection-scheme employed, etc.

Power electronic converters can operate in different states based on the operating conditions of the grid. The dynamic behavior of the converter under each of these operating states can be significantly different. The dynamics of the switching converters are modeled in a partitioned manner. The partitions are based on their operating states and are captured by looking into the input-output characteristics of the converter. This segmentation divides the system into several simpler linear models, which in combination covers most of the significant converter dynamics. Markov switching techniques are used to capture a wide array of system dynamics by switching between different states.

Developing detailed mathematical models to capture the inherent dynamic characteristics of aggregated power systems is critical to study power system reliability. Model reduction techniques (i.e., dominant pole, Routh-Pade, and Schur approximations) are used to obtain reduced order models that trade-off accuracy and computational complexity of the transient performance parameters. The reduced order models of the frequency domain are then converted into time domain representation for the analytical computation of transient performance parameters. The main focus is on designing reduced order models for the aggregated power systems model that accurately estimate system metrics such as the frequency nadir, the rate-of-change-of-frequency, and the settling time of frequency.

II. Key Figures

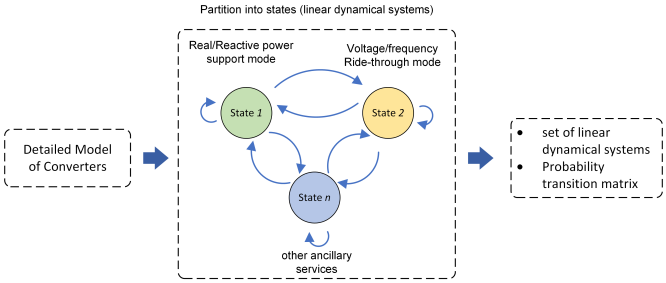

Fig. 1: Partitioned modeling of converters.

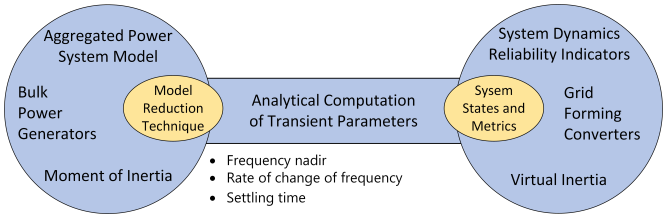

Fig. 2: Description of the model reduction process.

III. Conclusions and Future Work

A data-driven, black-box model for a grid-connected power electronic converter was developed from the logged dataset of grid voltage and current supplied by the inverter. In the future, the dynamics of the inverter under several operating conditions defined by the IEEE 1547 standard will be explored and combined to captures the most significant dynamics of the inverter. In addition, we will focus on designing reduced order models that accurately estimate system metrics.

References

[1] R. H. Byrne, T. A. Nguyen, D. A. Copp, B. R. Chalamala, and I. Gyuk, "Energy management and optimization methods for grid energy storage systems," *IEEE Access*, vol. 6, pp. 13 231–13 260, 2018.

Real-Time Overload Detection Algorithm with Combined Learning and Analytical Model

Fouad Hasan, *Student Member, IEEE,* Amin Kargarian, *Senior Member, IEEE*

***Abstract*—Reliable operation of the electric power system highly depends on a transmission network that is immune to mixed type contingencies and immediate actions against those contingencies. Operators run optimal power flow (OPF) in every 5-10 minutes resolution to determine transmission flow and to investigate any prospective overload in the system. However, for large scale systems, it becomes computationally costly and intractable. This paper presents a combined machine learning and analytical model-based scheme to make an early prediction of line congestion. The proposed method does not require solving OPF to determine branch loading that makes it suitable for real-time management of overload. Numerical results on the EPRI 39-bus system, IEEE 57-bus system, and the IEEE 118-bus system show the effectiveness of the proposed algorithm.**

I. Learning-Based Branch Flow Calculation

Key Equations:

Gen. Prediction: $\tilde{P}_g = \left[\tilde{p}_{g1}, \tilde{p}_{g2}, \tilde{p}_{g3} \cdots \tilde{p}_{gn}\right]^T \quad \forall n \in n_g$

Normal flow: $PL = SF \times K_P.\tilde{P}_g - K_D.P_d$

Cont. flow: $PL_l^C = PL_l + LODF_{l,k} \times PL_k$

$$Pre-contingency\ Loading\% = \frac{|PL|}{|PL_{max}|} \times 100$$

$$Post-contingency\ Loading\% = \frac{|PL^c|}{|PL_{max}^c|} \times 100$$

The branch flow state is classified into five classes, as shown in Table I.

TABLE I

Security class	Line loading (%)
Low risk	$PL \leq 25\%$
Normal	$25\% < PL \leq 50\%$
Alert	$50\% < PL \leq 75\%$
Emergency	$75\% < PL \leq 95\%$
Congested (or overloaded)	$PL > 95\%$

Figure 1 shows the promising accuracy of the proposed algorithm for early congestion/overload forecast during normal and contingency situations.

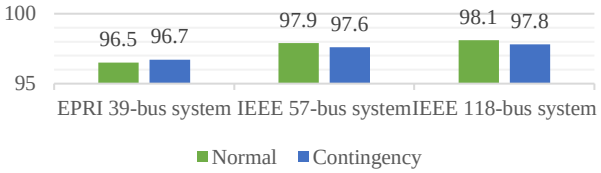

Fig. 1. Overall accuracy of classification by the combined algorithm.

As shown in Fig. 3, there is no mis-grouping with a multi-step jump (e.g., "Emergency" lines predicted to be in the "Low risk" category). An operator needs some actions if lines are either in emergency or congested zones. Other misclassifications are not crucial as loading conditions are in a safe operating zone.

II. Linear Sensitivity-Based Learning Algorithm

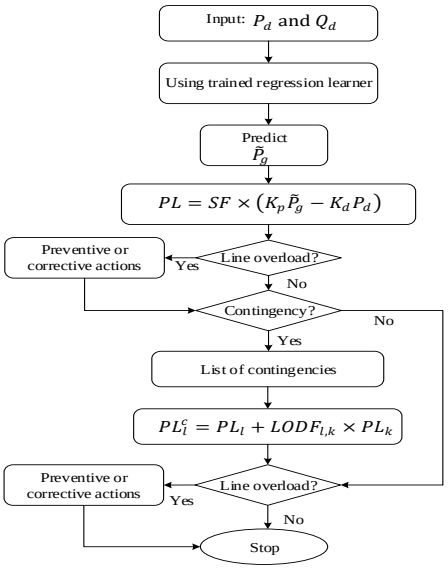

Fig. 2. Flowchart of the proposed algorithm.

III. Findings: Confusion Matrix of IEEE 118 System

		True state				
		Low	Normal	Alert	Emergency	Congested
Predicted state	Low	153599 82.6%	825 0.4%	0	0	0
	Normal	1228 0.7%	17735 9.5%	301 0.2%	0	0
	Alert	0	92 0.0%	7512 4.0%	16 0.0%	0
	Emergency	0	0	109 0.1%	3566 1.9%	3 0.0%
	Congested	0	0	0	1000 0.5%	14 0.0%
TPR		99.2%	95.1%	94.8%	77.8%	82.4%
		Accuracy=98.1%, Misclassification=1.9% **(IEEE 118-bus)**				

(a)

		True state				
		Low	Normal	Alert	Emergency	Congested
Predicted state	Low	152766 82.1%	626 0.3%	0	0	0
	Normal	2037 1.1%	17875 9.6%	362 0.2%	0	0
	Alert	0	86 0.0%	7253 3.9%	12 0.0%	0
	Emergency	0	0	410 0.2%	4010 2.2%	1 0.0%
	Congested	0	0	0	547 0.3%	15 0.0%
TPR		98.7%	96.2%	90.4%	87.8%	93.8%
		Accuracy=97.8%, Misclassification=2.2% **(IEEE 118-bus)**				

(b)

Fig. 3. Prediction accuracy of line flow classification during a) normal and b) contingency IEEE 118-bus system.

Real-Time Overload Detection Algorithm with Combined Learning and Analytical Model

Fouad Hasan, *Student Member, IEEE,* Amin Kargarian, *Senior Member, IEEE*

***Abstract*—Reliable operation of the electric power system highly depends on a transmission network that is immune to mixed type contingencies and immediate actions against those contingencies. Operators run optimal power flow (OPF) in every 5-10 minutes resolution to determine transmission flow and to investigate any prospective overload in the system. However, for large scale systems, it becomes computationally costly and intractable. This paper presents a combined machine learning and analytical model-based scheme to make an early prediction of line congestion. The proposed method does not require solving OPF to determine branch loading that makes it suitable for real-time management of overload. Numerical results on the EPRI 39-bus system, IEEE 57-bus system, and the IEEE 118-bus system show the effectiveness of the proposed algorithm.**

I. Learning-Based Branch Flow Calculation

Key Equations:

Gen. Prediction: $\tilde{P}_g = \left[\tilde{p}_{g1}, \tilde{p}_{g2}, \tilde{p}_{g3} \cdots \tilde{p}_{gn}\right]^T \quad \forall n \in n_g$

Normal flow: $PL = SF \times K_P.\tilde{P}_g - K_D.P_d$

Cont. flow: $PL_l^C = PL_l + LODF_{l,k} \times PL_k$

$$Pre-contingency\ Loading\% = \frac{|PL|}{|PL_{max}|} \times 100$$

$$Post-contingency\ Loading\% = \frac{|PL^c|}{|PL_{max}^c|} \times 100$$

The branch flow state is classified into five classes, as shown in Table I.

TABLE I

Security class	Line loading (%)
Low risk	$PL \leq 25\%$
Normal	$25\% < PL \leq 50\%$
Alert	$50\% < PL \leq 75\%$
Emergency	$75\% < PL \leq 95\%$
Congested (or overloaded)	$PL > 95\%$

Figure 1 shows the promising accuracy of the proposed algorithm for early congestion/overload forecast during normal and contingency situations.

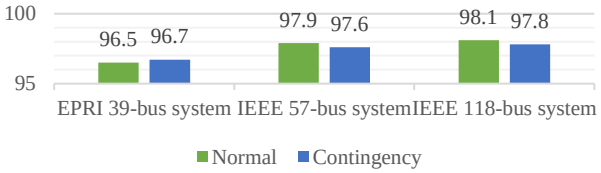

Fig. 1. Overall accuracy of classification by the combined algorithm.

As shown in Fig. 3, there is no mis-grouping with a multi-step jump (e.g., "Emergency" lines predicted to be in the "Low risk" category). An operator needs some actions if lines are either in emergency or congested zones. Other misclassifications are not crucial as loading conditions are in a safe operating zone.

II. Linear Sensitivity-Based Learning Algorithm

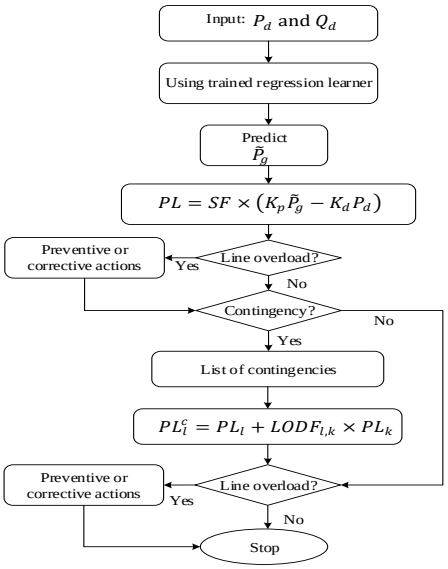

Fig. 2. Flowchart of the proposed algorithm.

III. Findings: Confusion Matrix of IEEE 118 System

		True state				
		Low	Normal	Alert	Emergency	Congested
Predicted state	Low	153599 82.6%	825 0.4%	0	0	0
	Normal	1228 0.7%	17735 9.5%	301 0.2%	0	0
	Alert	0	92 0.0%	7512 4.0%	16 0.0%	0
	Emergency	0	0	109 0.1%	3566 1.9%	3 0.0%
	Congested	0	0	0	1000 0.5%	14 0.0%
TPR		99.2%	95.1%	94.8%	77.8%	82.4%
		Accuracy=98.1%, Misclassification=1.9% **(IEEE 118-bus)**				

(a)

		True state				
		Low	Normal	Alert	Emergency	Congested
Predicted state	Low	152766 82.1%	626 0.3%	0	0	0
	Normal	2037 1.1%	17875 9.6%	362 0.2%	0	0
	Alert	0	86 0.0%	7253 3.9%	12 0.0%	0
	Emergency	0	0	410 0.2%	4010 2.2%	1 0.0%
	Congested	0	0	0	547 0.3%	15 0.0%
TPR		98.7%	96.2%	90.4%	87.8%	93.8%
		Accuracy=97.8%, Misclassification=2.2% **(IEEE 118-bus)**				

(b)

Fig. 3. Prediction accuracy of line flow classification during a) normal and b) contingency IEEE 118-bus system.

Impact of Imbalance Settlement System Design on a Risk-Averse Aggregator of Flexible Demand Side Resources

Lars Herre
School of Electrical Engineering and Computer Science
KTH Royal Institute of Technology, 10044 Stockholm, Sweden
Email: lherre@kth.se

***Abstract*—To maintain power balance, system operators have designed a spectrum of ancillary services acting on different time scales to maintain the frequency at its nominal value. In balancing markets, balance responsible parties can sell or buy additional energy. The system aims to minimize the real-time deviation of a balance responsible party from their day-ahead position. Real-time imbalance is today settled in different ways depending on the specific regulations. However, the design of the imbalance settlement system can have a high impact on the bidding strategy of a balance responsible party. In this paper, the bidding strategy of a balance responsible party under different imbalance settlement system designs is modeled. Specifically, the risk-aversion of a balance responsible party managing an aggregation of flexible loads under uncertainty and the impact on its profitability as well as overall power system balancing is investigated.**

***Index Terms*—demand side management, energy arbitrage, imbalance settlement, risk management.**

I. Introduction

To maintain power balance, system operators have designed a variety of ancillary services acting on different time scales to maintain the frequency at its nominal value. This is to ensure balance by penalizing the real-time deviation of a balance responsible party (BRP) from their day-ahead position. Real-time imbalance is today settled in different ways depending on the specific regulations. The design of the imbalance settlement system can have a high impact on the bidding strategy of actors.

In the Nordic Electricity Market (Nord Pool AS [1]), the imbalance is calculated by eSett OY [2] and broadcast ex-post. Therefore, a BRP such as an aggregator of flexible controllable loads, does not know the imbalance settlement price before the decision about the real-time consumption is made.

In some countries, a *one-price imbalance settlement system* is used, where the BRP benefits if it helps the system. For instance, a BRP would benefit from less consumption than the day-ahead bid at times when the system is up-regulating the supply side, or from more consumption when the system is up-regulating the supply side.On the other hand, when the BRP does not help the system, a disadvantageous imbalance settlement price results in a loss for the BRP. Other countries use a *two-price imbalance settlement system*, where the BRP can never make a profit from being in imbalance. If the BRP helps the direction of system up-or down-regulation, then then same price as the day-ahead price is used. If it does not help the system, a disadvantageous imbalance settlement price results in a loss for the BRP.

These two imbalance settlement systems can result in different day-ahead bidding strategies, as it is shown in this paper. The BRP faces uncertainty from imbalance settlement prices and needs to take an optimal decision on the day-ahead in a given imbalance settlement system. Furthermore, the risk-aversion of the BRP is an important parameter that affects the bidding strategy and the expected profits. A risk-averse BRP would expect lower profits, and be less prone to risk, whereas a risk-taking BRP can expect higher profits while taking higher risk. From another perspective, the type of imbalance settlement system also affects the risk-aversion of a BRP that wants to keep its conditional value at risk (CVaR) constant.

Today, in some markets like Sweden, a producer's imbalance is calculated by a two-price system while a consumer's imbalance is calculated by a one-price system. This means that consumers *can* profit from being in imbalance. A consuming BRP with flexible controllable loads can therefore strategically arbitrage energy between the day-ahead market and the imbalance settlement given perfect price information. Since price forecasts are uncertain, a risk-averse bidding strategy can support the BRP to maximize the expected profits. The cost minimization problem of the risk-averse aggregator under uncertainty is modeled with

$$\begin{aligned}
&\text{min.} && (1-\beta)\cdot\mathbb{E}\left[c_\omega\right]+\beta\cdot\text{CVaR} && \text{(1a)}\\
&\text{s.t.} && \text{Cost and revenues} && \text{(1b)}\\
& && \text{Electric power \& energy constraints} && \text{(1c)}\\
& && \text{Risk-aversion} && \text{(1d)}
\end{aligned}$$

II. Key Take-Aways

The uncertainty from prices has a major impact on the bidding strategy of the BRP. Different degrees of risk-aversion are analyzed. It is found that the yearly mean of expected profits is higher in a one-price imbalance settlement system.

References

[1] Nord Pool AS, "Historic Market Data," October 2018. [Online]. Available: http://www.nordpoolspot.com/historical-market-data/

[2] eSett Oy Settlement Service, "Nordic Imbalance Settlement," 2018. [Online]. Available: https://www.esett.com/

Computationally Efficient Formulations for Fault Isolation and Service Restoration in Distribution Systems

Mohammad Mehdi Hosseini, Masood Parvania
Department of Electrical and Computer Engineering, University of Utah, Salt Lake City, UT 84112
Emails: {mehdi.hosseini, masood.parvania}@utah.edu

***Abstract*—This paper proposes two computationally efficient mixed integer optimization models, in quadratic-constrained (QC) and linear forms, for optimal real-time fault isolation and service restoration (FISR) in distribution systems. The proposed models integrate an efficient integer programming formulation to model the automated switching operation, which use only one set of binary variables, and therefore are suitable to use in real-time switching application because of their relatively lower computational burden. The proposed models are implemented on the 32-bus and 123-bus test distribution systems under multiple fault scenarios in order to compare their accuracy and speed of computations. The simulations results show that the linear model can provide FISR solutions in almost real-time, with an acceptable accuracy compared to the QC model.**

***Index Terms*—Fault isolation and service restoration, automated switching, distribution system.**

I. Contributions & Highlights

The automatic FISR systems rely on switching algorithms and procedures to isolate the faulted line sections and restore interrupted load points through main feeder and alternative backup feeders. This paper investigates a mixed integer programming (MIP) approach for optimizing the real-time switching operation involved in automated fault isolation and service restoration (FISR) in distribution system. More specifically, integer programming is first utilized to formulate the automatic and real-time switching operation in distribution systems using binary variables showing the status of line switching in the network. The proposed real-time switching formulation is then utilized to formulate the real-time FISR problem in two MIP forms, namely, quadratic constrained (QC) and linear. The QC formulation integrates an accurate branch flow formulation to model distribution power flow, while the linear model utilizes the linear approximation of the formulas.

II. The Fault Isolation and Restoration Model

The proposed algorithm finds the best real-time switching sequence, based on the available automatic switches, and the fault location. Suppose the illustrative distribution system with two feeders, shown in Fig. 1, undergoes a fault at line l_{23}. The algorithm can find the second configuration in this figure, given the location of switches with automation capability, using a binary variable e_{ij} that shows energizing condition of lines, using the following real-time switching model:

$$|s_{ij} - s^d_{ij}| \leq a_{ij}, \ \forall i,j, \tag{1}$$

$$e_{ij} \leq 1 - f_{ij}, \ \forall i,j, \tag{2}$$

$$3e_{ij} \geq e_{ki} + s_{ij} + s_{ji} - 2, \ \forall i,j,k, \ j \neq k, \tag{3}$$

$$\sum_{j|(i,j)\in\mathcal{L}} e_{ji} \leq 1, \ \forall i,j, \tag{4}$$

By incorporating the proposed switching method in a grid operation model, multiple faults may be isolated given any fault location. In addition, depending on the objective of the optimization model, states of switches will change to, for example, maximize load restoration or reduce power loss. Both quadratic and linear power flow models are tested with the switching method, and it is shown that both models are highly efficient in selecting switching sequences, while the linear model is also fast enough to be used in real-time operations. The accuracy and computation time of the proposed models is compared with two common methods in Fig. 2, indicating substantial saving in computational time.

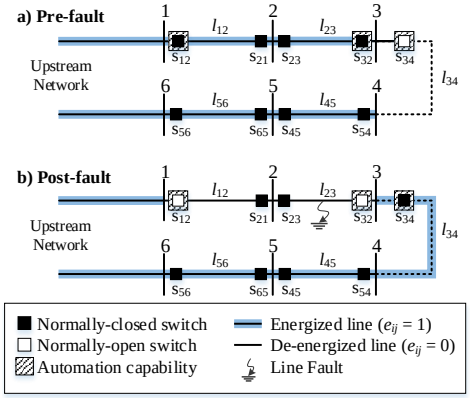

Fig. 1. FISR operation procedure

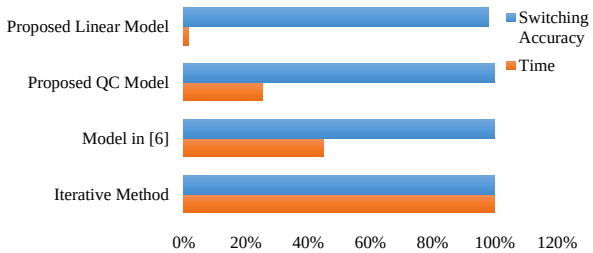

Fig. 2. Computation time and switching accuracy of four methods

A Multi-function AAA Algorithm Applied to Frequency Dependent Line Modeling

Lucas Monzón
Department of Applied Mathematics
University of Colorado, Boulder
Email: monzon@colorado.edu

William Johns, Spatika Iyengar, Matthew Reynolds,
Jonathan Maack, and Kumaraguru Prabakar
National Renewable Energy Laboratory
Email: matthew.reynolds@nrel.gov

***Abstract*—Modeling of power distribution system components that are valid for a wide range of frequencies are crucial for highly accurate modeling of electromagnetic transient (EMT) events. This has recently become of interest due to the improvements needed for the resilient operation of distribution systems. Vector fitting (VF) is used in electromagnetic transients programs, like EMTP-RV, PSCAD, and ATP-EMTP, for wide band representations of power system components in EMT simulations. In this research, we introduce a new multi-input rational approximation algorithm (MIAAA) based upon [1] and illustrate its advantages with respect to VF. We show that MIAAA not only outperforms VF in terms of achieving better accuracy using fewer poles, but also has no numerical issues achieving convergence. Also, in contrast to VF, MIAAA does not require good estimates for the location of the approximation poles.**

I. Key Methodology

Starting from K functions $\{\varphi_k\}_{k=1}^{K}$ with sample values from a common set $Z = \{z_n\}_{n=1}^{N} \subseteq \mathbb{C}$, we iteratively build approximations, by selecting a subset of M (support points) $\{z_n\}_{n=1}^{M}$ and finding corresponding weights w_n so that the quotient of barycentric representations

$$B_k(z) = \frac{\sum_{n=1}^{M} \frac{w_n \varphi_k(z_n)}{z - z_n}}{\sum_{n=1}^{M} \frac{w_n}{z - z_n}}, \quad k = 1, \ldots, K \tag{1}$$

are used to approximate the functions φ_k, $k = 1, \ldots, K$. Since all B_k have a common barycentric denominator, the final rational approximations, written in partial fractions form, have a common set of poles.

At each step of the iteration, a greedy choice is used to select an additional support point z_m from the initial sample set Z which is responsible for the largest deviation. We then use least squares to compute a set of common weights $w_1, ..., w_m$ for the intermediate barycentric approximations.

We terminate the iteration when $\max_k |B_k(z) - \varphi_k(z)|_{z \in Z}$ is less than the desired tolerance.

II. Results

To illustrate the performance of the algorithm with respect to VF, we consider a 6 by 6 terminal admittance matrix of a power distribution system already discussed in the literature [2]. The fitting errors achieved by both methods for two of the matrix entries, $f(1)$ and $f(2)$, are displayed in Figure 1. Results for other matrix entries are similar. Note that the MIAAA approximation is always below the target accuracy 10^{-6} and fits the linear section of the function with error close to double precision, while VF performs significantly worse. Importantly, MIAAA also provides a better approximation order since it only requires 36 common poles to reach the target accuracy in contrast with VF which requires 50 poles. Although MIAAA was also faster than VF, we do not provide speed comparisons since additional work is necessary for a more thorough comparison and, for the intended applications, the final number of poles used in the approximation is the dominant factor in running time and not the running time of VF or MIAAA.

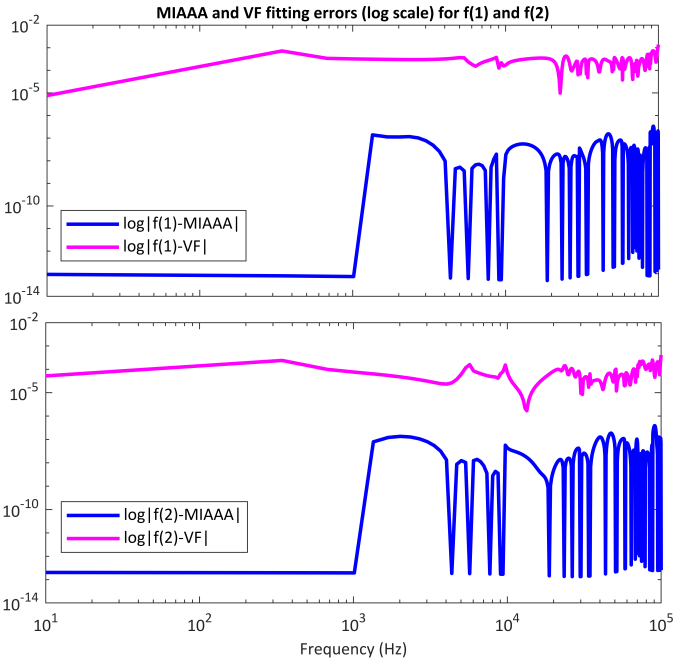

Fig. 1. Comparing vector fitting and MIAAA fitting errors on two entries, $f(1)$ and $f(2)$, of an admittance matrix.

References

[1] Y. Nakatsukasa, O. Sète, and L. Trefethen, "The aaa algorithm for rational approximation," *SIAM Journal on Scientific Computing*, vol. 40, no. 3, pp. A1494–A1522, 2018.

[2] B. Gustavsen, "User's guide for vectfit3.m," *SINTEF Energy Research, Trondheim, Norway*, 2008. [Online]. Available: www.sintef.no/projectweb/vectfit

A Reinforcement Learning Approach for Branch Overload Relief in Power Systems

Mariana Kamel
Dept. of Electrical Engineering and Computer Science
The University of Tennessee
Knoxville, TN, USA

Yawei Wang
Dept. of Computer Science
The George Washington University
Washington, DC, USA

Chen Yuan
GEIRI North America
San Jose, CA, USA

Fangxing Li
Dept. of Electrical Engineering and Computer Science
The University of Tennessee
Knoxville, TN, USA

Renchang Dai
GEIRI North America
San Jose, CA, USA

Guangyi Liu
GEIRI North America
San Jose, CA, USA

***Abstract*— This work presents a reinforcement learning (RL) approach to the problem of branch overload relief. An agent is trained to re-dispatch generators' real power output in order to adjust the power flow through the network so that none of its branches is overloaded. The generation re-dispatch agent is trained using the deep deterministic policy gradient (DDPG) algorithm. The proposed approach is tested on both the IEEE 14-bus and 39-bus systems. Once trained, the performance of the re-dispatch agents was compared against that of the classical optimal power flow (OPF) approach. The trained agents demonstrated better performance with both having: (a) close to a 100% success rate for cases which had an OPF solution; and (b) 70.14% and 46.48% success rates for cases which had no feasible OPF solution. Such results confirm the potential of the proposed DDPG-based RL re-dispatch approach as a reliable method for managing branch overloading.**

Keywords—Branch overload, deep deterministic policy gradient, generation re-dispatch, reinforcement learning

I. Control Methodology

In reinforcement learning, the agent interacts with the environment in discrete time-steps. At each time-step t, the agent observes the system states s_t, decides on an action a_t and receives a reward r_t. The RL agent learns progressively as it accumulates more and more experience until it learns an optimal control law. In this work, the system states, actions, and rewards are defined as follows: Given an N-bus system where $\mathcal{G}$ is the set of system generators (excluding the slack unit), $\mathcal{B}$ is the set of system branches, then; (1) System states are defined as: $S = \{s|s_t = \{I_{i,t} \; \forall \; i \in \mathcal{B}\} \cup \{P_{gj,t} \; \forall \; j \in \mathcal{G}\}$ where $I_{i,t}$ is the current of the i[th] branch, $P_{gj,t}$ is the real output power of the j[th] generator. (2) Action space is defined as: $A = \{a|a_{j,t} = \Delta P_{gj,t} \; \forall \; j \in \mathcal{G}\}$ where $\Delta P_{gj,t}$ is the amount of change in the real output power of the j[th] generator. (3) The reward function is formulated as: $r_t = -1 + r_{TML}$ where r_{TML} is equal to: +20 if $I_{i,t} \leq I_{i-max} \; \forall \; i \in \mathcal{B}$; ore -20 if power flow diverges; or 0 otherwise.

II. Results

The performance of the proposed RL-based control is investigated on both the IEEE 14-bus and 39-bus systems. The following are the training and testing results:

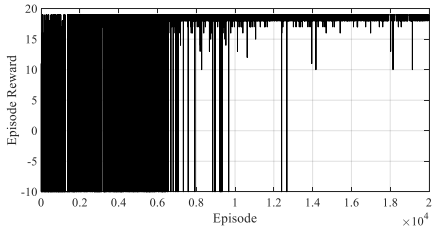

Fig. 1. Agent training results for the IEEE 14-bus system: episode reward.

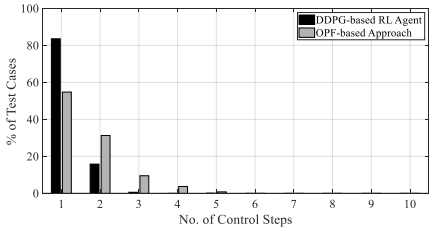

Fig. 2. Testing results for the IEEE 14-bus system: display of solved test cases according to the number of control steps taken to reach the solution.

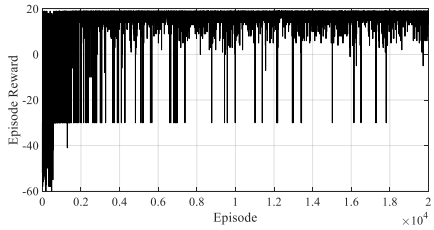

Fig. 3. Agent training results for the IEEE 39-bus system: episode reward.

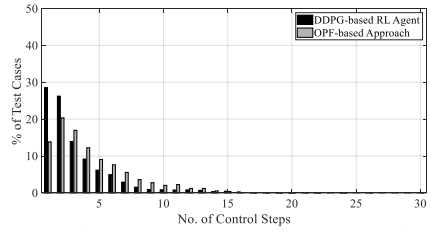

Fig. 4. Testing results for the IEEE 39-bus system: display of solved test cases according to the number of control steps taken to reach the solution.

III. Conclusion

The results obtained show the potential of the proposed DDPG-based RL control as a reliable tool for managing branch overloading.

Industrial Smart Load Using Five-Level Packed U-Cell Converter

Amirabbas Kaymanesh, *Student Member, IEEE* and Ambrish Chandra, *Fellow, IEEE*
Department of Electrical Engineering
École de Technologie Supérieure (ÉTS), Montréal, Canada
Emails: amirabbas.kaymanesh.1@ens.etsmtl.ca and Ambrish.Chandra@etsmtl.ca

***Abstract*—By far, numerous comprehensive control methods have been introduced for electric spring with versatile purposes such as stabilizing point of common coupling voltage and frequency. Although introduced controllers are technologically mature, there are few researches focusing on the electric spring topology. High switching frequency and voltage stress on switches, low-power application, high harmonics content of the output waveforms are some of the inherent demerits of the conventional two-level converters already employed in the electric spring configurations. This necessitates employment of a multilevel converter as electric spring, especially for medium-voltage industrial applications. Therefore, a five-level electric spring using PUC5 converter with a small-sized flying capacitor and an open-loop sensor-less voltage balancing method integrated into its modulation technique is introduced. Comparing with a two-level electric spring, which has two bulky capacitors, PUC5-based smart load has only one small size capacitor. Besides, although it has four more switches, the voltage and power rating of these switches are much lower. The steady-state and dynamic performance of the proposed five-level electric spring has been also validated.**

Keywords— Electric spring, PUC5, multilevel converter, power quality.

I. PUC5-ES2 Configutation and Controller

Topology of the proposed PUC5-based electric spring (PUC5-ES2) that should be connected in series with a noncritical load (NCL) to form an industrial smart load (SL) is shown in Fig. 1. Besides, a simplified diagram of the employed controller can be seen in Fig. 2.

II. Model Analisis and Results

The aim of this section is to evaluate the steady-state and dynamic operation of the PUC5-ES2. The modelled system considered here is a weak power system, which is powered by a conventional AC voltage source and a renewable energy emulator that is able to inject various amount of active and reactive power to grid through a distribution line. A resistive-inductive load is considered as NCL (12.93+j10.18) and a resistive load (19.225 Ω) is considered as critical load (CL).

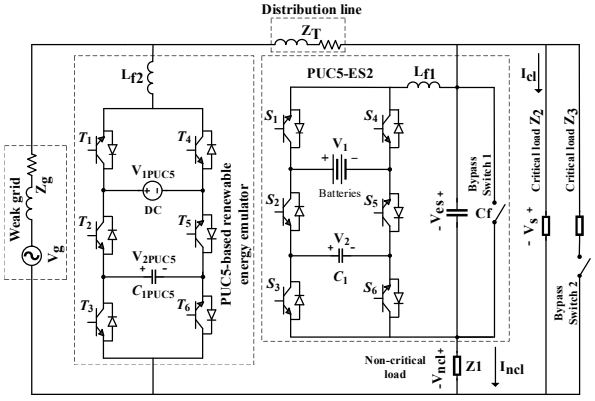

Fig. 1. Diagram of the simulated weak grid using Simscape Electrical

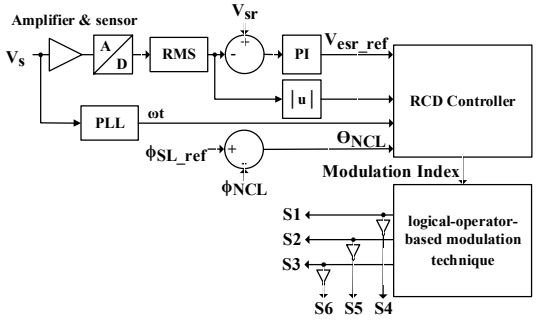

Fig. 2. Schematic of the utilized radial-chordal decomposition controller modified for PUC5-ES2 application

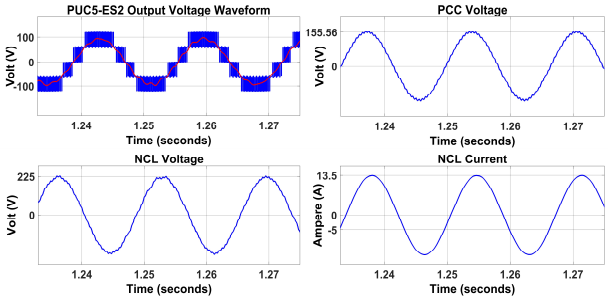

Fig. 3. Steady-state waveforms in a grid with extra power generation

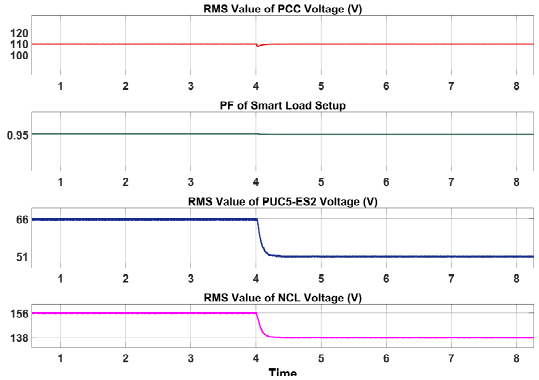

Fig. 4. Captured RMS values and PF of the SL during a transient

Fig. 3 depicts the recorded waveforms in the simulated grid with redundant generated active power. As illustrated, PUC5-ES2 has injected a five-level compensation voltage to the grid and consequently PCC voltage has been stabilized to its nominal value ($155.56/\sqrt{2} = 110\ V\ RMS$) and the PF of SL has been modified from 0.786 to about 0.95. For checking the dynamic performance, during this operation, resistance of the CL has been suddenly changed to around 15 Ω at $t = 4\ s$. Fig. 4 shows the recorded measurements. As it is clear, by modifying the NCL voltage, PUC5-ES2 has effectively managed to keep the PCC voltage at its nominal value and the modified amount of PF stable in the desired value.

Operating the Maui Power System with 100% Inverter Based Resources

Rick Wallace Kenyon[1,2], Anderson Hoke[2], Bri-Mathias Hodge[1,2]
[1]Electrical, Computer, and Energy Engineering; Renewable and Sustainable Energy Institute
University of Colorado Boulder, Boulder, USA
[2]Power Systems Engineering Center, *National Renewable Energy Laboratory, Golden, USA*

As power systems achieve higher instantaneous levels of renewable energy sources, the dynamical impacts of inverter based resources (IBRs), the typical interfacing technology for wind and solar energy, begins to play out [1]. This is exceedingly prevalent at higher instantaneous penetrations, which are being experienced today; the Hawaiian island of Maui achieved a peak instantaneous IBR penetration of 76% in 2018 [2]. The traditional control strategy for transmission connected IBRs is *grid-following* (GFL), where the IBR tracks an existing voltage waveform and injects current to achieve desired power set points. A valid question for relatively high shares of GFL IBRs is 'what's forming the grid?', with an anticipated instability at higher instantaneous penetrations. Fig. 1 depicts this general concept of instability with a bears on bicycles analogy. *Grid-forming* (GFM) inverters might solve this stability issue as they do not rely on an existing voltage waveform, but instead form the waveform frequency and magnitude directly. While GFM IBRs have existing, widespread application to microgrids, the operation of a high voltage, meshed transmission power system with only autonomously synchronizing GFM and GFL IBRs has not yet occurred. This work looks at the transient stability of the Maui power system with only GFM and GFL IBRs, a near future reality considering Hawaii's renewable energy goal of 100% by 2045.

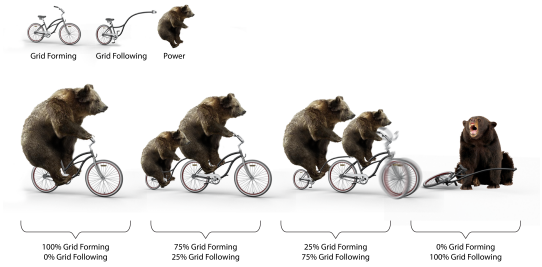

Fig. 1. Bears on bicycles analogy of GFM vs. GFL operational limits. Note that 'grid-forming' in this image implies any device forming the voltage waveform.

A model of the Maui power system has been developed and validated against field data, both in steady state and dynamically, with the electromagnetic transient program, power systems computer aided design (PSCAD). The Maui system PSCAD model incorporates parallel computing, allowing it to run on seven cores during simulations. General data about the system is provided in Table I. Full order dynamical models of GFM and GFL IBRs have been developed in PSCAD for application to the Maui power system. The GFL have grid support capabilities, such as frequency droop and synthetic inertia. The GFM is based on the droop control strategy.

TABLE I
PERTINENT PARAMETERS OF MAUI SYSTEM.
*: FUTURE INSTALLATION, **: HYPOTHETICAL

Aspect	Parameter	Quantity	Aggregate Rating
System	Buses	197	n/a
	Loads	93	Peak: 200 MW
Generation	Wind: Type 3	2 Plants	51 MW
	Wind: Type 4	2 Plants	24 MW
	Distributed PV	171 Aggregate	101 MW
	Utility-Scale PV	2 + Plants	5.4 MW
	GFL BESS	2 + 2* Plants	21 + 75* MW
	GFM BESS**	1–4** Plants	20–60** MW

The simulations performed with the PSCAD Maui model include standard transient stability scenarios such as load steps, generation losses, and various types of faults. For each simulation, the penetration of GFL versus GFM resources is varied in order to highlight the dependency of the system on GFM assets. Fig. 2 shows the frequency response of the system for a fault and subsequent generation loss, which was developed during the model validation process.

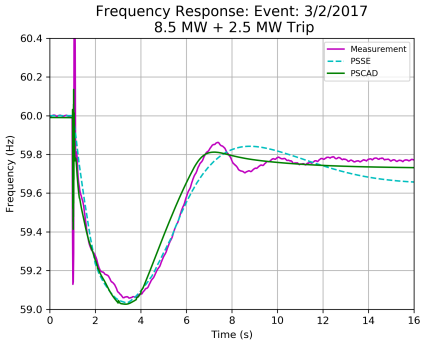

Fig. 2. Frequency response traces of validation efforts for the Maui System.

A special thanks to the Hawaiian Electric Company for their assistance with the model development and operational information.

REFERENCES

[1] B. Kroposki, B. Johnson, Y. Zhang, V. Gevorgian, P. Denholm, B. Hodge, and B. Hannegan, "Achieving a 100% Renewable Grid: Operating Electric Power Systems with Extremely High Levels of Variable Renewable Energy," *IEEE Power and Energy Magazine*, vol. 15, no. 2, pp. 61–73, Mar. 2017.

[2] R. W. Kenyon, A. Hoke, J. Tan, B. Kroposki, and B. M. Hodge, "Grid-Following Inverters and Synchronous Condensers: A Grid-Forming Pair?" Clemson University, Mar. 2020, p. 8.

Efficient Hosting Capacity Computation for Distribution Circuit

Mohammad Asif Iqbal Khan and Sumit Paudyal
Florida International University, Miami, FL, USA
Emails: {mkhan103, spaudyal}@fiu.edu

***Abstract*—Coordinating demand against variable whole-sale energy market or wide-area control signals requires responsive distributed energy resources (DERs) and at large scale it is valuable to guarantee that the coordination does not violate network measurements while maximizing the grid utilization. Developing on the dynamic behavior of the distribution grid, it is considered that the distribution feeder utilization can be maximized using a smart coordinator that allows further loads into the grid depending on the live grid measurements used as constraints to determine whether the grid has additional flexibility in real-time. Here, a demand dispatch scheme to maximize distribution feeder utilization is developed that guarantees network admissible DER/load coordination in presence of diverse group of DERs. In specific, this work develops a coordination scheme which evaluates the network parameters to calculate available flexibility of the network and aggregates the additional connections until the grid measurement constraints are violated. By using IEEE 13 node test feeder, we could demonstrate the maximization of DER connectivity using the developed coordination scheme under defined constraints.**

***Index Terms*—Distribution system, Power flow analysis, Scheduling optimization**

I. Key Equations

The Newton Raphson (NR) method can be built as:

$$\begin{bmatrix} \Delta P \\ \Delta Q \end{bmatrix}^T = \begin{bmatrix} J1 & J2 \\ J3 & J4 \end{bmatrix}^T \begin{bmatrix} \Delta \delta \\ \Delta V \end{bmatrix}^T \tag{1}$$

where the Jacobian elements are as following:

$$\begin{bmatrix} J_1 & J_2 \\ J_3 & J_4 \end{bmatrix}^T = \begin{bmatrix} \frac{\partial P}{\partial \delta} & \frac{\partial P}{\partial V} \\ \frac{\partial Q}{\partial \delta} & \frac{\partial Q}{\partial V} \end{bmatrix}^T \tag{2}$$

Using the Jacobian element the active power grid flexibility can be calculated per time step T:

$$\left[\text{Flexibility}\right]^T = \left[J_2 * (V_{\text{measurement}} - V_{\text{threshold}})\right]^T \tag{3}$$

where $V_{\text{threshold}}$ is defined as the under voltage floor of grid i.e. 0.95 (p.u.) and $V_{\text{measurement}}$ is the actual measurement from the grid.

II. Constraint-aware coordinator logic

The major constraints to the coordinator are:

- The voltage limit of the bus (V)
- The active power sensitivity/flexibility (P)
- The transformer rating/capacity limit (X)

This coordinator logic in the coding environment can be summarized as in the Algorithm 1 below:

Result: Managing aggregated coordination at every time iteration k:
Get $P_{\text{flexibility}}[k]$;
Get $V_{\text{bus}}[k]$;
Get $\text{Transformer}_{\text{capacity}}[k]$;
if $0.95 < V_{bus}[k] < 1.05$ and $P_{remaining\ flexibility}[k] > 0$ and $Transformer_{remaining\ capacity}[k] > 0$ **then**
  Aggregate network usage;
  Update $P_{\text{remaining flexibility}}[k]$;
  Update $\text{Transformer}_{\text{remaining capacity}}[k]$;
else
  break;
end

Algorithm 1: Coordinator algorithm

III. key Results

In the Fig. 1, the flexibility and the impact of flexible loads at node 675 of IEEE 13 node feeder are shown for a day.

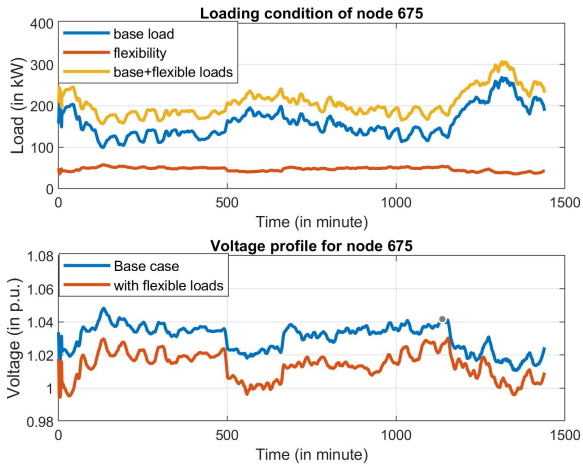

Fig. 1. Availability (top) and impact of addition of flexible loads (bottom)

PMU-Based Evaluation of Transmission Bus Strength through Angle Sensitivity Metrics

Taehyung Kim, Alvaro Furlani Bastos, and Surya Santoso, *The University of Texas at Austin*
W. Mack Grady, *Baylor University*
Patrick Gravois, Megan Miller, Nemica Kadel, John Schmall, Shun Hsien (Fred) Huang, and Bill Blevins, *ERCOT*

***Abstract*—As the share of wind power generation increases, the power system stability may be adversely affected. Wind interconnection studies are conducted to evaluate and anticipate the interactions between the wind project and the power system. Various metrics have been developed to evaluate the system strength at the point of interconnection: short-circuit ratio, voltage stability limit, and system inertia. These metrics, unfortunately, rely on network data which may not be readily available. In this paper, a voltage phase angle based index is proposed for evaluating a transmission bus strength. The proposed metric describes the sensitivity of the change of voltage phase angle to the change of active power flow. The proposed metric requires no network information but solely rely on PMU measurements. The validity of the proposed metric is demonstrated by applying it to analyzing the system strength of the Panhandle region of the ERCOT transmission network. Through field data, it is shown that the proposed metric correctly identifies buses as strong or weak. Moreover, the metric can determine the system strength caused by varying wind power production. It is shown that the system strength decreases during high wind power generation, and vice versa.**

I. Introduction

We propose a new method to estimate the system strength using PMU measurements only. Instead of frequency and inertia, voltage angle and power measurements are used to calculate the angle sensitivity to power. This method has been tested on the Panhandle region of the ERCOT network using actual measurement data. This paper is organized as follows. The theoretical background of angle sensitivity is discussed in the first section. Then the approach to calculating the angle sensitivity with PMU data is presented Finally, bus strengths of the Panhandle region using the proposed method are presented in the last section.

II. Proposed Metric

We propose a phase angle-based metric as follows:

$$\frac{\Delta\delta}{\Delta P} = \frac{X_{eq}}{\sqrt{(V_1 V_{ref})^2 - (P_0 X_{eq})^2}} \tag{1}$$

The proposed metric is affected by Voltage magnitude, line power flow, and equivalent reactance of bus. Fig. 1 shows the algoritm to compute the angle sensitivity.

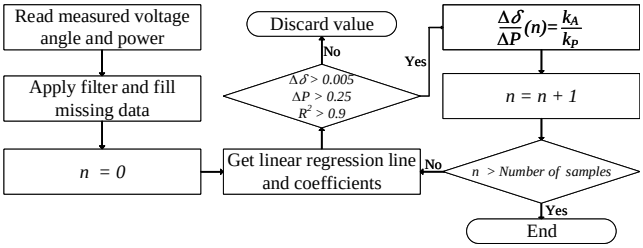

Fig. 1. The flow chart to calculate the angle sensitivity.

III. Evaluating Panhandle Region Line Strength

Fig. 2 shows the relative angle sensitivity of buses in the Panhandle region. It can be seen that Alibates and Tule Canyon are the weakest buses, and Clear Crossing is the strongest bus.

IV. Conclusion

This paper proposes a new method to evaluate transmission bus strength. The angle sensitivity calculated using PMU measurements is used to evaluate the system strength, and it was applied to the Panhandle region of the ERCOT network. From the case study, the results confirm those previously evaluated using a WSCR method, i.e., buses at the remote region tend to be weaker than those closer to the center of the ERCOT grid.

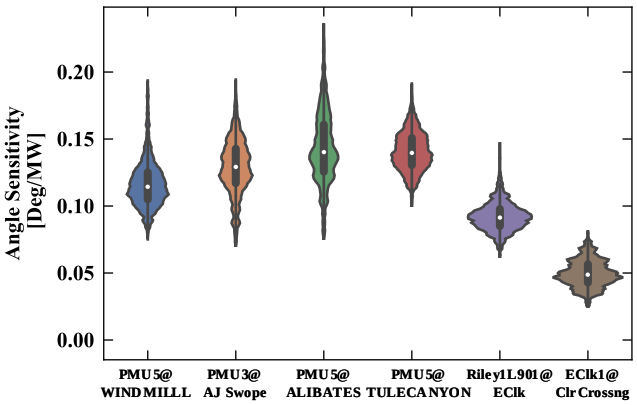

Fig. 2. Angle sensitivities of the buses measured by selected PMUs

WTG Active Power Control for Transient Stability Enhancement

Stavros Konstantinopoulos and Joe H. Chow

***Abstract*—This work discusses the benefits of coordinating the active and reactive power control of renewable resources, utilizing their fast-acting converters and low inertia characteristics. The proposed control scheme aims at improving the transient stability margin of an adjacent large synchronous generator (SG). The control design is developed for a Type-3 wind turbine generator (WTG) to act as a controllable braking resistor, slowing down the acceleration of the SG after a fault. Simultaneously, the reactive power control uses a sliding-mode based design,/ to assist in dynamic voltage recovery and damp the power swings. The method is tested on a single-machine infinite-bus system.**

***Index Terms*—DFIG, transient control, sliding mode control**

I. WTG and SG Infinite Bus System

The system used for the design is the single machine infinite bus system noted in Fig. 1

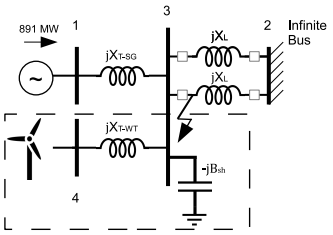

Fig. 1. SMIB and WTG System.

A. Active Power Control Design

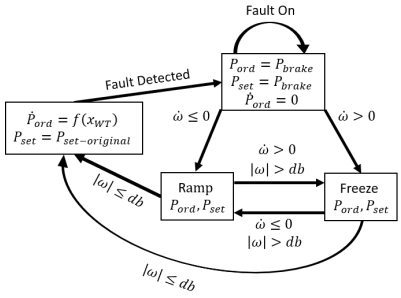

Fig. 2. Transient Active Power Management Logic.

Fig. 2 shows that when a fault is detected, the power command P_{ord} is reset to a low value. After the fault is cleared, P_{ord} is ramped to the pre-fault power setpoint. This power reduction will increase the electrical power demand on the faulted SG, decelerating it. This is called the dynamic power reduction (DPR). By monitoring the acceleration of the SG, the ramp can be temporarily frozen (adaptive DPR) if the SG starts to accelerate, improving swing mode damping.

B. Sliding Mode Reactive Power Control Design

The electromechanical model of the SG is adopted and the controller can be designed as the input is in affine form. The swing equations are

$$\dot{\delta} = \Omega\omega, \;\; 2H\dot{\omega} = \hat{f}(\delta) + \hat{g}(\delta)I_Q \tag{1}$$

With $\hat{f}(\delta) = P_m - F(\delta)$. With $\lambda, k(\delta) > 0$, we choose [1]

$$s = \omega + \lambda(\delta - \delta_{SEP}) \tag{2}$$

$$I_Q = \frac{-\hat{f}(\delta) - \lambda\omega}{\hat{g}(\delta)} + k(\delta)\text{sgn(s)} \tag{3}$$

$$L(s) = \frac{s^2}{2} \implies \dot{L}(s) = k(\delta)\hat{g}(\delta)|s| < 0 \tag{4}$$

since $\hat{g}(\delta) < 0$. I_Q denotes the reactive current injection of the WTG, δ, ω the SG rotor angle and speed and δ_{SEP} the stable equilibrium's rotor angle.

II. Single Machine Infinite Bus System Results

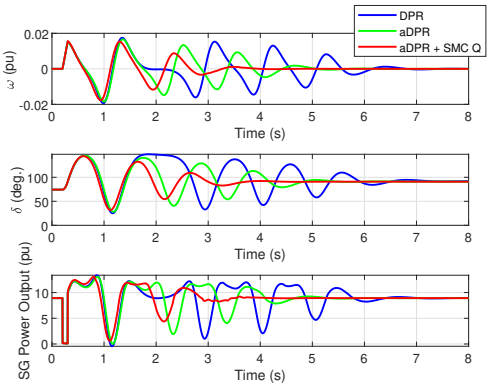

Fig. 3. SG Response for Different Controller Configurations.

The critical clearing time of the system improved from 4.5 cycles with native controls, to 6.1 cycles with aDPR.

References

[1] V. Utkin, "Variable structure systems with sliding modes," *IEEE Trans. Autom. Control*, vol. 22, no. 2, pp. 212-222, April 1977.

Stavros Konstantinopoulos and Joe H. Chow are with the Department of Electrical and Systems Engineering, Rensselaer Polytechnic Institute, Troy, NY, USA. e-mail:{konsts,chowj}@rpi.edu.

Lissajous Parameters based Islanding Detection of Multiple DGs in Microgrid

Avinash Kumar, Rakesh Kumar Panda, Abheejeet Mohapatra, and S. N. Singh
Department of Electrical Engineering, Indian Institute of Technology Kanpur, Kanpur, India 208016
Email: kumarav@iitk.ac.in; rpanda@iitk.ac.in; abheem@iitk.ac.in; snsingh@iitk.ac.in

***Abstract*—This poster proposes a new passive technique for quick Unintentional Islanding Detection (UID) of multiple DGs, even in the case of zero power mismatch/ power balance, by the use of the Lissajous pattern. Point of Common Coupling (PCC) voltage and current phasors are estimated by Moving Window Discrete Fourier Transform (MWDFT). The Lissajous pattern and the associated parameters, such as slant angle, major and minor axes, are evaluated from these phasors. Based on these parameters, UI is detected. The proposed approach is tested on Real-Time Digital Simulator (RTDS).**

***Index Terms*——Islanding Detection, Lissajous pattern, Moving Window Discrete Fourier Transform, Microgrid Protection.**

I. Introduction

UID aids in seamless transition of DGs between grid following and grid forming modes of operation and also assists in control capabilities of the microgrid to regulate voltage and frequency. The existing UID can be classified as passive, active, and hybrid approaches. The passive approaches are simple and commercially accepted, as they avoid power quality and stability issues, and have decentralized control.

II. Proposed Method using Lissajous Parameters

The proposed approach only requires the fundamental components of the voltage and current phasors at the PCC, which are obtained from MWDFT. By using these estimated phasors, the Lissajous pattern is constructed [1].

$$\frac{\hat{i}_{pcc}^2}{\hat{I}_{mp1}^2}+\frac{\hat{v}_{pcc}^2}{\hat{V}_{mp1}^2}-\frac{2\hat{i}_{pcc}\hat{v}_{pcc}\cos(2\hat{z}_d)}{\hat{I}_{mp1}\hat{V}_{mp1}}=\sin^2(2\hat{z}_d) \quad (1)$$

A. Lissajous Parameters

The Lissajous parameters such as slant angle, major and minor axes are evaluated as

$$\begin{aligned}\tan(2\theta_p)&=\frac{2\hat{V}_{mp1}\hat{I}_{mp1}\cos(\hat{z}_d)}{\hat{V}_{mp1}^2-\hat{I}_{mp1}^2}\\ a_m&=\frac{\hat{V}_{mp1}^2\hat{I}_{mp1}^2}{\hat{I}_{mp1}^2+\{2\hat{I}_{mp1}\cos(\hat{z}_d)+\hat{V}_{mp1}\}\hat{V}_{mp1}\tan(\theta_p)} \quad (2)\\ b_m&=\frac{\hat{V}_{mp1}^2\hat{I}_{mp1}^2}{\hat{V}_{mp1}^2+\{2\hat{V}_{mp1}\cos(\hat{z}_d)+\hat{I}_{mp1}\}\hat{I}_{mp1}\tan(\theta_p)}\end{aligned}$$

The authors would like to thank the DST/Indo-US Science and Technology Forum (IUSSTF), New Delhi, India for providing financial support to carry out this research work under projects IUSSTF/EE/2017282B and DST/EE/2018174D.

B. Operation of Proposed method

To discriminate UI from non-islanding events, slant angle jump ($SAJ=\theta_p^{pre}-\theta_p^{dis}$) is inspected. $SAJ\neq 0$ indicates the occurrence of a disturbance in the microgrid. After one cycle, $\Delta a_m=|a_m^{pre}-a_m(t)|$ and $\Delta b_m=|b_m^{pre}-b_m(t)|$ are evaluated.Thereafter, the average values of Δa_m and Δb_m over a half cycle are monitored to discriminate UI from fault/switching events. To discriminate UI from other events, $\Delta a_{m_{avg}}$ and $\Delta b_{m_{avg}}$ both should be less than 0.1pu.

III. RTDS based Simulation Results

The proposed approach of UID of DGs in a microgrid is tested in RTDS on a test microgrid. It consists of multiple DGs, where DG1 is IIDG, DG2 is battery storage and DG3 is a diesel generator. The proposed UID is also tested for different load quality factor Q_f, PMC, Load Switching (LS), Capacitor Switching (CS), faults, and DG out cases.

TABLE I
Simulation Results of Various Load Q_f

Q_f	R (Ω)	L (mH)	C (mF)	f_r (Hz)	$\Delta a_{m_{avg}}$	$\Delta b_{m_{avg}}$
0.5	0.4608	2.4442	2.8778	60.01	0.0427	0.0317
1	0.4608	1.2219	5.7546	60.02	0.0337	0.0295
1.77	0.4608	0.6779	10.3444	60.1	0.0343	0.0291
2.5	0.4608	0.4877	14.3553	60.15	0.0487	0.0366
3	0.4608	0.4061	17.2120	60.2	0.0331	0.0252

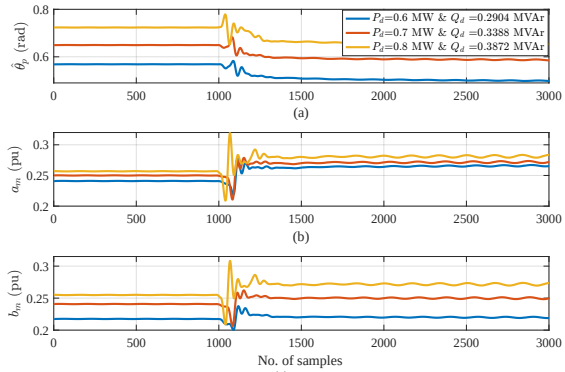

Fig. 1. (a) θ_p (b) a_m and (c) b_m for different PMC

References

[1] B. D. Smith and S. H. Ward, "On the computation of polarization ellipse parameters," Geophysics, vol. 39, no. 6, pp. 867–869, 1974.

Reinforcement Learning for Optimal Allocation of Superconducting Fault Current Limiters

Xiejin Ling [1], Yinhong Li [1*]

[1]State Key Laboratory of Advanced Electromagnetic Engineering and Technology, Hubei Electric Power Security and High Efficiency Key Laboratory, School of Electrical and Electronic Engineering, Huazhong University of Science and Technology, Wuhan 430074, China

Abstract-Superconducting fault current limiter (SFCL) is a new type of current limiting equipment that can restrict the short circuit current level in power systems without impacting on their normal operations. However, the existing SFCL allocation methods have disadvantages of long computation and unstable convergence. Recent advances in the area of artificial intelligence provide the possibility to achieve the optimal SFCL allocation with the consideration of both speed and convergence. To this end, the SFCL allocation is converted into a Reinforcement Learning (RL) problem in this paper. A designer to find the optimal SFCL allocation is viewed as an agent, and the power system is regarded as the environment. The agent adjusts the location and size of SFCLs to respond to the feedback from the environment optimally. The Q-learning algorithm is applied to solve the RL problem. The experimental results demonstrate the effectiveness and superiority of the proposed method.

I. Key Model

A. Problem Formulation

$$\begin{aligned} &\min\ C=\sum_{l=1}^{N_{SFCL}}\left(CZ_l\cdot zf_l+CI_l\right)\\ &s.t.\quad zf_l\le zf_{\max},\ l=1,2,\ldots,N_{SFCL}\\ &\qquad I_k\le I_k^{\max},\quad k=1,2,\ldots,N \end{aligned} \tag{1}$$

B. Reinforcement Learning

$$s_t=\left[zf_l\right]_{1\times L}\quad\left(0\le zf_l\le zf_{\max}\right) \tag{2}$$

$$a_{t,l}=\left[0,0,\ldots,\Delta z,\ldots,0\right]_{1\times L} \tag{3}$$

$$s_{t+1}=s_t+a_{t,l} \tag{4}$$

$$r_{t+1}\left(s_t,a_{t,l}\right)=\begin{cases} M-C, & \text{if } s_{t+1} \text{ is } T_s\\ -1000, & \text{if } s_{t+1} \text{ is } T_f\\ 0, & \text{others}\end{cases} \tag{5}$$

II. Numerical Results

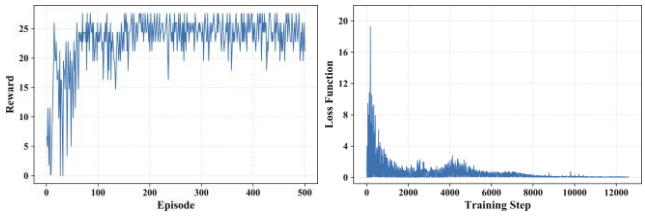

Fig. 1. (a): The curve of rewards, (b): The curve of the loss function.

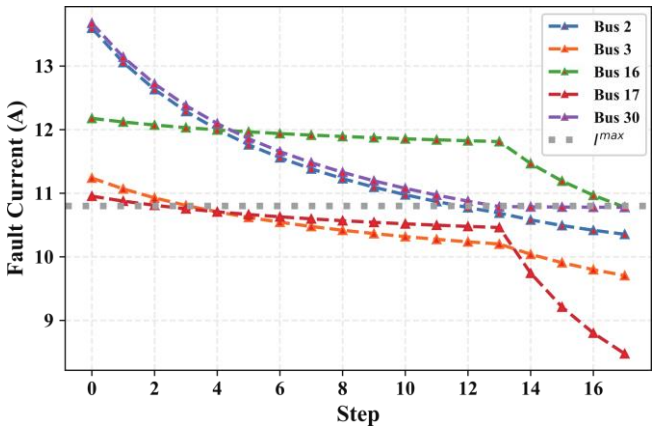

Fig. 2. The reduction processes of the fault currents

Table I: The statistical results of ten experiments

Method	Lowest Cost	Mean Cost	MSE	Time
GA	3.217	4.823	1.386	65.349
PSO	3.217	4.478	1.344	4.119
IMINLP	3.217	3.217	0	1079.432
RL	3.217	3.217	0	39.581

III. Conclusion

This paper proposes an RL approach to solve the optimal SFCL allocation problem. The test results show that the proposed method is superior to other algorithms in the calculation speed and the convergence performance. The method has great potential for application to other optimization problems.

A Scenario-adaptive Online Learning Algorithm for Demand Response

Linwei Sang, Qinran Hu, *Member, IEEE*, Yuan Zhao, Ruhuai Han, Zaijun Wu, Xiaobo Dou

***Abstract*—This paper introduces a scenario-adaptive online learning algorithm for aggregating demand side resources. The problem of dispatching demands is formulated under a contextual combinatorial multi-armed bandit framework with the objective to minimize the mismatch between actual aggregated demand adjustment and the reduction target from system operator. Comparing with previous online learning framework for demand aggregation, this paper considers temporal and spatial factors and creates a scenario-adaptive mechanism to model the behavior of demands. The simulation results show the proposed method achieves less mismatch and more reliable aggregation performance than conventional methods.**

***Keywords*—Multi-armed bandit, demand response, online learning, regret analysis, contextual bandit**

I. Introduction

Demand side resources, as flexible grid assets, have been playing important roles in facilitating power system operations. With the development of Internet of Things (IoT) technologies, utility companies have started to explore the possibilities of enabling real-time demand response.

In this paper, we extend the work in [1], and take the temporal and special factors, which may influence the behavior of demands, into consideration. Thus, this paper adopts Contextual-CMAB algorithm and proposes scenario-based probability to model users' profile.

Contribution: 1) we propose the contextual combinatorial upper confidence bound (Contextual-CUCB) algorithm based on CMAB framework; 2) the regret of the proposed algorithm is analyzed. We prove the upper *regret* bound of our algorithm over T times, n users and $|\chi|$ scenarios are $O(n^3|\chi|\log(T/|\chi|))$; 3) simulation results show Contextual-CUCB algorithm outperforms CUCB-Avg which does not consider the scenarios.

II. Main Results

Denote the set of n users as $[n]$. At time t, only some of the users S_k (belong to $[n]$) receive commands to realize the aggregated demand reduction. The aggregator generates the commands based on the reduction target D from power system. The loss at t time step is depicted by the square deviation of aggregated demand reduction from the target (1).The problem can be formulated as follows:

$$\min_{S_k \subseteq [n]} \mathrm{E}\Big(\sum_{i \in S_k} X_{i,t}^z - D\Big)^2 \qquad (1)$$
$$\text{s.t} \quad X_{i,t}^z \sim Bern(p_i^z)$$

The Contextual-CUCB learning algorithm is proposed to solve the problem, as following:

Algorithm: Contextual-CUCB

1. **Inputs:** α>2, D , contexts
   Initialization: For each scenario z, create a instance
2. knowledge $know_z$ which contains the users' profile under z, and set the initial parameters.
3. **for** each round t **do**
4. Choose the $know_z$ with $z = z_t$
5. Calculate the UCB for each i in $know_z$

$$U_i^z(t) = \min\left(\bar{p}_i^z(t-1) + \sqrt{\frac{\alpha \log N_z}{2T_i^z(t-1)}}, 1\right)$$

6. Sort $U_i^z(t)$ in descending order satisfying:

$$U_{id(1)}^z(t) \geq \cdots \geq U_{id(n)}^z(t)$$

7. Find the largest $k > 0$ such that

$$\sum_{i=1}^{k} \bar{p}_{id(i)}^z(t-1) < D + 1/2$$

8. Send signals to selected users$\{id(1),\ldots,id(k)\}$
9. Updating the $know_z$ according to the feedback $X_{i,t}^z$:

$$\bar{p}_i^z(t) = \bar{p}_i^z(t-1) + \frac{1}{N_z(t-1)+1}\left(X_{i,t}^z - \bar{p}_i^z(t-1)\right)$$
$$N_z(t) = N_z(t-1) + 1$$
$$T_i^z(t) = T_i^z(t-1) + 1$$

10. **end for**

We study the performance of the Contextual-CUCB algorithm. Then, we compare its results to the offline optimal algorithm and CUCB-Avg algorithm.

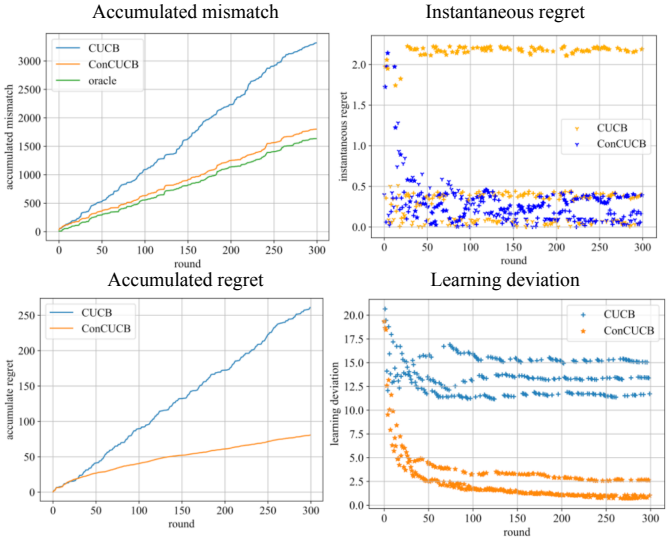

Fig.1 The accumulated mismatch, instantaneous regret, accumulated regret, and learning deviation of the Contextual-CUCB, CUCB-Avg and oracle algorithm

Reference

[1] Y. Li, Q. Hu, and N. Li, "Learning and Selecting the Right Customers for Reliability: A Multi-Armed Bandit Approach," in *2018 IEEE Conference on Decision and Control (CDC)*, Miami Beach, FL, 2018, pp. 4869–4874

SALSA-Based Method for Identifying Critical Component and Critical Component Outage Causality with Cascading Failure Data

Lu Liu, Hao Wu

College of Electrical Engineering, Zhejiang University, Hangzhou, China

***Abstract*—Component outages in power system cascading failure play different roles such as facilitating outage propagation or being vulnerable to other component outages. The component outage propagation relationship between two components can be described by the component outage causality (COC). Recognizing the roles of component outages and quantifying the high-impact COCs are helpful for identifying critical components and critical COCs that are crucial in cascading failure propagation. This paper proposes a method based on Stochastic Approach for Link-Structure Analysis (SALSA) for identifying critical components and critical COCs with cascading failure data, in which component outage and causality are compared to the web page and directed link respectively. Verification on the IEEE 118-bus system with fault chains generated by cascading failure simulation, demonstrates the mitigation measure on identified critical COCs can effectively reduce cascading failure risk.**

I. Methodology

A. Cascading Failure Structure

Cascading failure process can be described by fault chain (FC) $L_i = \{l_1^{(i)}, \cdots, l_j^{(i)}, l_{j+1}^{(i)}, \cdots\}$, where $l_j^{(i)}$ is j-th component outages, and component outage causality (COC) $l_j^{(i)} \to l_{j+1}^{(i)}$ is propagation relationship between two consecutive component outages.

B. Critical COC Identification

This paper aims to identify high-risk COCs from massive FCs based on SALSA approach. Define component outages collection appeared in FCs as ν, hub-components collection as V_h, authority-components collection as V_a. Then bipartite graph $G_b = (V_h, V_a, W)$ can be constructed for describing COCs.

$$\begin{aligned} V_h &= \{l | l \in \nu, O(l) > 0\}, \\ V_a &= \{l | l \in \nu, I(l) > 0\}, \\ W(l_h, l_a) &= N_{l_h \to l_a}/N, (l_h \in V_h, l_a \in V_a), \end{aligned} \tag{1}$$

where $O(l)$ is out-degree, and $I(l)$ is in-degree. The adjacency matrix $W \in \mathbb{R}^{n \times n}$ presents propagation probability of COCs. Two-step random walks are conducted on G_b for correlation indicator calculation, by picking up different role-type component randomly. One step walk starts from authority-component to hub-component, and another from hub to authority. Then two transition matrices H and A, which correspond to two Markov chains generated by two walks respectively, can be computed:

$$\begin{aligned} A &= W_c^T W_r, \\ H &= W_r W_c^T, \end{aligned} \tag{2}$$

where W_r is row normalization matrix, W_c is column normalization matrix. A (H) reveals correlation between authority(hub)-components. Principal eigenvalues π_a and π_h are calculated using power method in (3), the higher entries of which can be used for identifying critical components. Critical hub-component is more likely to facilitate outage propagation, and critical authority-component is more vulnerable to other outages.

$$\begin{aligned} \pi_a^{(k+1)T} &= \pi_a^{(k)T} A, \\ \pi_h^{(k+1)T} &= \pi_h^{(k)T} H. \end{aligned} \tag{3}$$

C. Critical COC Identification

COC is quantified comprehensively considering factors of component criticalness, propagation probability and influence on cascading failure blackouts. Critical COC is identified by risk indicator using (4).

$$RI_{i \to j} = \pi_h(i) W(i,j) \Gamma(i,j) \pi_a(j), \tag{4}$$

where $\Gamma \in \mathbb{R}^{n \times n}$ is causality impact matrix, representing average impact of COC $i \to j (i \in V_h, j \in V_a)$ on FCs.

$$\Gamma(i,j) = \frac{1}{N_{i \to j}} \sum_{q \in \Omega_{i \to j}} \frac{d_{l_{s_{i-1}}^{(q)}} - d_{l_{s_j}^{(q)}}}{d_{l_{s_j}^{(q)}}}, \tag{5}$$

where $\Omega_{i \to j}$ is FC collection containing $i \to j$, $N_{i \to j}$ is FC number in $\Omega_{i \to j}$, $d_{l_{s_j}^{(q)}}$ is accumulative load loss of q-th FC at stage s_j.

II. Case Study and Results

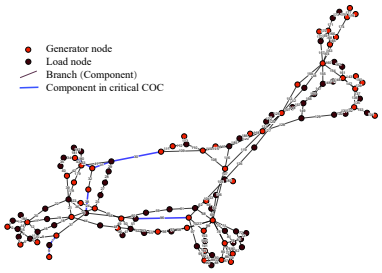

Fig. 1. IEEE 118-bus system graph.

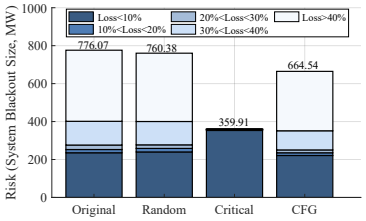

Fig. 2. System blackout size after mitigation measures.

The proposed method have totally identified 2029 COCs with non-zero risk indicators, and components of top 10 critical COCs (e.g. $9 \to 96, 7 \to 96, 9 \to 38, 7 \to 38, 31 \to 33, 33 \to 30, 33 \to 31, 96 \to 33, 31 \to 30, 33 \to 96$) are presented in topological connection graph of IEEE-118 bus system in Fig.1. It shows that critical COCs are not necessarily topologically connected, and components of COCs are coincidentally located on important flow transmission channels topologically.

The mitigation measures are adopted for validating identification results, which simulate relay operation in cascading failure process by reducing component outage probability by 90% temporarily according to critical COCs information. Different mitigation cases are simulated: 1) original system without mitigation, 2) mitigation measure with 10 randomly selected COCs, 3) mitigation measure with top 10 critical COCs, 4) mitigation measure with comparison method, and results are shown in Fig.2.

Fig.2 shows that blackout risks decreases from 776.07MW to 760.38MW, 359.91MW, 664.54MW in case2,3,4 respectively. The mitigation effect on reducing system blackout risk is slight under case2. Case3 and case4 have different mitigation effects, and case3 especially performs better in mitigation of large-scale blackouts with system load losses greater than 10%. It verifies that critical COCs are effectively identified by the proposed method.

Efficient Algorithm for Solving Combined T & D Power Flow and Dynamic Simulation

M Al Mamun
Florida International University
mmamu011@fiu.edu

Arun Suresh
University of North Carolina at Charlotte
asuresh4@uncc.edu

Mohammad Asif Iqbal Khan
Florida International University
mkhan103@fiu.edu

Sukumar Kamalasadan
University of North Carolina at Charlotte
skamalas@uncc.edu

Sumit Paudyal
Florida International University
spaudyal@fiu.edu

***Abstract*—Increased penetration of distributed energy resources will lead to increased interaction of transmission and distribution system and have significant impact on the operations of bulk transmission systems. This has lead to development of co-simulation platform for solving transmission and distribution (T&D) systems simultaneously for steady state as well as dynamic studies. Most of co-simulation methods in current literature follow a decoupled approach, where transmission and distribution systems are decoupled at interface buses and solved independently either one after other or simultaneously depending on parallelizing capability of processing unit used. Since the bench-marking solutions to T&D co-simulation are not available, first this work presents a unified T&D co-simulation as a benchmark which can aid validating the results obtained using other co-simulation approaches. However, this method may suffer from significant computational burden when the system becomes larger. An approach to tackle this issue is to exploit the the parallel computational techniques on a accelerated platform to solve and analyse unified system. Secondly, a decoupled dynamic simulation is also performed on the transmission network where the distribution network is considered as a lumped load connected to a node of the transmission network to observe the transient stability. In this case, all the nonlinear differential algebraic equations (DAEs) of the system are discretized using the Backward Euler method first and, then, the network state and algebraic variables are divided into two sub-systems. After that the Gauss Jacobi Waveform Relaxation algorithm, which is parallel in nature, is used to determine the network variables for each sub-system and, thus, the system dynamics is observed and analyzed. Finally, rigorous MATLAB simulation results verify the effectiveness of the proposed algorithms.**

I. Preliminary Results

A test integrated T&D system is created with 9 bus transmission system and a part of load at bus 8 is replaced by connecting a 123 bus distribution system a shown in Fig. 1(a). Simulation results of Decoupled and Unified approaches and error between both approaches for A phase is shown in Fig. 1(b).The dynamics using waveform relaxation for rotor angles of three generators in the transmission network is shown in Fig. 1(c) .

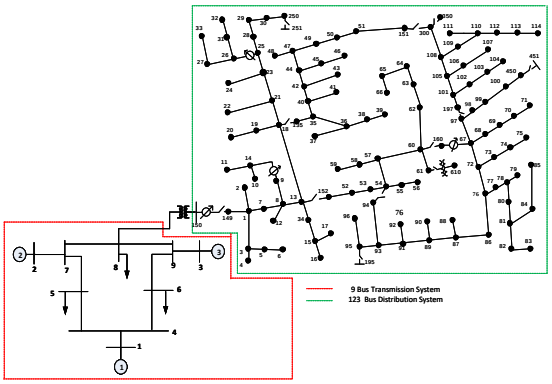

((a)) One Line Diagram

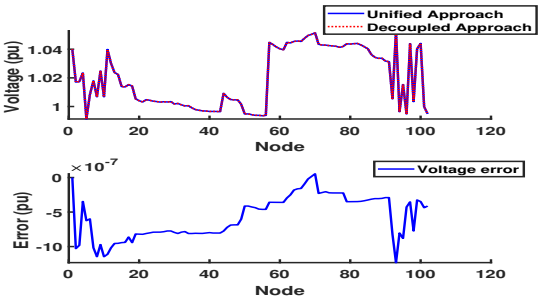

((b)) Load flow Results Phase A

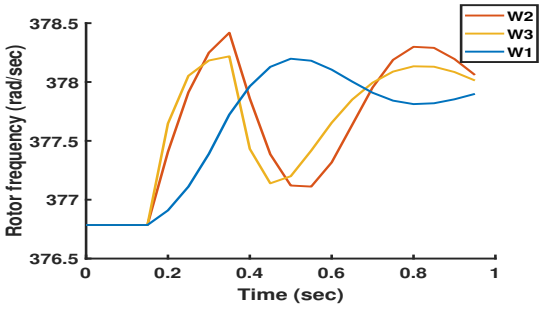

((c)) Generator rotor frequencies

Fig. 1: Preliminary Results

Probabilistic short-circuit analysis: a new approach integrating intermittent power injection

Daniella de Barcellos Martins, Wandry Rodrigues Faria, Benvindo Rodrigues Pereira Júnior
University of São Paulo, São Carlos, Brazil

***Abstract*—This paper presents a new approach for probabilistic short-circuit analysis based on a Monte Carlo Simulation (MCS) and a hybrid compensation technique to determine the fault currents in an unbalanced distribution network with Distributed Generators (DGs). The probabilistic short-circuit approach proposed considers the main uncertainties inherent to the fault problem, such as the intermittent power production from DG, load demand, fault location, fault type, and fault resistance. This type of approach does not consider only extreme values in the fault current determination, allowing a better protection system sizing and a better risk and costs analysis.**

I. Probabilistic short-circuit analysis

A probabilistic short-circuit approach does not consider only extreme values in the fault current determination, allowing a better protection system sizing and a better risk and costs analysis. The flowchart in Fig. 1 illustrates the proposed methodology applied to estimate the Probability Density Function (PDF) of fault currents.

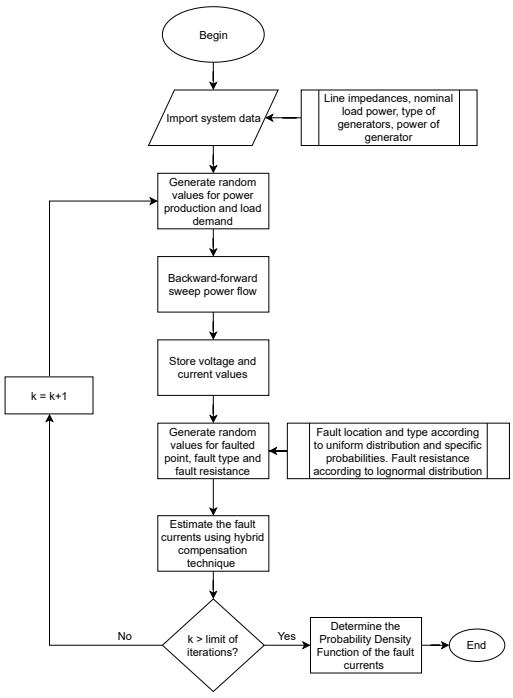

Fig. 1. Flowchart of the proposed method.

For the pre-fault conditions of the system, it was considered the variation of power production and load demands, using weibull and gaussian distributions, respectively. For the fault location, fault resistance, and fault type, the uniform distribution, the lognormal distribution, and different probabilities of fault occurrence were considered, respectively. To evaluate the methodology, 50,000 fault cases were simulated using the MCS in a real distribution system.

The authors would like to acknowledge the CNPq for the financial support (grants 134386/2018-3 and 424489/2018-0).

II. Results

From Fig. 2, it is possible to verify the influence of DGs in short-circuit levels; the currents without the generators present higher values due to the contribution of the substation only. When considering the generators, the substation contribution decreases, and the frequency of the lower currents becomes higher. From Fig. 3, it is possible to observe that the occurrence of currents lower than 1560 A represents 95% of all the simulated cases.

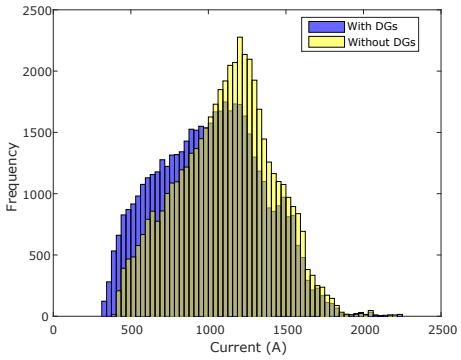

Fig. 2. Fault current at the substation branch for both with and without DGs.

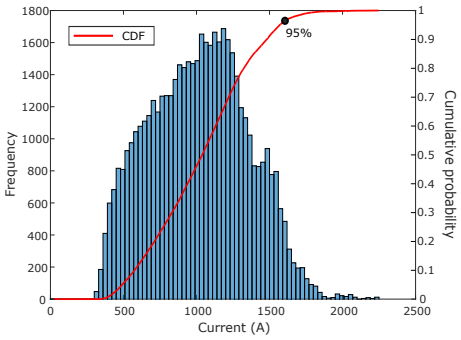

Fig. 3. CDF for substation fault currents with DGs.

This probabilistic approach may be useful for distribution companies in protection system planning and design.

Risk-constrained Bi-level Optimization for Virtual Bidder Bidding Strategy in Day-Ahead Electricity Markets

Hossein Mehdipourpicha, Rui Bo, *Senior Member, IEEE*
Missouri University of Science and Technology, Rolla, USA (rbo@mst.edu)

***Abstract*—Virtual bidders place virtual offers/bids into day-ahead (DA) electricity market, and the cleared energy is settled at the price difference between day-ahead market and real-time (RT) market. With high volatility in the price difference, virtual bidders face great uncertainties and financial risks in their decision making. Therefore, this paper proposes a risk-constrained bi-level optimization model for virtual bidders bidding strategy. In this model, uncertainties related to the other market participants offers/bids and RT market prices are modeled through scenarios. Financial risk associated with bidding decisions is modeled using conditional value-at-risk (CVaR) metric. A case study is presented to demonstrate the effectiveness of the proposed method.**

Keywords*— *Bidding strategy, Bi-level optimization, Conditional Value-at-Risk (CVaR), Uncertainties, Virtual bidder, Stochastic.

I. INTRODUCTION

Virtual bidders, as a purely financial players, can submit incremental offers (INCs) or decremental bids (DECs) into the day-ahead market without the obligation of providing/consuming the physical energy in the real-time market. The net energy in DA market and RT market must be zero, while the net profit is calculated in the two-stage settlement process based on the price difference between DA and RT markets. Virtual bidders can make profit by arbitraging the price difference between DA and RT markets. However, they are exposed to the risk of profit volatile due to the uncertainties of other market participants strategies, which can change the DA market prices, and RT market prices. In order to account for the virtual bidder's impact on DA market price and consider the uncertainties of the RT market price forecast and other participants' offers/bids, we propose a risk-constrained bi-level optimization model to optimize bidding strategy of virtual bidders in the DA market. The upper-level problem seeks to maximize the profit of a virtual bidder, whose revenue is calculated based on the cleared DA market price obtained at the lower-level problem which represents the market clearing process. The upper-level model incorporates scenario-based uncertainties of RT market price and other market participants' offers/bids. Lastly, the conditional value-at-risk (CVaR) is included to quantify the risk of profit associated with different bidding strategies. By virtue of Karush-Kuhn-Tucker optimality conditions, strong duality theorem and Fortuny-Amat Transformation, the bi-level model is converted to a single-level mixed integer linear programming model.

II. CASE STUDY

The proposed model is tested on the 24-bus Reliability Test System. One virtual bidder is considered in this system that can offer from 5 different buses. Assume the maximum generation/ demand that virtual bidder can offer in the DAM is 100MW. We assume the power quantities offered by other market participants (generators/demands) are known by the virtual bidder, and their offer/bid prices are unknown. These uncertain offer/bid prices are modeled as 5 scenarios and RTM price uncertainty is modeled as 3 scenarios (A, B and C). Fig. 1 depicts the efficient frontier that shows the expected profit decreases as the weighting factor β increases. It means that, when the virtual bidder takes the risk-taker position, the resulting optimal strategy allows the virtual bidder to make higher expected profit; however, it may incur significant losses in some scenarios (such as RTM Scenario A and C in conjunction with DAM scenario 2, as shown in Fig. 2). On the contrary, when the virtual bidder takes the risk-averse position, its expected profit is reduced, while the corresponding optimal bidding strategy guarantees positive profits in all scenarios (as seen in Fig. 3).

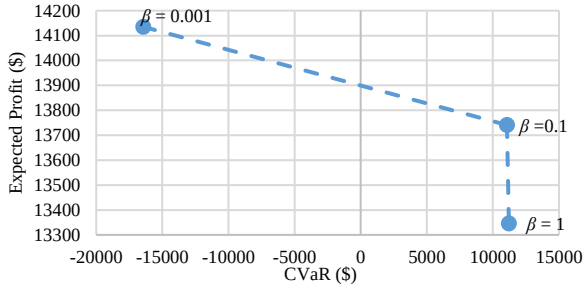

Fig. 1. Efficient Frontier: expected profit vs CVaR

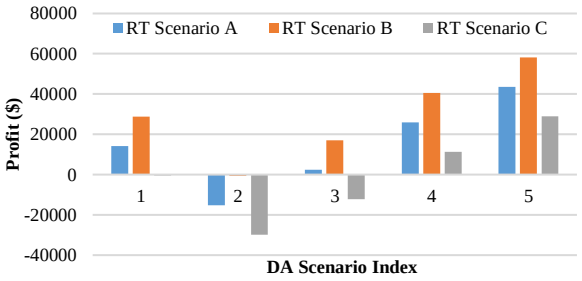

Fig. 2. Profit of risk-taker virtual bidder (β=0.001)

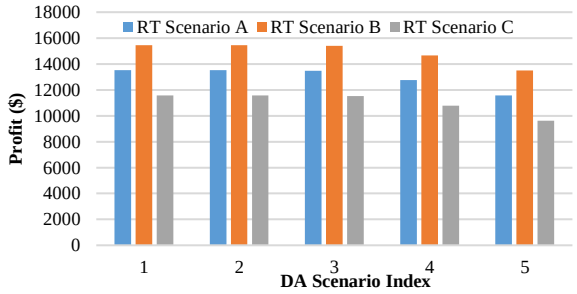

Fig. 3. Profit of risk-averse virtual bidder (β=1)

III. CONCLUSION

Virtual bidders face a variety of uncertainties when making bidding decisions in DAM. Scenario-based modelling is used to model these uncertainties, and CVaR metric is used to model the financial risk of the decisions. A risk-constrained bi-level optimization model is proposed to derive the optimal bidding strategy of a virtual bidder in participating in DAM market. A case study shows that the proposed model allows virtual bidders to choose a risk level that will balance between the expected profit across all scenarios and the potential losses in certain scenarios.

A Unified Droop-Free Distributed Secondary Control for Grid-Following and Grid-Forming Inverters in AC Microgrids

Sheik M. Mohiuddin and Junjian Qi
Department of Electrical and Computer Engineering
University of Central Florida
Orlando, Florida 32816 USA

***Abstract*—The inverter-based distributed generators (DGs) in microgrids usually operate in either grid-following (GFL) or grid-forming (GFM) control mode. In GFL mode the DG follows the voltage and frequency of the microgrid while in GFM mode it dictates voltage and frequency for the microgrid. In this paper, we propose a unified droop-free distributed secondary control for both GFL and GFM inverters based on distributed optimization. The proposed control regulates the frequency to nominal frequency, regulates the global average voltage in the microgrid to the rated voltage, and ensures accurate active and reactive power sharing among all GFL and GFM inverters. The DGs can communicate through a sparse communication network and share information about average voltage estimates and nominal active/reactive power. The effectiveness of the proposed control is validated through simulations on an eight-DG test microgrid with four GFL inverters and four GFM inverters.**

***Index Terms*—AC microgrid, distributed control, distributed optimization, frequency regulation, grid-following inverter, grid-forming inverter, power sharing, voltage regulation.**

I. Short Summary

Most existing papers on microgrid control only consider either GFL or GFM control mode. However, for exploiting the plug and play features of the microgrid and enabling a smooth transition between grid-connected and islanded modes, it is essential that DGs with both types of control capabilities be properly coordinated. In this paper, we propose a unified droop-free distributed secondary control for both GFL and GFM inverters. The contributions are summarized as follows.

1) A novel unified droop-free distributed secondary control framework utilizing a single communication network is developed for both GFL and GFM inverters based on a formulated distributed optimization problem.
2) The proposed control has a very similar structure for both GFL and GFM inverters and is very easy to implement. Both GFL and GFM inverters are coordinated to participate in frequency and voltage regulation.
3) Steady-state analysis shows that the proposed control can regulate the frequency to nominal frequency, regulate the average voltage of all inverter output buses to rated voltage, and achieve active and reactive power sharing among all GFL and GFM inverters.

II. Secondary Control for GFL and GFM Inverters

The design objectives of the secondary frequency and voltage control include 1) regulating the frequency back to nominal frequency, 2) regulating the average voltage of the output buses of all inverters to the rated voltage, and 3) achieving proportional active and reactive power sharing among all GFL and GFM inverters. Therefore, we define the following objective function for the secondary control:

$$\min f = \sum_{i=1}^{N} f_i, \tag{1}$$

with

$$f_i = \frac{N\alpha}{2}\left(V_{\mathrm{r}} - \overline{V}\right)^2 + \frac{1}{2}\sum_{j\in\mathcal{N}_i^c} a_{ij}(\lambda_{P_i} - \lambda_{P_j})^2 + \frac{1}{2}\sum_{j\in\mathcal{N}_i^c} a_{ij}(\lambda_{Q_i} - \lambda_{Q_j})^2, \tag{2}$$

where $\alpha > 0$ is a design parameter, $\overline{V} = \sum_{k=1}^{N} V_k/N$ is the average voltage of all inverter output buses, V_{r} is the rated voltage (i.e., 1.0 in per unit), $\mathcal{N}_i^c$ denotes the neighbors of DG i in $\mathcal{G}$, and $\lambda_{P_i} = P_i/\overline{P}_i$ and $\lambda_{Q_i} = Q_i/\overline{Q}_i$ are the active and reactive power utilization ratios for inverter i with $\overline{P}_i$ and $\overline{Q}_i$ as the corresponding active and reactive power limits. The proposed secondary control for the GFL and GFM inverters are shown in Fig. 1.

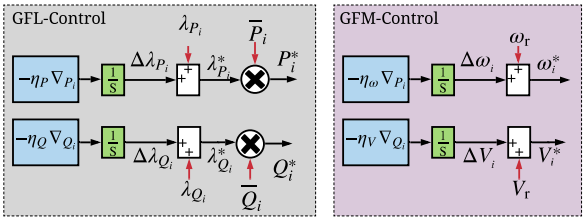

Fig. 1. Secondary control for the GFL and GFM inverters.

The performance of the proposed unified distributed control is validated through simulations on an eight-DG test microgrid implemented in Matlab/Simulink which demonstrates the controller success in frequency and voltage regulations as well as achieving the objectives of equal active and reactive power sharing among all the inverters.

A Game-Theoretic Approach to Model Interruptible loads: Application to Micro-Grid Planning

Soheil Mohseni, Alan C. Brent, Daniel Burmester, Will N. Browne
Sustainable Energy Systems, Faculty of Engineering, Victoria University of Wellington, Wellington, 6140, New Zealand
Email: {soheil.mohseni, alan.brent, daniel.burmester, will.browne}@vuw.ac.nz

***Abstract*—Exploiting the flexibility offered by demand response (DR) resources could have a significant impact on the long-term economic viability of renewable and sustainable energy systems (RSESs). While several mature DR programs exist in the literature, the potential savings offered by forming coalitions in the models of electricity sector decision-making is less well explored. Accordingly, using insights from cooperative game theory that provides a platform to enforce and sustain cooperation among the involved players, this study presents the first long-term demand-side resource projection framework tailored towards the design optimization of RSESs.**

Keywords—Microgrids, Sizing, Demand response, Game theory.

I. Key Contributions

Notably, two novel generalizations of standard renewable energy system planning are established: (1) a characterization of the epistemic uncertainty associated with the delivery of incentive-responsive loads in the long run, and (2) a quantitative analysis of the strategic, interacting choices of economic agents involved in the game – the utility, demand response aggregators (DRAs) that parcel up a set of smaller active loads, and end-users – based on cooperative game theory.

II. Key Test System and Model

The conceptualized microgrid (MG), shown in Fig. 1, consists of solar photovoltaic (PV), wind turbine (WT), and micro-hydro (MH) power generation technologies, a super-capacitor (SC) bank, an inverter, an electrolyzer, a hydrogen tank, a fuel cell (FC), and electric vehicle supply equipment (EVSE) to serve different customer classes mediated by DRAs. A customer comfort-preserving optimization model that uses the tit-for-tat strategy was developed for the long-term equipment capacity planning of grid-independent MGs, the flowchart of which is shown in Fig. 2.

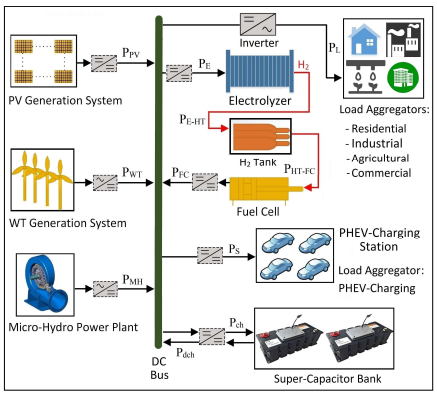

Fig. 1. Schematic diagram of the conceptualized test-case micro-grid system.

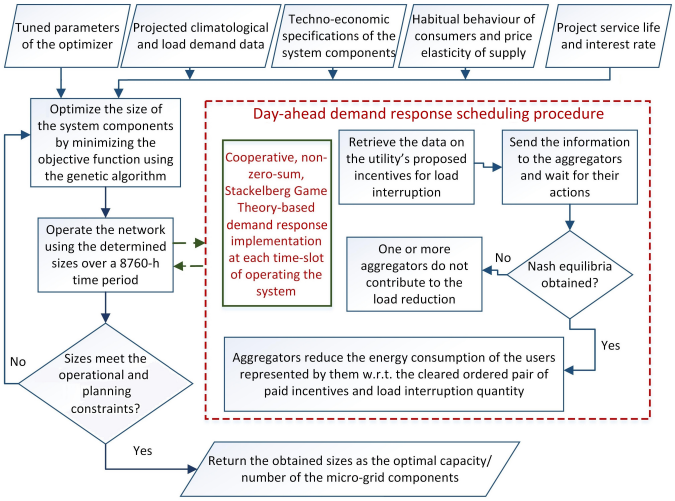

Fig. 2. Flowchart of the DR-integrated MG design optimization model.

III. Key Results and Discussion

The impact of the proposed game-theoretic DR scheduling framework (GT-DR) on the load curve fed into the optimization model is compared to its non-game-theoretic counterpart (NGT-DR) and the baseline scenario (NO-DR) in Fig. 3 for the day where the annual peak demand occurs. The figure reveals that the cooperative arrangement of DR resources can play a key role in peak load shaving. As Table I demonstrates, the improved load factor, by leveling out seasonal demand fluctuations in the light of identifying the best coalitions of the agents and an optimal distribution of the resulting total payoffs, enables significant savings in the total net present cost (TNPC).

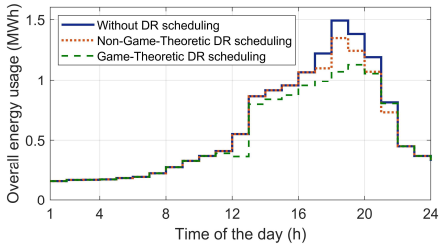

Fig. 3. Impact of demand response on the shape of the daily load profile.

TABLE I. MG Design Optimization Results For Different Scenarios

Scen.	PV (kW)	WT (kW)	MH (kW)	FC (kW)	SC (kWh)	Elec. (kW)	Tank (kg)	Inv. (kW)	EV-SE (kW)	TN-PC ($)
GT-DR	243	1.1k	588	860	77.1	1.1k	680	1.3k	66	9.7m
NGT-DR	243	1.5k	784	920	84.1	1.3k	713	1.4k	88	11.1 m
NO-DR	243	1.6k	882	975	91.6	1.5k	749	1.5k	154	12.0 m

Overcurrent Protection Scheme for the IEEE 13-Node Benchmark Test Feeder with Improved Selectivity

Muhammad Yousaf *, Kashem M. Muttaqi, Danny Sutanto
School of Electrical, Computer and Telecommunications Engineering
University of Wollongong, NSW 2500, Australia
*my701@uowmail.edu.au

***Abstract*—The IEEE 13-node test system has been used widely for evaluating the protection strategies. This paper focuses on the design of a robust overcurrent protection (OCP) scheme for the IEEE 13-bus test feeder using standardized procedures to provide a benchmark protection data for future research studies. The protection strategy used in this paper employ the coordination study among the relaying protective devices and fuses to improve the selectivity of the designed OCP scheme. The designed protection strategy has been validated for all types of fault events to demonstrate a realistic scenario. The proposed protection data will be utilized for the future protection studies performed on IEEE 13-node benchmark test system.**

***Index Terms*—fault studies, overcurrent protection, IEEE 13-node test feeder, protection devices.**

I. Introduction

THE IEEE has developed the IEEE 13-node radial test feeder for use by researchers for the verification of their research outcomes, due to its semblance with a real distribution network with unbalanced loading conditions. Currently, no data is available in the literature for the protection setting of this test feeder. This paper proposes an OCP scheme for the IEEE 13-node radial test feeder by the comparing the load flow and fault studies results with the published literature. The paper presents n novel protection strategy that need to be developed for the reliable operation of the power networks using the IEEE 13-node radial test feeder under different fault scenario. The proposed allocation of optimal placement of the protective devices (PDs) and the determination of their protection setting can be utilized for future protection studies conducted on this benchmark test system as shown in Fig. 1.

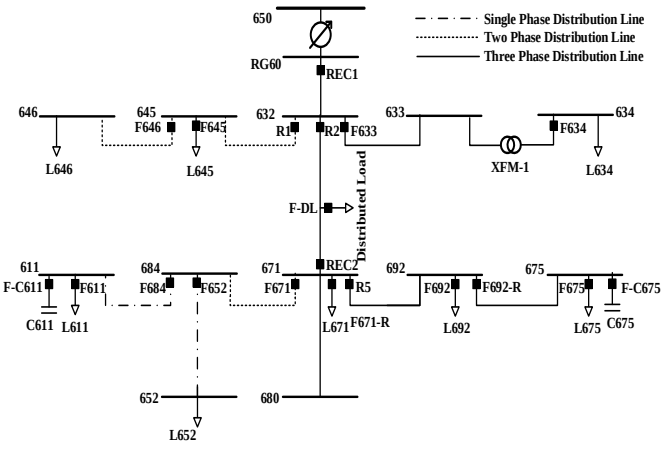

Fig. 1: The one line diagram of the IEEE 13-Node test feeder with optimal placement of the PDs

II. Proposed Overcurrent Protection Scheme

The proposed protection strategy incorporates the impact of future integration of distributed generations (DGs) on the original protection setting as well. If the branch current lies into the fault zone, this will lead to differentiate between fault locations as shown in Fig. 2. Each zone of protection will be tested to sort out the exact fault location to maximize the selectivity of the designed protection scheme. In case of loss of the coordination for recloser-fuse, the recloser's fast operation will be revised in the precise steps to restore the coordination. If the fast operation of recloser reaches its limitation, this will be followed by the upgradation of fuse. For long laterals with series fuses, fuse-fuse coordination will be restored by optimal upgradation of the fuse size unlike the relaying PDs.

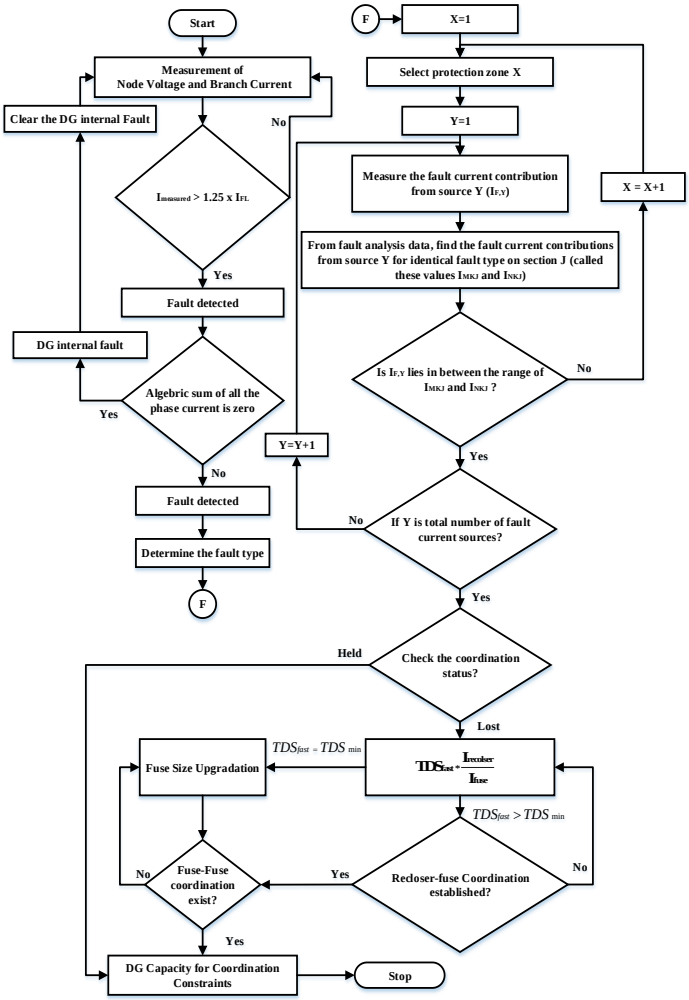

Fig. 2: Proposed Protection scheme for IEEE 13-node test feeder

Hidden Protection Challenges of Unbalanced Distributed Networks for Higher Concentration of Distributed Energy Resources

Muhammad Yousaf *, Kashem M. Muttaqi, Danny Sutanto
School of Electrical, Computer and Telecommunications Engineering
University of Wollongong, NSW 2500, Australia
* E-mail: my701@uowmail.edu.au

***Abstract*— Integration of the distributed energy resources (DERs) has empowered the electric power utilities to meet the increasing load demands efficiently at the reduced cost. Despite several benefits, there are some hidden protection challenges due to the large-scale integration of DERs with unbalanced distribution networks (DNs), which have not been properly addressed in literature. This research work investigates the impacts of higher concentration of DERs on the voltage swelling of the unfaulted phases during fault events for different DERs penetration level. Increase in voltage unbalance of real DNs having unbalanced voltage profile has been analyzed for uneven allocation of single-phase rooftop photovoltaic (PV) units. Impact of the grounding strategies of DERs on the operation of different types of protection strategy has been assessed for different grounding impedance followed by the mitigation strategy.**

Keywords*— Distributed energy resources, fault studies, overcurrent protection, distribution networks, grounding strategies.

I. INTRODUCTION

This research work focuses on quantifying the impacts of DGs on the hidden protection challenges. Section II examines the impact of DG penetration level on the overvoltage surges of unfaulted phases during ground faults. Rise of zero-sequence voltage has been explored in section III for unbalanced allocation of photovoltaic (PV) sources. Section IV discusses the grounding strategies for DERs units on the operation of PDs.

II. VOLTAGE SURGES FOR UNFAULTED PHASES

According to IEEE Standards C62.92.3-1993, the voltage increase in the unfaulted phase for a ground fault is equal to the net value of fault voltage and voltage drop across the fault impedance. The rise in the unfaulted phase is caused by the flow of the fault current through the capacitance to ground of these phases. Furthermore, this issue also depends on the grounding configuration and methodology of the network as depicted by simulation results shown in Fig. 1.

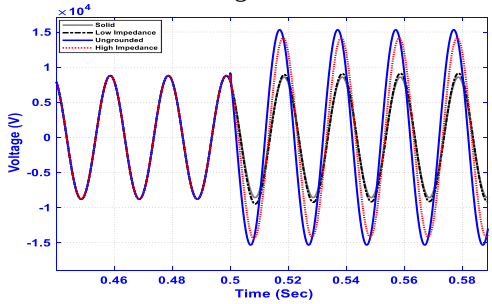

Fig. 1: Comparison of the voltage rise of unfaulted phases for different grounding strategies

III. IMPACT ON INCREASED NEUTRAL CURRENT

High concentration of the uneven allocation of DER units with the real unbalanced DNs may enhance the unbalanced voltage profile among different phases. This enlarged unbalanced among the phases will result in the rise of neutral potential rise (NPR) as illustrated in Fig. 2 generating high neutral current (I_N) through the neutral grounding wire causing health and safety hazards.

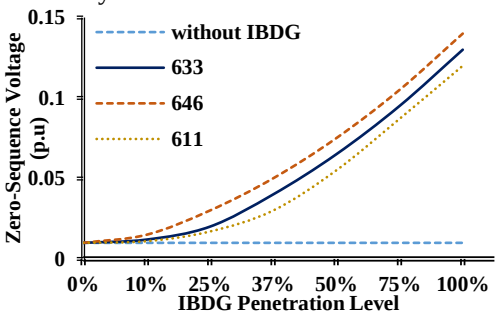

Fig. 2: Zero-sequence voltage for different IBDG concentrations for bus 632

IV. GROUNDING SCHEME FOR DISTRIBUTED GENERATION

Grounding configuration of the DGs defines its fault current contribution during the ground faults that may affect the operation of overcurrent PDs as shown in Fig. 3.

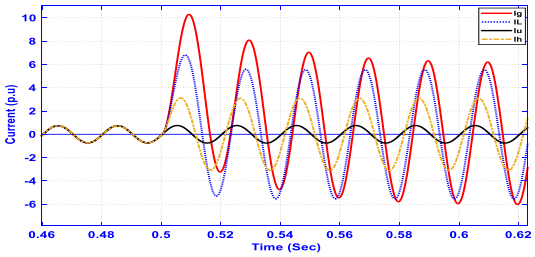

Fig. 3: Fault current contribution from SBDG for different grounding strategies

The proposed hybrid grounding scheme can be illustrated by the following flow chart as shown in Fig. 4. During grid connected (GC) mode, the high impedance grounding (Z_{GC}) will be designed to limit the zero-sequence current through the generator rotor according to its thermal capability during the ground faults. During the islanded (IL) mode of operation, the low impedance grounding (Z_{IL}) is recommended for the reliable operation of the overcurrent PDs and the reduced overvoltage stress on the unfaulted phases.

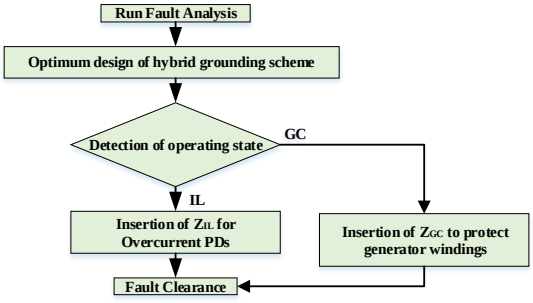

Fig. 4: Proposed strategy for design of hybrid grounding scheme

AMI Based Communication Scheme for Decentralized Volt/VAR Control

Valliappan Muthukaruppan
North Carolina State University
Raleigh, NC, USA
vmuthuk2@ncsu.edu

Mesut E. Baran
North Carolina State University
Raleigh, NC, USA
baran@ncsu.edu

***Abstract*—With the recent introduction of smart inverters to provide reactive power (VAR) support, the number of voltage support devices on the distribution system is expected to increase. However, integrating these devices with current centralized volt/var schemes is challenging due to increased real-time data requirements. This study investigates the use of two communication schemes for implementing a decentralized volt-var control scheme that can manage smart inverters along with traditional voltage regulation devices using the existing automatic metering infrastructure (AMI). A design guide is proposed to help with the placement of additional collectors needed for Volt/VAR, and the latency in communication is utilized to assess the performance of the two schemes using the IEEE 123 Node prototype system.**

***Index Terms*—Smart grid communication, volt/var control, radio mesh network, smart distribution system, automatic metering infrastructure.**

I. Introduction

Integrated volt/var control (IVVC) is the state-of-the-art control scheme utilized by the utilities to maintain the voltage on distribution systems within the ANSI standard. Current approaches are central control schemes, and they are seriously challenged by the increasing DER penetration in distribution feeders, primarily due to the high volume of data that needs to be sent to the controller. Recently, research is focused on developing distributed and decentralized volt/var optimization schemes that can address this challenge. However, very few studies have looked into the feasibility of incorporating such algorithms in present distribution feeders. The issue is that current distribution systems have minimal communication infrastructure.

The goal of this study is to develop a communication scheme based on existing AMI infrastructure for implementing a decentralized VVO scheme. The contribution of this paper is as follows:

- Provide a design guide for locating the collectors for a given distribution system
- Develop an analytical method to estimate the performance of the proposed communication scheme considering latency in communication.

II. Communication Scheme

Radio Frequency (RF) mesh based communication scheme and a model-based master-slave architecture for volt/var optimization is adopted in this study. Figure 1 illustrates the architecture of the VVO scheme. For a successful operation of VVO, the master needs the load data from all the nodes in the system. Hence, the communication can be split into two layers: layer-1 corresponds to data collection (upstream communication of load data) and layer-2 corresponds to the control loop (downstream communication of control commands). Since the number of smart inverters is typically lower than the load nodes in a distribution system and further grouping of these smart inverters under slaves makes the latency associated with layer-2 communication negligible. Hence in this study, only the layer-1 communication is investigated for performance assessment.

The two data collection schemes analyzed in this study are:

- **Scheme 1:** The smart meters at each house communicates its load data directly back to the master through the local collector.
- **Scheme 2:** The load data from the smart meters at each house connected to a distribution transformer is aggregated at the distribution transformer using an explicit data aggregator and then communicated back to the master through the local collector.

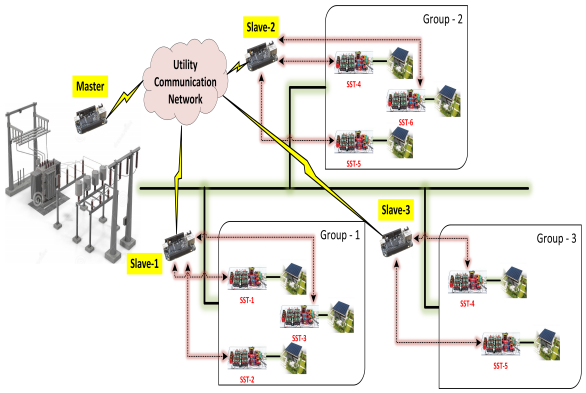

Fig. 1. The architecture of the adopted VVO scheme

Using a closed form equation for data generated by smart meters and the overall bandwidth degradation of channels inherent to RF mesh networks the overall latency in communication is estimated and utilized to compare the performance of the proposed communication schemes.

Distributed Dynamic State Estimation for Microgrids

Bang L. H. Nguyen
ECE Department
Clarkson University
Potsdam, NY, USA
bangnguyen@ieee.org

Tuyen V. Vu
ECE Department
Clarkson University
Potsdam, NY, USA
tvu@clarkson.edu

Thomas H. Ortmeyer
ECE Department
Clarkson University
Potsdam, NY, USA
tortmeye@clarkson.edu

Tuan Ngo
Electric Power Engineers
EPE Consulting
Austin, TX, USA
ngotuan@utexas.edu

***Abstract*—Conventionally, the dynamic state estimation of variables in power networks is performed based on the forecasting-aided model of bus voltages. This approach is effective in the stiff grids at the transmission level, where the bus voltages are less sensitive to variations of the load. However, in microgrids, bus voltages can fluctuate significantly under load changes, the forecasting-aided model may not sufficiently accurate. To resolve this problem, this paper proposes a dynamic state estimation scheme for microgrids using the state-space model derived from differential equations of power networks. In the proposed scheme, the branch currents are the state variables, whereas the bus voltages become the inputs which can vary freely with loads. As a result, the entire microgrids system can be partitioned into local areas, where neighbor areas share the common inputs. The proposed estimation scheme then can be implemented in a distributed manner. A novel Kalman-based filtering method is derived to estimate both states and inputs simultaneously. Only information of common inputs is exchanged between neighboring estimators. Simulation results compare the proposed method (SIE) with the conventional weighted least squared (WLS) and tracking state estimation (TSE).**

***Keywords*— Bad data detection, dynamic state estimation, distributed scheme, data fusion, microgrids.**

I. Contributions

The main contributions of this paper are as follows: 1) This work pioneer to resolve the problem of unknown inputs in dynamic state estimation using state-space models, 2) A novel Kalman-based filtering method is derived to simultaneously estimates both states and inputs, 3) The distributed implementation of proposed estimation scheme is introduced. 4) The communication and bad data detection protocol are presented.

II. Formulations

The dynamic model of branch currents in *dq*-frame are expressed as:

$$\frac{di_{ij,dq}}{dt} + j\omega_o i_{ij,dq} = -\frac{R_{ij}}{L_{ij}} i_{ij,dq} + \frac{1}{L_{ij}}\left(v_{j,dq} - v_{i,dq}\right), \quad (1)$$

where i, j denote the bus index; $\bullet_{dq}$ denotes as $(\bullet_d + j\bullet_q)$; ω_o is the angular frequency of the dq-rotating frame. Combined with PMU-based measurements, the state-space models of microgrids can be described in discrete form as:

$$\begin{cases} x_k = A_d x_{k-1} + B_d u_{k-1} + w_{k-1}, \\ z_{x,k} = C x_k + v_{x,k}, \ z_{u,k} = D u_k + v_{u,k}. \end{cases} \quad (2)$$

The input-to-output relationship of the system can be derived

$$z_{x,k} = CA_d x_{k-1} + CB_d u_{k-1} + Cw_{k-1} + v_{x,k}. \quad (3)$$

Combining (3) with the previous state estimates and input measurements, the following set of equations can be achieved.

$$\begin{bmatrix} \hat{x}_{k-1} \\ z_{u,k-1} \\ z_{x,k} \end{bmatrix} = \begin{bmatrix} I & 0 \\ 0 & D \\ CA & CB \end{bmatrix} \begin{bmatrix} x_{k-1} \\ u_{k-1} \end{bmatrix} + \begin{bmatrix} e_{x,k-1} \\ v_{u,k-1} \\ Cw_{k-1} + v_{x,k} \end{bmatrix}, \quad (4)$$

The WLS solution of (4) can be expressed as:

$$\begin{bmatrix} \hat{x}_{k-1} \\ \hat{u}_{k-1} \end{bmatrix} = (\mathcal{O}^T R^{-1} \mathcal{O})^{-1} \mathcal{O}^T R^{-1} \begin{bmatrix} \hat{x}_{k-1} \\ z_{u,k-1} \\ z_{x,k} \end{bmatrix}, \quad (5)$$

The predicted state vector and its covariance can be achieved as

$$\hat{x}_{k|k-1} = A_d \hat{x}_{k-1} + B_d \hat{u}_{k-1}, \quad (6)$$

$$P_{x,k|k-1} = [A_d \quad B_d] U_{k-1} \begin{bmatrix} A_d \\ B_d \end{bmatrix} + Q. \quad (7)$$

The state estimate and its covariance can be obtained as

$$\hat{x}_k = \hat{x}_{k|k-1} + K_k\left(z_{x,k} - C\hat{x}_{k|k-1}\right), \quad (8)$$

$$P_{x,k} = (I - K_k C) P_{k|k-1}. \quad (9)$$

where $K_k = P_{x,k|k-1} C^T \left(C P_{x,k|k-1} C^T + R_x\right)^{-1}$

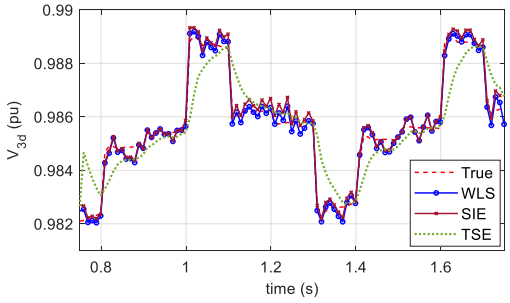

Figure 1. The comparison of estimates of $\boldsymbol{v_{3d}}$

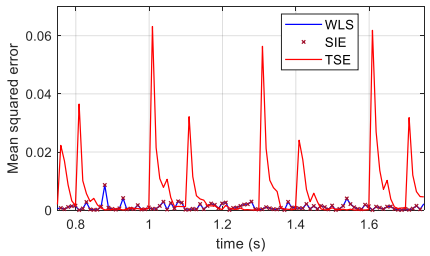

Figure 2. The comparison of mean squared errors.

Efficient Operation of Distribution Grids with High Penetration of DER through Cluster Control

Shyamal Patel, *Student Member, IEEE,* Adedoyin Adedokun, *Student Member, IEEE,* Krishna Murari, *Member, IEEE,* Sukumar Kamalasadan, *Senior Member, IEEE,* Sumit Paudyal, *Member, IEEE*

***Abstract*—The proposed approach of distribution grid clustering and feeder-head error minimization was tested on IEEE 123-bus distribution feeder with 10 PVs and 10 energy storage systems. The cluster controller primarily controls the energy storage on the feeders to minimize the error on the tie-line flows. The optimal number of clusters was determined using the eigen gap analysis. managed by an optimal power flow framework.**

***Index Terms*—Power balance, Resiliency, DER, Clustering**

I. Proposed Approach

We propose a hierarchical approach for controlling DERs connected to distribution feeders as shown in Fig. 1. At the top hierarchy, Distribution System Operator (DSO) solves optimal power flow (OPF) problem to find set points of legacy control devices (tap changer, cap banks, network switches), and aggregate dispatch of the areas (set points to area controller). The area controller solves a second OPF problem at finer resolution using a distributed approach [1] and develops set points for DER clusters. The distribution feeder with high DER penetration is clustered optimally using spectral clustering [2]. The cluster boundaries are virtual and would be changing dynamically with changing grid conditions. The loads within each cluster are primarily addressed by the distributed generation present in that cluster. The measurement taken across feeder connecting the clusters provides tracking error (i.e, dispatch minus response). These errors for each cluster are minimized by the individual cluster controllers. The remaining error is aggregated and the area controller tries to minimize the aggregate error at the area level. If the further error persists, then it is the role of the DSO to dispatch resources to minimize the net error seen from the sub-station. An OPF problem in general can be formulated as:

$$\underset{V,p,q}{\text{argmin}} \quad f(V,p,q) \tag{1}$$

$$\text{subject to :} \quad S_{ij} = V_i \left(V_i^* - V_j^*\right) y_{ij}^* \tag{2}$$

and with power and voltage limits. Spectral Clustering framework can be described as

$$L = DA \tag{3}$$

Here, L is the lagrangian matrix, D is a diagonal matrix and A is the powerflow based adjacency matrix.

$$L_n = D^{-\frac{1}{2}} L D^{-\frac{1}{2}} \tag{4}$$

Here, L_n is the normalized lagrangian matrix

This material is supported by the U.S. Department of Energy under Award Number DE-EE0008774. Authors are with the University of North Carolina at Charlotte and Florida International University.

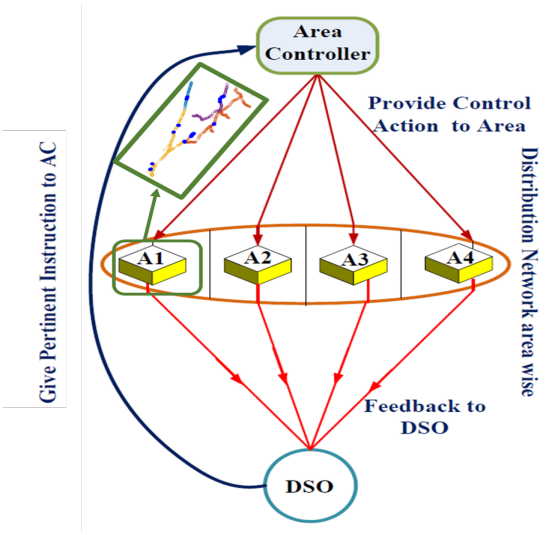

Fig. 1: Flowchart: Proposed approach

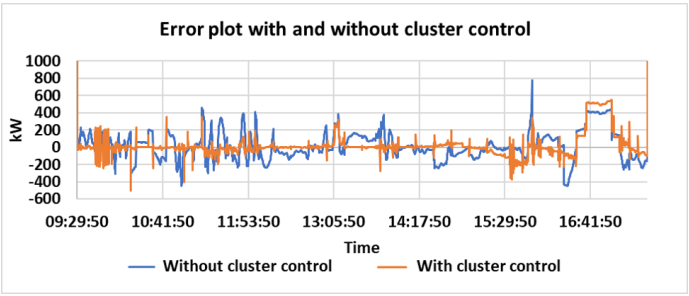

Fig. 2: Power error as observed at feeder head by area controller

II. Results

The proposed approach of distribution grid clustering and feeder-head error minimization was tested on IEEE 123-bus distribution feeder with 10 PVs and 10 energy storage systems. The cluster controller primarily controls the energy storage on the feeders to minimize the error on the tie-line flows. The optimal number of clusters were determined using the eigen gap analysis. Fig. 1 shows the distribution grid clusters for a snapshot of power flow. The resulting error observed by area controller is shown in Fig. 2.

References

[1] A. Thakallapelli and S. Kamalasadan, "Alternating direction method of multipliers (admm) based distributed approach for wide-area control," in *2017 IEEE Industry Applications Society Annual Meeting*, 2017, pp. 1–7.

[2] R. J. Sánchez-García, M. Fennelly, S. Norris, N. Wright, G. Niblo, J. Brodzki, and J. W. Bialek, "Hierarchical spectral clustering of power grids," *IEEE Transactions on Power Systems*, vol. 29, no. 5, pp. 2229–2237, 2014.

Peer-to-Peer Energy Trading in Smart Grids Considering Network Utilization Fees

Amrit Paudel, Yang Jiawei, Hoay Beng Gooi
Nanyang Technological University, Singapore

***Abstract*—In the P2P approach, each actor negotiates directly with a set of trading partners. A proper market clearing mechanism is necessary to facilitate energy transactions among different parties. This work proposes a decentralized market clearing mechanism for P2P energy trading, considering the privacy of the agents as well as utilization fees for using the third party owned network. Grid-related costs in P2P energy trading are considered by calculating network utilization fees using an electrical distance approach.**

I. System Model

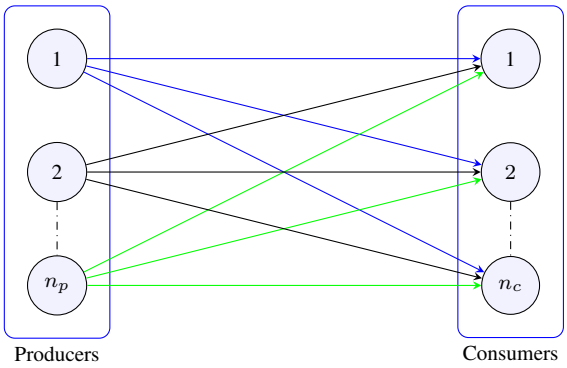

Fig. 1. The schematic model of P2P energy market

II. Simulation Results

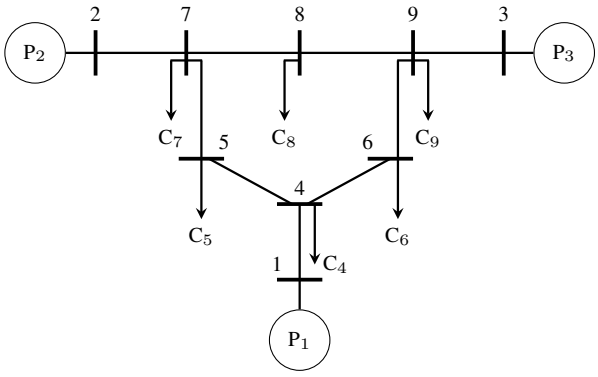

Fig. 2. IEEE 9-bus system for simulation studies

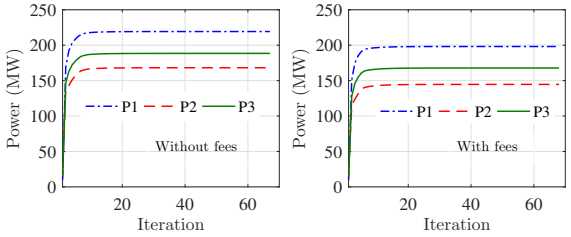

Fig. 3. Evolution of supply of producers in 9-bus system

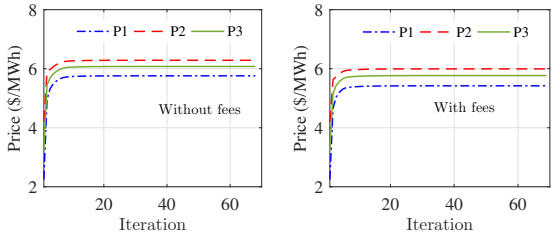

Fig. 4. Evolution of price of producers in 9-bus system

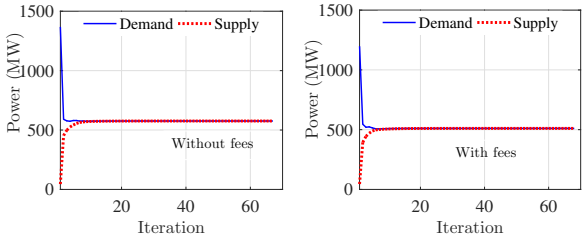

Fig. 5. Evolution of total demand and supply in 9-bus system

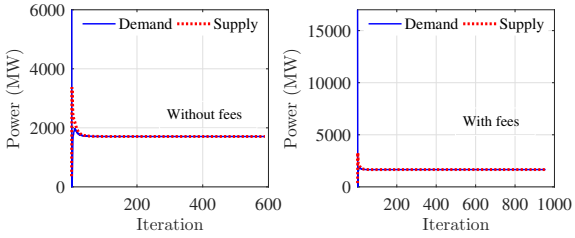

Fig. 6. Evolution of total demand and supply in 39-bus system

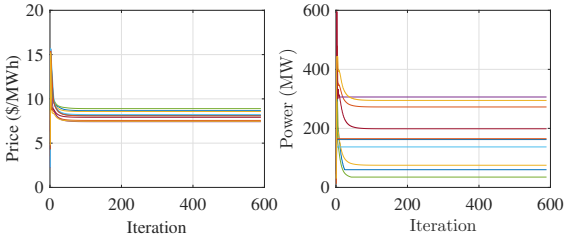

Fig. 7. Evolution of prices (left) and supply (right) without network fees in 39-bus system

III. Conclusion

This work presented a fully decentralized market clearing mechanism for P2P energy trading. It has been found that the trading decision of consumers not only depends on the prices offered by producers but also depends on the electrical distance from producers if network utilization fees are considered in P2P trading.

Impact Assessment of Real Time Demand Control on Active AC/DC Hybrid Distribution Networks

Subho Paul, *SIEEE*
Electrical Engineering, IIT Roorkee
Roorkee, India
spaul@ee.iitr.ac.in

Narayana Prasad Padhy, *SMIEEE*
Electrical Engineering, IIT Roorkee
Roorkee, India
nppeefee@iitr.ac.in

***Abstract*— Large penetration of DC distributed energy resources and DC electrical loads into the existing AC distribution network transforms the conventional AC network to an AC/DC hybrid distribution network (HDN). However, intermittent renewable energy, uncertain market energy price and vulnerable load demand causes serious real time power imbalance situation. To address the above deficiency, this paper assesses the impact of real time demand control on AC/DC HDN by designing a multi-objective, non-linear, convex, real time energy management algorithm based on Lyapunov optimization technique, which works only by knowing the updated present data of the uncertain parameters rather than their probabilistic estimated values.**

I. Introduction

For the last few decades, exhaustive burning of fossil fuels and increasing global warming threat forced the power sector to integrate renewable energy resources in the electrical energy generation portfolio. A significant share of green energy comes from battery collocated photovoltaic panels, which produces DC power. These DC distributed energy resources and evolution of DC loads necessitate the unification of DC networks with the existing AC networks, and results AC/DC HDN. The proposed real time algorithm aims to control the load demand at each bus of the network against abrupt change in energy price and PV generation. The proposed multi-objective strategy simultaneously minimizes the energy cost and maximizes the usefulness of the consumed power, designed as value function. The strategy is formulated as non-linear convex optimization problem. The defined real time demand control process is solved by using merger of queuing theory and Lyapunov optimization process. The proposed solution process does not require the probabilistic estimated values of the uncertain parameters and works only with their present values.

II. Real Time Optimization Framework

The main aim of the optimization problem is to minimize the energy cost i.e. pay off to the main grid. However, it also has the responsibility to satisfy its customers with less load curtailment Therefore, objective function for the optimization problem is given by,

$$\underset{\Omega_t}{Min}\ \ O_t\left(\Omega_t\right)=C_t-\sum_{n\in N}V_{n,t}\left(X_{n,t}^{L}\right) \tag{1}$$

$$\Omega_t=\left[X_{n,t}^{PV},Y_{n,t}^{PV},X_{n,t}^{grid},Y_{n,t}^{grid},X_{n,t}^{bat},Y_{n,t}^{bat},X_{n,t}^{L},Y_{n,t}^{L},M_{nm,t},\left|V_{n,t}\right|,\theta_{n,t}\right]$$

$$\text{Here, } C_t=\sum_{n\in N}X_{n,t}^{grid}\rho_t^{RTP}\Delta t \tag{2}$$

$$\text{And } V_{n,t}\left(X_{n,t}^{L}\right)=\gamma_t X_{n,t}^{L,\max}\left(1-\exp\left(-\xi_t X_{n,t}^{L}\right)\right),0<\xi_t<1 \tag{3}$$

Now, if the load control operation is implemented at each time span separately, then overall benefit is acquired by minimizing the long term value of the equation (1) as specified below,

$$\underset{\Omega_t}{Min}\ \ \lim_{T\to\infty}\frac{1}{T}\sum_{t=0}^{T-1}\mathrm{E}\left[O_t\left(\Omega_t\right)\right] \tag{4}$$

Difficulty regarding time average objective function, choice of battery charging/discharging time and load curtailment hours are resolved here by implementing the concept of merger of queueing theory and Lyapunov optimization. The revised real time optimization problem is given by,

$$\min_{\Omega_t}\ \ \mathbb{Z}=V\sum_{n\in N}\left(Q_{n,t}X_{n,t}^{bat}\Delta t\right)-\sum_{n\in N}\frac{L_{n,t}X_{n,t}^{L}}{X_{n,t}^{L,\max}-X_{n,t}^{L,\min}}+AO_t\left(\Omega_t\right) \tag{5}$$

Subject to operating constraints of each network components and the hybrid distribution network architecture.

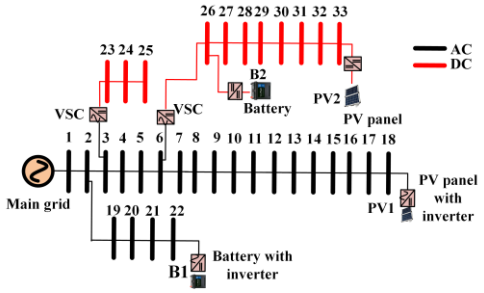

Fig. 1 Modified IEEE 33 bus AC/DC hybrid distribution network

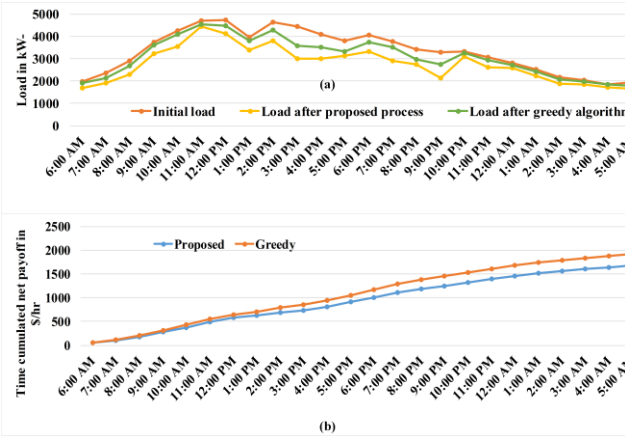

Fig. 2 Simulated output- (a) load demand, (b) time cumulated net pay off of the AC/DC HDN after applying proposed and greedy process

III. Simulation Results

The formulated real time demand control process is validated on modified IEEE 33 bus AC/DC HDN as shown in Fig. 1. The simulation outcomes depicted in Fig. 2(a) shows that the proposed real time load control process reduces the demand at each time step and that results the peak reduction of 6.04% (from 4730.4 kW to 4444.39 kW). Comparisons of proposed process with the greedy algorithm based solution technique are depicted in Fig. 2. As can be seen from Fig. 2(a) that the demand reduction is more in case of proposed one (4.1% for greedy process) and that results low time accumulated net pay off for the distribution network owner (Fig. 2(b)). Solution time at each time step for the proposed strategy to reach the global optimum ranges from 5.57 sec to 5.62 sec, which is quite low. Hence, the proposed technique is a real time strategy as the solar generation, load and energy price do not update within 5 to 6 sec.

Ground Source Heat Pump Modeling and Aggregation for Services Provision in Electricity Markets

Dario Peralta, *Student, IEEE*, Kankar Bhattacharya, *Fellow, IEEE*, and Claudio Cañizares, *Fellow, IEEE*
Department of Electrical and Computer Engineering
University of Waterloo, Waterloo, Ontario, Canada
{d2peralt, kankar, ccanizar}@uwaterloo.ca

***Abstract*—This poster presents a thermal load aggregator model to determine the optimal heating load dispatch to control the house temperature for a community comprising many houses, considering two heating alternatives: Heating Ventilation and Air Conditioning (HVAC) system, and the proposed Ground Source Heat Pump (GSHP) system. The study presented here considers a load aggregator that would submit demand bids to the utility operator and purchase electricity for its clients, considering two different strategies: maximizing the customer comfort (Base Case), and minimizing the aggregator's total electricity cost.**

***Index Terms*—Ancillary services, electricity market, ground source heat pump, HVAC, load aggregator.**

I. Introduction

There are not many comparisons between aggregated GSHP and HVAC loads for power consumption reduction, and no load aggregator models have yet been reported for optimal power dispatch of heating/cooling loads with GSHP systems. Therefore, a thermal load aggregation approach to minimize the aggregator's energy procurement costs is discussed in this work, based on a mathematical model that includes the GSHP characteristics to optimize the electricity usage by end-users, while considering household thermal comfort.

II. Test System and Results

The load aggregator is assumed to provide electricity to 800 houses, as in [1], and that each house has the same thermal characteristic. The aggregator collects information on the uncontrolled loads in the house, the house thermal and heating system characteristics, and the current and forecasted ambient temperature, in order to optimally schedule the heating load of each house. The energy purchase strategy of the aggregator is implemented through its participation in the Day-ahead (DA) and Real-Time (RT) markets, as illustrated in Fig. 1.

Tables I and II present a summary of the aggregator's total procurement cost and the total heating energy over a 24-hour period, also its total peak load demand and the time when it occurred. Furthermore, the differences between HVAC and GSHP systems are summarized in Table III, demonstrating the effectiveness of the proposed two-stage strategy for optimal aggregator load dispatch of HVAC and GSHP systems, and the advantages of GSHP compared to HVAC.

This work has been supported by the NSERC Energy Storage Technology (NEST) Network, Canada, http://www.ryerson.ca/nestnet/

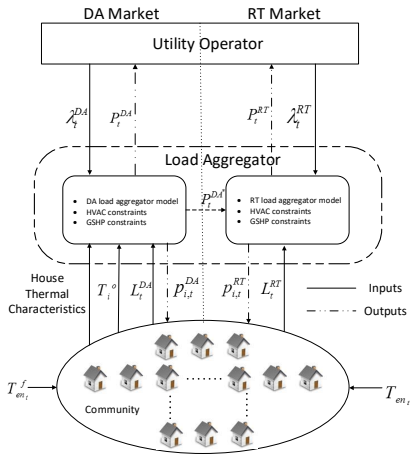

Fig. 1: Framework of the load aggregator participating in the electricity market.

TABLE I: Aggregator with HVAC systems.

			Total Energy (kWh)	Peak Demand (kW)	
		Total Cost ($)	Heating Load	Demand	Hour
Base Case		5,700	68,645	6,585	19:00
Aggregator	DA	4,944	65,229	6,550 (-0.54% *)	17:00
	RT	133	65,625 (-4.4% *)	6,303 (-4.3% *)	17:00
	Total	5,078 (-10.9% *)			

* With respect to Base Case

TABLE II: Aggregator with GSHP systems.

			Total Energy (kWh)	Peak Demand (kW)	
		Total Cost ($)	Heating Load	Demand	Hour
Base Case		4,999	53,655	5,800	8:00
Aggregator	DA	4,576	52,096	5,750 (-0.86% *)	17:00
	RT	68	52,735 (-0.21% *)	5,787 (-0.21% *)	17:00
	Total	4,645 (-7.1% *)			

* With respect to Base Case

TABLE III: HVAC vs GSHP systems.

		Δ Cost* ($)	Δ Heating energy* (kWh)	Δ Peak load* (kW)
Base Case		-12.3%	-21.8%	-11.9%
Aggregator	DA	-7.4%	-20.1%	-12.2%
	RT	-48.8%	-19.6%	-8.2%
	Total	-8.5%		

* With respect to HVAC

References

[1] S. Chen, Q. Chen, and Y. Xu, "Strategic bidding and compensation mechanism for a load aggregator with direct thermostat control capabilities," *IEEE Transactions on Smart Grid*, vol. 9, pp. 2327–2336, May 2018.

Coupling Effects and Impact of EHV AC Cable Circuits on LV AC Systems within a Tunnel

Nils Pfeifer
Mustafa Kizilcay
Simon Papenheim
Pawel Malicki
University Siegen
Chair of Electrical Power Systems
Siegen, Germany
nils.pfeifer@uni-siegen.de

***Abstract*— The power generation by wind farms in the north and northeastern area of Germany has significantly increased during the last ten years. Within the scope of transmission system expansion plan of Germany new EHV transmission lines at the 380-kV level will be erected as mixed lines consisting of several underground cable and overhead line (OHL) sections. The easiest way for the cable installation are trenches in the ground, but this is not always possible, so that erection of cable tunnels is inevitable in certain areas. Within such a tunnel, several transmission systems are intended to be placed, resulting in a high electromagnetic field intensity and therefore coupling effects. Due to the used equipment, it may happen that a low-voltage system is also required within the tunnel to supply those equipment. In this investigation the influence from the EHVAC systems to LV AC systems in different configurations is analyzed and some measures to reduce those coupling effects are examined.**

***Index Terms*—Coupling Effects, EMI, HVAC Tunnel System, Magnetic Field**

I. INTRODUCTION

In addition to the ever-increasing demand for energy, the changeover to renewable energy sources in Germany requires a transmission grid reinforcement to increase the transmission capacity from North to South. Already during the planning, problems arise with laws and expectation of the rural communities, which usually prefer underground cables to the erection of new overhead lines. Therefore, a "mixed" line with overhead and underground cable sections will be the compromise, because a complete implementation with cables is technically not possible. In this investigation a 380-kV cable section is studied, whereat the coupling within a tunnel due to the electromagnetic field and the narrow space between the cables is the main focus.

There are two methods to place the cables in the underground. The usual one uses a cable trench and protective pipes. Hence, for this method the soil must be free for earthworks, which may not be possible in urban regions. The alternative is a cable tunnel, whereby the digging over the complete length is not necessary anymore. In addition to the actual tunnel, integrated buildings will be constructed, which are needed for the installation and for maintenance. Between those buildings low-voltage (LV) supply or communication lines are needed and can be placed within the tunnel. Due to the narrow space inside the tunnel, there is high field strength caused by EHV cables, which leads to strong coupling effects that may cause high stress on LV cables and/or equipment. Consequently, the field strength and the resulting coupling must be examined to ensure proper operation of the low voltage components inside the tunnel.

In this investigation the interaction of 380-kV AC cables with a parallel LV cable system in a cable tunnel is analyzed. The HVAC part consists of two independent three-phase systems. For the full power transmission, two circuits with two single-core cables per phase are required, so that overall twelve EHV cables are installed in the tunnel. The schematic cross section of the tunnel is shown in Figure 1.

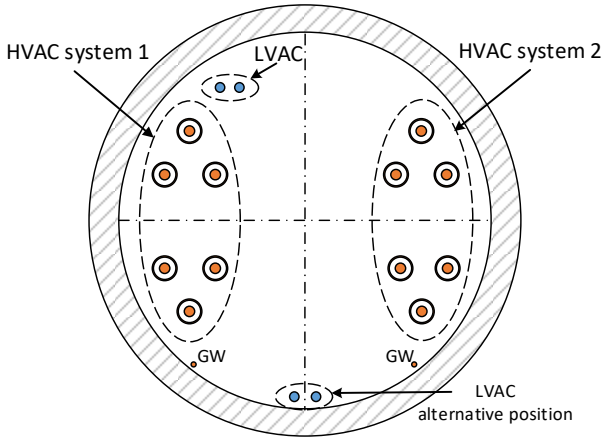

Figure 1. Schematic tunnel layout

On each side of the tunnel an EHV AC system with six cables belonging to the 380-kV transmission grid is located. The positions of the LV systems and several mitigation alternatives are studied with the aim to reduce the influence of the 380-kV AC system on the LV system. In addition, different cases with cross-bonding of cable sheaths and several operational states are analyzed.

For this purpose steady-state and transient analyses will be performed using EMTP-ATP (ElectroMagnetic Transients Program, Version Alternative Transients Program).

Generation of Synthetic Multi-Resolution Time Series Load Data via Generative Adversarial Networks

Andrea Pinceti, Lalitha Sankar, and Oliver Kosut
School of Electrical, Computer and Energy Engineering
Arizona State University
Tempe, AZ, 85287

I. Introduction

Historically, power system research has been based around the development of simplified physical models and the study of their interactions within a system. However, in recent years, the field of machine learning has matured and improved to the point where it can provide real value to power system operations; for this reason, a large portion of the research work focuses on applying machine learning techniques to power system applications. This change in direction represents a major shift: moving away from physics-based device models to a data-centric analysis of system behaviors.

Within this new paradigm, the availability of large amounts of real data is crucial. Unfortunately, while power system models of all kinds are readily available, data is a much more scarce resource. The few researchers who have relationships with electric utilities can get access to real measurements through long processes involving non-disclosure agreements; in general though, the broader research community must rely on the very few and limited datasets that are publicly available.

The goal of our project is to develop an open source tool for the generation of synthetic time-series load data at varying sampling rates and for different time lengths. Leveraging a proprietary dataset of high resolution measurements from hundreds of phasor measurement units (PMUs) across many years of operation, we can model the behavior of real system loads and subsequently generate realistic-looking data on demand. The focus on load data is motivated by the fact that loads are one of the main drivers of power system behaviors and they represent a latent variable: loads depend on phenomena outside of the power system itself (consumer behaviors, weather, etc.). Thus, realistic load profiles can be used as an input to existing power system programs and, running dynamic simulations, electric quantities such as voltages and currents can be accurately determined.

II. Load Generation Scheme

Having access to a dataset of almost 100 TB of uncompressed PMU data allows us to observe load profiles at 30 samples per second for many consecutive years, thus capturing fast dynamic behaviors as well as long term seasonal patterns. By first decomposing and down-sampling the raw PMU load data at different levels, we can use advanced generative adversarial networks (GANs) to learn a generative model for each time horizon and resolution. GANs are a powerful machine learning algorithm in which a generator (usually a deep neural network) is trained to generate realistic data by making it "compete" against a discriminator whose job is to distinguish between real samples and those created by the generator.

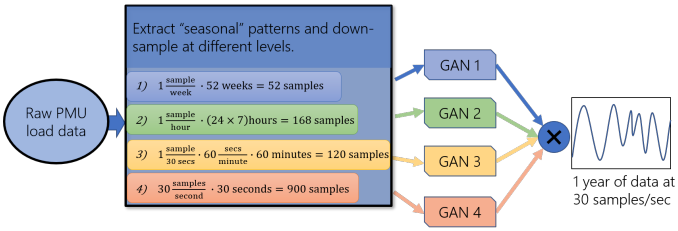

Fig. 1. Overview of the time-series load data generation scheme.

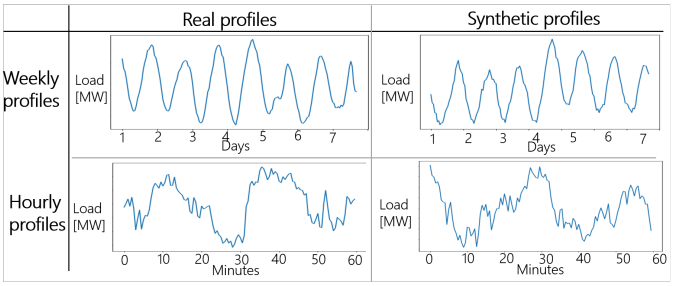

Fig. 2. Overview of the time-series load data generation scheme.

Figure 1 shows an overview of the generation scheme. The raw PMU load data is down-sampled at four different levels: 1) yearly profile, 2) weekly profile, 3) hourly profile, and 4) minute profile. A GAN model is trained individually for each level. The fully trained model can then be shared and used by researchers to generate any type of data required by their specific application. For example, for a dynamics study, two hours of data at 30 samples per second might be required; GANs 3 and 4 will be used to generate the hourly patterns and sub-second patterns, respectively. Figure 2 shows examples of real and generated load profiles at the weekly and hourly levels; the GANs learn to create completely new realistic-looking profiles.

A Dynamic Model of Small Modular Reactor Based Nuclear Plant for Power System Studies

Bikash Poudel*, *Student Member, IEEE*, Ramakrishna (Rama) Gokaraju*, *Senior Member, IEEE*
*Department of Electrical and Computer Engineering, University of Saskatchewan, Saskatoon, SK, Canada
Email: bikash.poudel@usask.ca, rama.krishna@usask.ca

***Abstract*—Small modular reactors (SMRs), an emerging nuclear power plant technology, are suitable for large grids as well as remote load centers and offer load following and frequency response capabilities. This poster presents a dynamic model of an integral pressurized water reactor (iPWR)-type SMR, modeled in Siemens PTI PSS/E, to assess the contribution of the reactor to the power system dynamics. The proposed SMR model mimics the heat generation process and subsequent heat transfer process with the inclusion of the reactor core based on point kinetics, primary coolant based on natural circulation, and a simplified three lump representation of the steam generator (SG). The SMR model is integrated with the modified IEEE standard GGOV1 turbine-governor system and a power system study is conducted. Results show the power system and reactor responses when subjected to electrical variations of 20% rated electrical output (REO) with a valve rate limit of ±80% REO/min.**

I. Key Figures

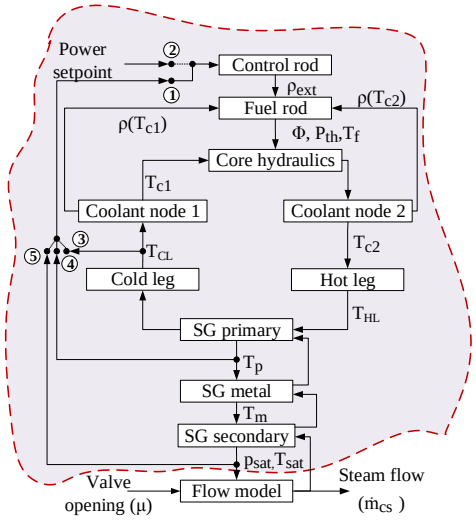

Fig. 1. SMR block diagram. Shaded region shows the reactor components.

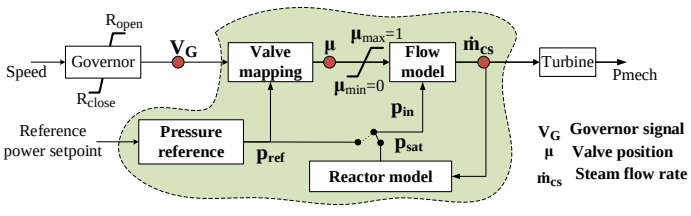

Fig. 2. GGOV1 modified and integrated with the SMR model. Shaded region shows the modifications with new modules.

II. Key Equations

The core neutronics is described by the average neutron flux (ϕ) formulated as a point kinetics model. The reactor thermal power (P_{th}) is proportional to the average neutron flux in the core. The mechanical power (P_{mech}) is a function of the enthalpy difference (Δh) and steam flow rate ($\dot{m}_{cs}$).

$$\frac{d\phi}{dt} = \frac{\rho}{\Lambda} - \frac{\beta}{\Lambda}\phi + \lambda C \tag{1}$$

$$P_{th} = \phi P_{th}^{r} \tag{2}$$

$$P_{mech} = \eta_T \Delta h \dot{m}_{cs} \tag{3}$$

III. Key Results

The proposed dynamic model is implemented in a single machine based power system model. The electrical load changes from 100% to 80% REO at 20 s. At 400 s, a 20% step increase brings the load back to 100% REO. The results show the importance of an SMR model for an accurate representation of system dynamics.

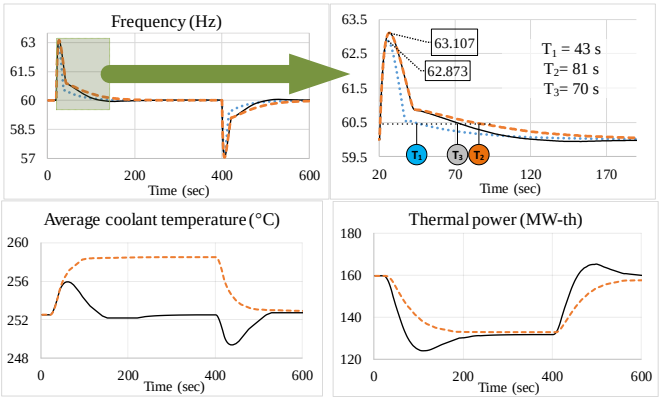

Fig. 3. Dynamic responses. Legends: Case I-Without Reactor (.....), Case II-With Uncontrolled Reactor (- - -), Case III-With Controlled Reactor (—).

References

[1] B. Poudel, K. Joshi, and R. Gokaraju, "A Dynamic Model of Small Modular Reactor Based Nuclear Plant for Power System Studies," *IEEE Trans. Energy Convers.*, IEEE Early Access, Nov. 30, 2019. DOI: 10.1109/TEC.2019.2956707

[2] T. Inoue, T. Ichikawa, P. Kundur, and P. Hirsch, "Nuclear plant models for medium- to long-term power system stability studies," *IEEE Transactions on Power Systems*, vol. 10, no. 1, pp. 141–148, Feb 1995.

[3] S. E. Arda and K. E. Holbert, "Implementing a pressurized water reactor nuclear power plant model into grid simulations," in *2014 IEEE PES General Meeting — Conference Exposition*, July 2014, pp. 1–5.

Security Constrained Unit Commitment with Corrective Demand Response

Arun Venkatesh Ramesh, *Student Member, IEEE*, and Xingpeng Li, *Member, IEEE*

***Abstract*—This work highlights the benefits of considering demand response by considering flexibility offered by controllable loads as a corrective action for post-contingency emergencies in day-ahead operations. A security-constrained unit-commitment (SCUC) with explicit corrective demand response actions is proposed and simulation results point cost savings. Since line and generator contingencies are infrequent, economic benefits are achieved without compromise in comfort level of customers in most cases. Currently, system operators predominantly utilize demand response program as a preventive action by shifting demand from peak to non-peak hours for system reliability but neglect the importance of such actions for post-contingency scenarios. The proposed model can bridge this gap, and it was tested on IEEE 24-bus system which shows significant cost savings in daily operations.**

I. Introduction

Smart grid technology advancements have brought two-way communications possible through sensing and control signals. Through the advanced metering infrastructure, system operators can determine and send signals to enable demand response (DR) for controllable loads. Typically, system operators use security-constrained unit-commitment (SCUC) to commit and obtain dispatch signals for generators to meet a forecasted day-ahead demand.

System operators often utilize preventive and corrective control actions to maintain system reliability. Mostly, DR through controllable loads are considered as a preventive action. DR benefits the system by moving non-critical deferrable loads from peak hours to non-peak hours increase the system flexibility while also increasing demand side market participation through financial incentives [1-2]. Though there are emergency DR plans that several system operators implement [3], they are solely based on supply and demand balance for frequency regulations and typically this is factored in the SCED process where operators handle DR through capacity markets and/or real-time markets [4-6].

Currently, the use of corrective demand response (CDR) in response to contingency is mostly not considered in the SCUC process, to the best knowledge of the authors. CDR can increase power system operational performance by reducing the operational costs when co-optimized with SCUC.

II. Key Modelling Equations

SCUC objective considering cost of CDR:

$$\text{Min: } operational\ cost + \sum_{n,c,t}(\pi_c * Lcost_n * DShed^c_{n,t}) + \sum_{n,j,t}(\pi_j * Gcost_n * DShed^j_{n,t}) \quad (1)$$

Post-contingency modeling of nodal balance with CDR:

$$\sum_{g\in g(n)} P_{g,c,t} + \sum_{k\in\delta^+(n)} P_{k,c,t} - \sum_{k\in\delta^-(n)} P_{k,c,t} = d_{n,t} - DShed^c_{n,t} \quad (2)$$

$$\sum_{g\in g(n)} P_{g,j,t} + \sum_{k\in\delta^+(n)} P_{k,j,t} - \sum_{k\in\delta^-(n)} P_{k,j,t} = d_{n,t} - DShed^j_{n,t} \quad (3)$$

$$DShed^c_{n,t}\ \&\ DShed^j_{n,t} \le \beta_n * d_{n,t} \quad (4)$$

where c is the contingent line; j is the contingent generator; t denotes the time period; $P_{g,c,t}/P_{g,j,t}$ and $P_{k,c,t}/P_{k,j,t}$ denotes the contingent generator dispatch of generator g and power flow on line k respectively; $d_{n,t}$ is the demand at node n. Here, $\pi_c * Lcost_n$ and $\pi_j * Gcost_n$ represents the probabilistic penalty cost associated CDR with respect line and generator contingency as shown in (1); $DShed^c_{n,t}$ and $DShed^j_{n,t}$ denotes the nodal demand curtailed as a corrective action for nodal balance for contingency of line c and generator j, respectively in (2)-(3). CDR is implemented only on participating non-critical demand denoted by a fractional value, β_n, of nodal demand in (4).

III. Results

The proposed SCUC-CDR was validated against traditional SCUC on the IEEE 24-bus system. The mathematical model was implemented using AMPL and solved using Gurobi solver for a 24-hour (Day-Ahead) load period.

The difference in overall cost of SCUC-CDR and SCUC demonstrates a cost saving of $ 15,348 (2.3% of total cost) by considering corrective demand curtailment of about 49.4 MW cumulatively for all line contingencies and about 316.2 MW cumulatively for all generator contingencies.

TABLE I. Operational cost and post-contingency demand curtailed

	SCUC	SCUC-CDR
Total Cost ($)	671,835	656,487
MIPGAP (%)	0.95%	0.84%
Solve time (s)	3,814.59	4,489.34
$\sum_{n,c,t,} DShed^c_{n,t}$	NA	49.4 MW
$\sum_{n,j,t,} DShed^j_{n,t}$	NA	316.2 MW

IV. References

[1] C. Su and D. Kirschen, "Quantifying the Effect of Demand Response on Electricity Markets," *IEEE Transactions on Power Systems*, vol. 24, no. 3, pp. 1199-1207, Aug. 2009.

[2] H. Wu, M. Shahidehpour, and A. Al-Abdulwahab, "Hourly demand response in day-ahead scheduling for managing the variability of renewable energy," IET Gen. Transm. Distrib., vol. 7, no. 3, pp. 226–234, 2013

[3] M. H. Albadi and E. F. El-Saadany, "A summary of demand response in electricity markets," Elect. Power. Syst. Res., vol. 78, no. 11, pp. 1989–1996, Nov. 2008.

[4] Demand response strategies, PJM [Online]. Available: https://www.pjm.com/markets-and-operations/demand-response.aspx

[5] Load Resource Participation in the ERCOT Markets, ERCOT [Online]. Available: http://www.ercot.com/services/programs/load/laar

[6] Demand response and load participation, CAISO [Online]. Available: http://www.caiso.com/participate/Pages/Load/Default.aspx

Deadband Voltage Control and Power Buffering to Enable Extreme Fast Charging of Electric Vehicles

Waqas ur Rehman, *Student Member, IEEE*, Rui Bo, *Senior Member, IEEE*
Missouri University of Science and Technology, Rolla, USA

***Abstract*— Integration of an extreme fast charging (XFC) station with AC power grid may cause power quality issues that adversely affect neighboring loads. It can introduce dynamic and steady-state voltage violations in the host power grid. As EVs arrive and depart, power swings of ±400 kW (as per the latest CHAdeMO 2.0 protocol) are expected to be experienced by the power grid. Consequently, transient over-voltage and under-voltage may occur, damaging other equipment on the grid. Reactive power compensation capability of bi-directional electric vehicle (EV) chargers can prove essential in mitigating the steady-state voltage violations caused by the EV charging itself or changes in the neighboring loads. Use of stationary energy storage system (ESS) for power buffering can be utilized to address the voltage transients (sags and swells) as a result of EV charging at the XFC station. In order to address the controller 'hunting' issue with conventional deadband voltage control (V-control) methods, this paper proposes a Q-sign triggered deadband V-control method at the point of common coupling (PCC). In addition, to ensure the ramp rate of power flow from grid is within the allowable limits set forth by the grid code, a ramp rate control is proposed that uses the ESS as a 'power buffering' device, which not only can help with voltage transient mitigation but also can reduce the long-term wear and tear in the conventional voltage regulating devices. Lastly, different from most reported work in the literature where no explicit limit of the power electronic converters (PECs) is considered during the V-control, this work takes into account a reasonable apparent power capacity limit of the PECs when achieving the V-control. This limit also affects the amount of active power that can be obtained from the power grid, and subsequently may require ESS to function as 'load sharing' device to provide supplemental active power to satisfy EV load. A case study simulated in MATLAB/Simulink (interfaced with PLECS) is presented to demonstrate the efficacy of the proposed control approaches for the operation of XFC station.**

Keywords—extreme fast charging, deadband voltage control, ESS power buffering, ramp rate control.

I. XFC Station Control Schematic

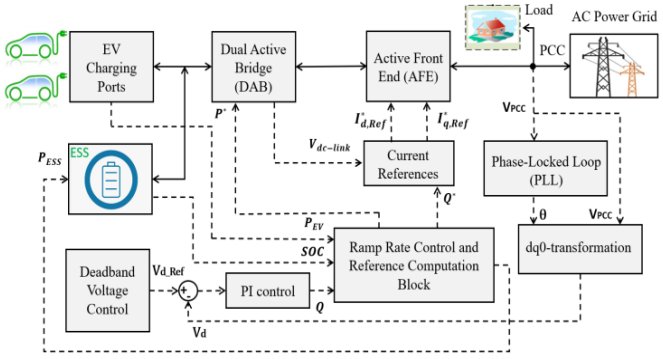

Fig. 1. High-level control schematic of XFC station

II. Case Study Results

Following cases are considered for the case study results:

Case 1: Without voltage and ramp rate control (base case)

Case 2: With deadband voltage control:

a. Without ramp rate control (i.e., w/o power buffering)
b. With ramp rate control (i.e., with power buffering)

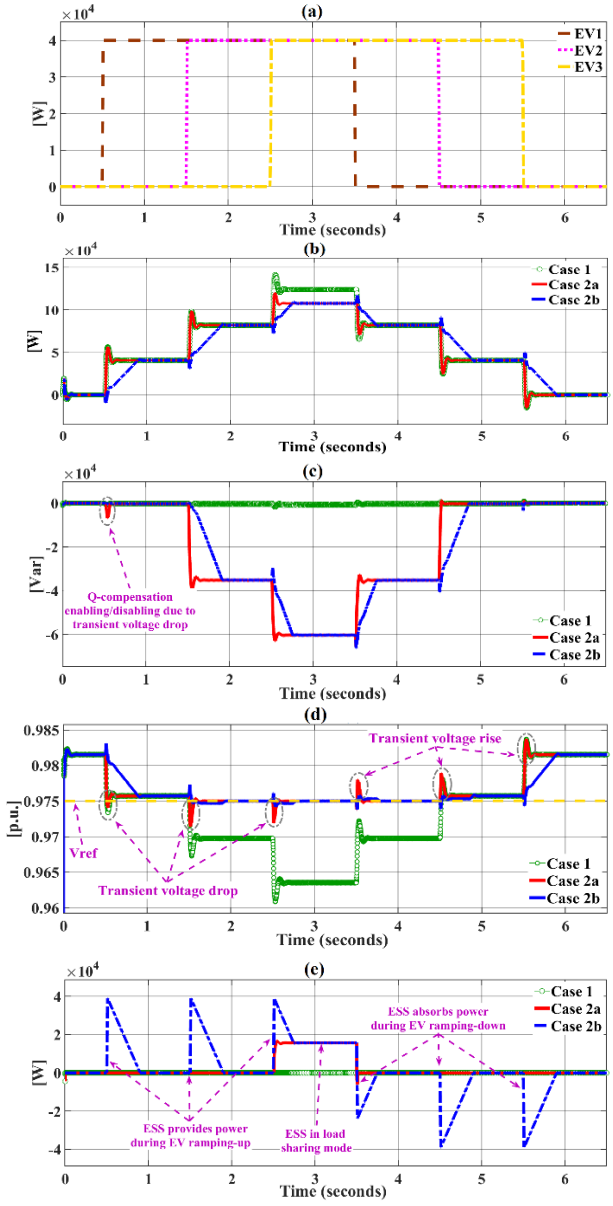

Fig. 2. Case study results: (a) EVs load, (b) measured active power at PCC (c) measured reactive power at PCC (d) PCC voltage, (e) ESS power

A Method for Power System Transient Stability Assessment Based on Transfer Learning

[1]Junyu Ren, [1]Jinfu Chen, [2]Benyu Li, [2]Ming Zhao, [2]Hengchu Shi, [2]Hao You
[1]State Key Laboratory of Advanced Electromagnetic Engineering and Technology,
Huazhong University of Science and Technology, Wuhan, China
[2]Yunnan Electric Power Dispatching and Controlling Center, Kunming, China

***Abstract*—Traditional machine learning models are subject to changes in the data distribution. Once the topology of power grid changes, the distribution of power grid data will change, resulting in the consequence that the former transient stability assessment model based on machine learning is no longer applicable and needs to be retrained. However, the power network after the topology changes cannot provide enough data for the training of the new model. To solve the problem above, this paper proposes a method of power system transient stability assessment based on transfer learning, which fully taps the potential of past data and assists a small amount of newly acquired data in training the model. The simulation results on the CEPRI36 system show that the proposed method can effectively improve the accuracy of original classification models, especially for weak classifiers with insufficient generalization ability. The disadvantage of transfer learning lies in the long training time, which still needs to be improved.**

***Keywords*—transfer learning, power system, transient stability assessment**

I. Introduction

Transient stability assessment (TSA) is significant to the maintenance of the stability of the whole power system. However, the problem of power network topology change is still an essential and unavoidable challenge in the research of transient stability assessment based on machine learning for following reasons: (1) The original machine learning model is no longer applicable because of the change of data distribution with the shift in power network topology.(2) Retraining the model is inefficient because the grid with changed topology often fails to provide enough newly labeled data in time.

Therefore, based on the idea of transfer learning, this paper presents a new method of power system transient stability assessment.

II. Proposed Methodology

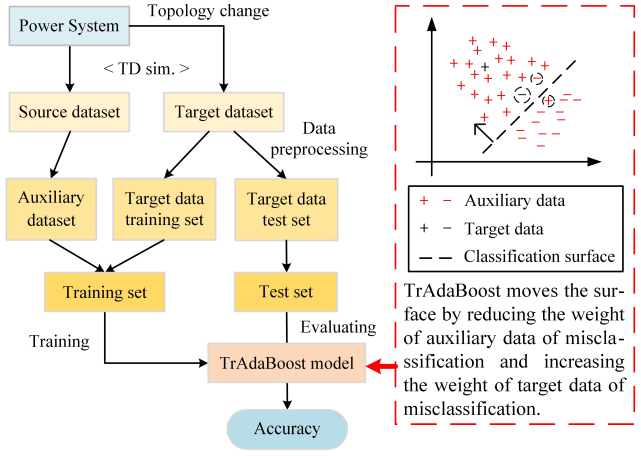

Fig. 1. Modeling process of TSA model based on transfer learning.

III. Case Analysis

The test is on CEPRI36 system, which is a 220 kV/500 kV AC power network with 8 generators and 26 AC lines.

TABLE I. Test Results of Transfer Learning Model

Target Data Volume	Decision Tree	Transfer Learning	Increase (%)
3600	0.949	0.973	2.4
3000	0.951	0.971	2.0
…	…	…	…
400	0.924	0.936	1.2

TABLE II. Test Results of Transfer Learning Model with Different Dataset Combination Scenarios

No.	Dataset Scenarios		Accuracy of	Accuracy for Target Data	
	Source Data	Target Data	Original Model	Original Model	Transfer Model
DS1	TS1	TS2	0.964	0.776	0.960
DS2	TS1	TS3	0.964	0.651	0.966
…	…	…	…	…	…
DS10	TS5	TS4	0.959	0.833	0.967

(DS: Dataset Scenario; TS: Topology Scenario)

TABLE III. Test Results of Different Models

Target Data Volume	DT	TrDT	Increase (%)	RF	TrRF	Increase (%)
3600	0.949	0.973	2.4	0.974	0.979	0.5
3000	0.951	0.971	2.0	0.971	0.975	0.4
…	…	…	…	…	…	…
400	0.924	0.936	1.2	0.936	0.948	1.2

TABLE IV. Time for Training of Transfer Learning Model

Target Data Volume	DT(s)	TrDT(s)
3600	0.00232	3.259
…	…	…
400	0.00058	0.941

IV. Conclusion

(1) For the scenarios of power system topology change, transfer learning can improve the accuracy of machine learning models by using data from similar fields.

(2) The transferability of the transfer learning model is related to the basic classifier and the amount of target data. The strong generalization ability of the basic classifier itself will restrict the transferability of the transfer learning model. In a certain range, the larger the amount of target data, the better the transfer effect.

(3) The training time of the transfer learning model is longer than that of the basic classifier.

Impact of Photovoltaic Generation Integration on Protection of Distribution Systems

Shuaiang Rong, *Student Member*, *IEEE*, Lina He, *Member*, *IEEE*
Electrical and Computer Engineering, University of Illinois at Chicago, Chicago, U.S.A.
Email: srong4@uic.edu, lhe@uic.edu

***Abstract*— The increasing penetration of photovoltaic distributed generation (PVDG) leads to significant challenges on the protection of distribution systems. It is important to study the impact of the integration of PVDG on the protection of distribution systems and clarify the corresponding technical challenges to enhance their resilience. This paper develops a generic distribution system integrated with a PVDG system, and identified the resulting impact on the overcurrent protection of distribution systems. A numerical study in this paper shows that the control of inverters can limit the fault current fed by PVDG systems significantly during a short-circuit (SC) fault. This makes the SC current too low to trigger the circuit breaker, leading to a protection failure (should operate but does not). To verify this conclusion, a comparison case with the connection of a traditional synchronous generator (SG) is provided.**

I. Introduction

The emerging environmental issues and sustainable concerns have inspired higher penetration of renewable energy resources (RES) in distribution systems. Among these RES, the PVDG is most prevailing due to its environmental-friendly and ecological sustainable characteristics. The high-level penetration of the PVDG can alleviate overloads and reduce the capacity of feeders and substation transformers effectively. Yet, these power electronic-interfaced PVDG systems pose challenges to the traditional protection of distribution systems especially consider the control behavior of the inverters. The traditional protection systems are designed based on the fault current characteristic of SGs, which can no longer protect the distribution systems with PVDG due to different fault current characteristics of PVDG systems. To guide the upgrades of the protection of the future distribution systems, this paper presents a quantitative analysis of the SC fault characteristics of a PVDG system, and a comparison case with a distributed SG.

II. Key Distribution System Configuration

Historically, the traditional distributed power supply comes from diesel generators, which are SGs. With the development of solar PV, the distributed generation will be mostly replaced by the PVDG system. To study the impact of the PVDG integration on the protection of the distribution systems, a benchmark system is designed with the connection of a SG as shown in Fig.1. A system with identical power flows is designed where the power generated by the SG is taken over by a PVDG system, as shown in Fig.2.

In both systems, when the fault occurs at location F, the fault currents will flow from the substation and the distributed generation system (SG or PVDG). Due to the same initial state of the systems with same power flows, the fault current fed by substation *If* are identical in both cases, which can be detected by relay R1. The circuit breaker CB1 will trip and isolate the fault from the substation. To study the difference of fault current characteristics of the SG and PVDG, their fault currents flow through the relay R2 are measured and compared in the Fig.3.

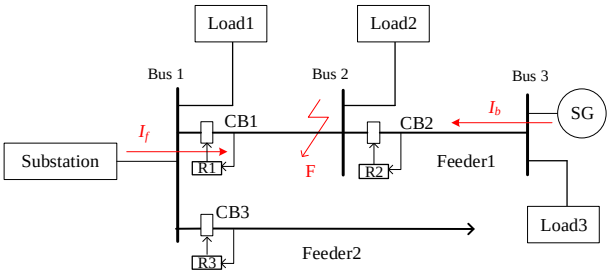

Fig.1 The benchmark system with SG

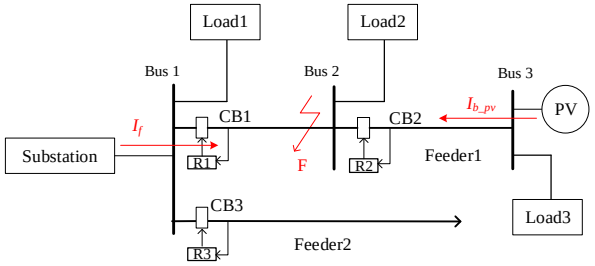

Fig.2 Distribution system with PVDG system

III. Key Results

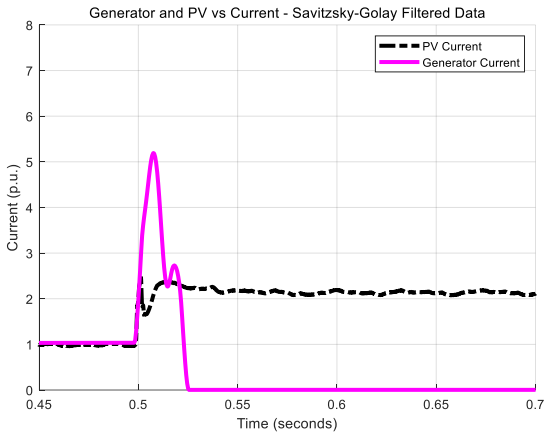

Fig.3 Fault currents generated from SG and PVDG

IV. Conclusion

As in Fig.3, the magnitude of the fault current fed by SG (I_b) can reach 5 times the current rating, which is large enough to be detected by the overcurrent relays. The relay R2 can trip the circuit breaker CB2, so that the fault current is interrupted and drop to 0. However, in the case of the distribution system integrated with the PVDG system, the current fed by the PVDG (I_{b_pv}) will be limited by the current limiter in the controller of the PV inverter. This fault current has a low magnitude (2 times the current rating) similar to the transient currents and overload currents, which can no longer be detected by the relay R2. This protection failure can cause damage of electrical equipment, leading to huge economical losses to the power system.

Signal Dispatching Method for Secondary Frequency Control Based on Area Requirement Change and Merit-Order

Masaru Saida, Masaki Imanaka, Muneaki Kurimoto, Shigeyuki Sugimoto and Takeyoshi Kato
Department of Electrical Engineering
Nagoya Univercity
Nagoya, Japan
saida.masaru@a.mbox.nagoya-u.ac.jp

Kouichiro Hata and Yoshiki Nakachi
Chubu Electric Power Co., Inc
Nagoya, Japan

***Abstract*— In Japan, after establishing the control reserve market in 2021, a Merit-Order (MO) method based on cost per kWh of each generator will be applied to a Load Frequency Control (LFC). A conventional Ramp-Rate (RR) method dispatches LFC signal based on ramp-rate of each LFC generator. In MO method, the frequency fluctuation may be increased compared to RR method, because the aggregated ramp-rate of all LFC generators may not be fully utilized. To solve this problem, we propose an LFC signal dispatching method considering the change of Area Requirement (AR) calculated from the frequency deviation. The effectiveness of the proposed method is evaluated using the IEEJ AGC30 model. As a result, the proposed method is able to reduce the frequency fluctuation compared to a simplified MO method, and the operating cost compared to RR method.**

Keywords—Load frequency control, Area requirement, Control reserve market, Merit-order, Ramp-rate, Simulation

I. Introduction

Load Frequency Control (LFC) is a control method which calculates the Area Requirement (AR) from the frequency deviation and dispatches the signal to multiple LFC generators so that the output of these generators follow demand fluctuations of cycles in several minutes to several ten minutes. After establishing the control reserve market in Japan, an LFC signal dispatching method based on the order of electricity generation cost per kWh (Merit-Order (MO) method) will be applied. One concern of using MO method is the increase in frequency fluctuation due to the decrease in total ramp-rate arising from that generators of lower cost tends to have lower ramp-rate and the aggregated ramp-rate of all generators may not be fully utilized.

Fig. 1 illustrates the time series change in LFC signal for two types of LFC signal dispatching methods, i.e. Simplified MO (S-MO) method, and proposed ΔAR-MO method. In Figure 1, $L_{AR}(t)$, which is simply simulated as a triangular wave of four minutes cycles is dispatched to two generators, L and H, having low and high cost per kWh respectively. In S-MO method, incremental fuel cost is calculated from the power output of each LFC generator every T [s] of LFC control cycle to create an MO list. When $L_{AR}(t)$ is positive, the ascending MO list is used to dispatch $L_{AR}(t)$. When $L_{AR}(t)$ is negative, the descending MO list is used. As a result, the difference between $L_{f\_sum}(t)$ (= $L_{f\_L}(t)$ + $L_{f\_H}(t)$) and $L_{AR}(t)$ is caused. It is indicated as "over" in Fig. 1(a).

In order to eliminate the over calculated $L_{f\_sum}(t)$ against $L_{AR}(t)$ in S-MO method, we propose a method in which ascending or descending MO list is switched over and LFC signal is calculated in a different way depending on the combinations of the signs of $L_{AR}(t)$ and the direction of change in $L_{AR}(t)$ ($\Delta L_{AR}(t)$). In Fig. 1(b), when $L_{AR}(t)$ and $\Delta L_{AR}(t)$ are both positive (time zone I) or negative (zone III), $L_{AR}(t)$ is dispatched in the same way as in S-MO method. When $L_{AR}(t)$ is positive and $\Delta L_{AR}(t)$ is negative (zone II), $\Delta L_{AR}(t)$ is dispatched using the descending MO list. When $L_{AR}(t)$ is negative and $\Delta L_{AR}(t)$ is positive (zone IV), vice versa.

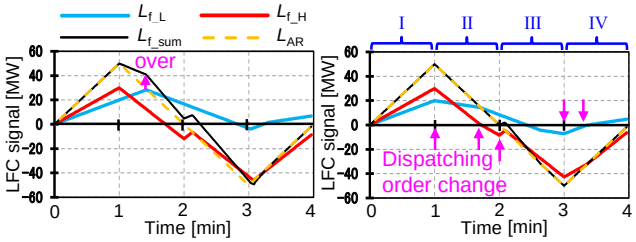

(a) S-MO method (b) ΔAR-MO method

Fig. 1. Examples of signal dispatching

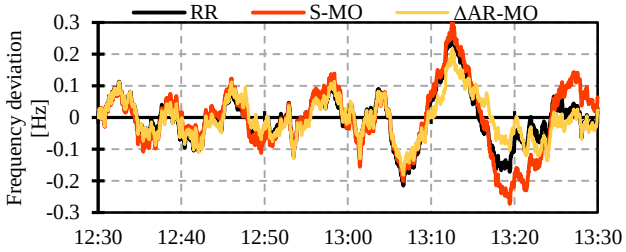

Fig. 2. Frequency deviation in each method

Table 1. Comparison of evaluation index (12:30~13:30)

method	C_{LFC} [10^3 yen]	Δf_{MAD} [Hz]	Δf_{max} [Hz]	L_{ave} (Coal) [MW]	L_{ave} (LNG) [MW]	L_{ave} (LNG-CC) [MW]	L_{ave}^{tot} [MW]
RR	-96	0.0609	0.280	2.9	1.3	1.8	6.0
S-MO	-626	0.0812	0.300	73.1	-48.3	-17.9	139.2
ΔAR-MO	-200	0.0533	0.217	12.6	-7.7	-1.8	22.1

II. Main Results

The effectiveness of ΔAR-MO method is evaluated by using the IEEJ AGC 30 model. Fig. 2 shows the frequency deviation result of each LFC method from 12:30 to 13:30. The magnitude of frequency deviation in ΔAR-MO method is the smallest among the three methods. Table 1 shows various evaluation indexes regarding the performance of LFC. From left to right: cost of LFC (C_{LFC}), mean absolute deviation of frequency (Δf_{MAD}), maximum frequency deviation (Δf_{max}), average of LFC signal of each type of LFC generator (L_{ave_i}), the sum of absolute L_{ave_i} (L_{ave}^{tot}). The cost of LFC of ΔAR-MO method is smaller than that of RR method.

Computational Efficiency Comparison of UC-OPF Formulations

Alper Savasci, *Student Member, IEEE,* Biswajit Dipan Biswas, *Student Member, IEEE,* Md Mahmud-Ul-Tarik Chowdhury, *Student Member, IEEE,* Sumit Paudyal, *Member, IEEE,* Sukumar Kamalasadan, *Senior Member, IEEE*

***Abstract*—The main objective of this paper is to investigate the existing literature on Unit Commitment and Optimal Power Flow (UC-OPF) optimization models and build a combined model that improves the solution in terms of computational and monetary cost leveraging the convex optimization techniques. The goal is to provide a unique UC-OPF framework that can be utilized by independent system operators (ISOs) and Regional Transmission Organization (RTOs).**

***Index Terms*—Unit Committment, Efficiency Comparisons, Optimal power flow**

I. Introduction

Generally, UC and OPF problems have high computational complexity. As a combined problem, the UC-OPF problem is also challenging because of the problem nature is nonconvex and nonlinear due to the existence of integrality restrictions from the UC part and nonlinear power flow equations from the OPF part. It can be even more difficult to obtain a high-quality solution when the system scale becomes larger. The UC-OPF, in its basic form, can be rendered as Mixed-Integer Nonlinear Programming (MINLP) problem.

The drawbacks of this basic form are the lack of scalability and tractability. To better scale and obtain high-quality solutions, different optimization techniques have been proposed in the literature. These techniques can be classified into three groups: decomposition techniques, linearization, and conic optimization techniques. In the first category, a general MINLP problem is decomposed into mixed-integer linear programming (MILP) and nonlinear programming (NLP) problems and solved by an iterative algorithm such as branch-and-bound and cutting plane (outer approximation) methods. In the second category, the MINLP problem is solved by linearizing the objective and constraints, which are in nonlinear form, using piece-wise linearization so that it can be formed as MILP, which is generally more tractable than MINLP.

Even though using the linearization techniques results is tractable optimization models, it might not capture challenging nonlinear nature precisely. Therefore, third category techniques use conic optimization methods, which can guarantee global UC-OPF solutions under specific network constraints in polynomial time, capturing the nonconvex nature of the feasible space in general [1], [2]. Mixed-Integer Semidefinite (MISDP) and Mixed-Integer Second-Order Cone Programming (MISOCP) are the main methods in the third category. The following mixed-integer conic optimization methods, as well as non-convex formulations, are planned to be considered and extensive computational simulations to be conducted and comparisons will be presented in terms of computation time, exactness, and optimality on IEEE test systems.

This material is supported in part by the U.S. Department of Energy under Award Number DE-EE0008774. Authors are with the University of North Carolina at Charlotte and Florida International University.

II. Key Equations

Power Flow Model:

$$P_i = |V_i| \sum_{k=1}^{n} |V_k| \left(\mathbf{G}_{ik} \cos\left(\theta_i - \theta_k\right) + \mathbf{B}_{ik} \sin\left(\theta_i - \theta_k\right)\right) \quad (1)$$

$$Q_i = |V_i| \sum_{k=1}^{n} |V_k| \left(\mathbf{G}_{ik} \sin\left(\theta_i - \theta_k\right) - \mathbf{B}_{ik} \cos\left(\theta_i - \theta_k\right)\right) \quad (2)$$

UC/OPF Model:

$$\underset{u_{t,g}, P_{t,g}, Q_{t,g}}{\operatorname{argmin}} \sum_{t \in \mathcal{T}, g \in \mathcal{G}} C(P_{t,g}) \quad (3)$$

$$u_{t,g}\, P_g^{Min} \leq P_{t,g} \leq u_{t,g} P_g^{Max}, \qquad \forall t \in \mathcal{T}, \forall g \in \mathcal{G} \quad (4)$$

$$u_{t,g}\, Q_g^{Min} \leq Q_{t,g} \leq u_{t,g} Q_g^{Max}, \qquad \forall t \in \mathcal{T}, \forall g \in \mathcal{G} \quad (5)$$

$$P_{t,g} - P_{t-1,g} \leq RU_g u_{t-1,g}, \qquad \forall g \in \mathcal{G}, \forall t \in \mathcal{T} \quad (6)$$

$$P_{t-1,g} - P_{t,g} \leq RD_g u_{t,g}, \qquad \forall g \in \mathcal{G}, \forall t \in \mathcal{T} \quad (7)$$

$$(x_{t-1,g} - TU_g)(u_{t-1,g} - u_{t,g}), \geq 0, \qquad \forall t \in \mathcal{T},\ \forall g \in \mathcal{G} \quad (8)$$

$$(x_{t-1,g} - TD_g)(u_{t-1,g} - u_{t,g}), \leq 0, \qquad \forall t \in \mathcal{T}, \forall g \in \mathcal{G} \quad (9)$$

$$u_{t,g} \in \{0, 1\}, \qquad \forall t \in \mathcal{T}, \forall g \in \mathcal{G} \quad (10)$$

Power Flow Equations : Eq(1) - (2)

III. Key Results

An initial computational comparison of MINLP and MISDP multi-period UC-OPF ($t = 1$ to 3) formulations on 3-generator 6-bus test network is shown in Table I. The shows that MISDP formulation can ensure exact solution for this system. For larger system if the MINLP fails to provide global optimal solution, MISDP can ensure that.

TABLE I: MINLP vs. MISDP

	t = 1		t = 2		t = 3	
	MINLP	MISDP	MINLP	MISDP	MINLP	MISDP
Gen1 (MW)	98.35	98.35	103.977	103.976	161.6	161.6
Gen2 (MW)	0	0	0	0	150	150
Gen3 (MW)	0	0	0	0	0	0
Demand	95	95	100	100	300	300
Loss	3.35	3.35	3.977	3.976	11.6	11.6

References

[1] X. Bai, H. Wei, K. Fujisawa, and Y. Wang, "Semidefinite programming for optimal power flow problems," *International Journal of Electrical Power and Energy Systems*, vol. 30, no. 6-7, pp. 383–392, 7 2008.

[2] J. Lavaei and S. H. Low, "Zero duality gap in optimal power flow problem," *IEEE Transactions on Power Systems*, vol. 27, no. 1, pp. 92–107, 2012.

Sensitivity Analysis of Time-of-Use Rates on Operations of Home Energy Management Systems

Ashwin Shirsat
Department of Electrical and Computer Engineering
North Carolina State University
Raleigh, NC 27695, USA
ashirsa@ncsu.edu

Wenyuan Tang
Department of Electrical and Computer Engineering
North Carolina State University
Raleigh, NC 27695, USA
wtang8@ncsu.edu

***Abstract*—Widespread adoption of distributed energy resources, especially solar PV, is observed in present times for residential applications. A similar trend is observed with distributed storage. Falling energy storage costs, the intermittent nature of solar PV, and the mismatch between the solar output and residential load demand are promoting the use of storage. The self-sufficiency provided by the storage can lead to a strained relationship with the utility. In this paper, we develop a model predictive control based residential-scale DC-coupled PV-storage system and analyze the sensitivity of its daily operations to perturbations in the start time, duration, and value of the time-of-use rate along with the variations in the flat PV sell back price. The results can assist the process of designing effective tariff schemes, such that the rate structure is of significant value to the customers, as well as benefits the utility in achieving its goals.**

I. Introduction

Coupling storage with PV alleviates over-generation and excessive curtailment but disrupts the relationship between the customers and the load serving entity (LSE). This strained relationship is due to the self-sufficiency offered to the customers by the PV-storage systems. This results in the reduced utilization of grid services by the customer, which leads to reduced compensation to the LSE, and can potentially disrupt the utility business. However, the presence of the utility is necessary since the PV-storage systems cannot be wholly relied upon due to the volatile nature of solar energy. An approach to address this problem is to design new tariff schemes that can prove to be economical to the customers, increase the residential PV-storage penetration, and also help utilities run their business without losses.

Most of the existing literature is limited to the optimal operations of the system given a specific tariff scheme. A gap exists when it comes to the sensitivity of the PV-storage system operations to variations in the time-of-use (TOU) tariff schemes and rates. To bridge the gap in the literature on DC-PVSS control algorithms and their sensitivity to TOU rates, our contributions are as follows:

1) A realistic MPC based residential-scale DC-PVSS optimization model incorporating the converter losses, and the flexibility to shift controllable loads.
2) Sensitivity analysis of the TOU tariff scheme on the daily operational performance of the DC-PVSS by varying TOU rate value, start time, and duration.

II. Results

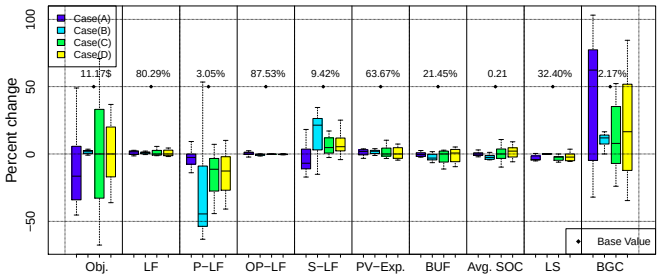

Fig. 1. System sensitivity to variation in TOU rates.

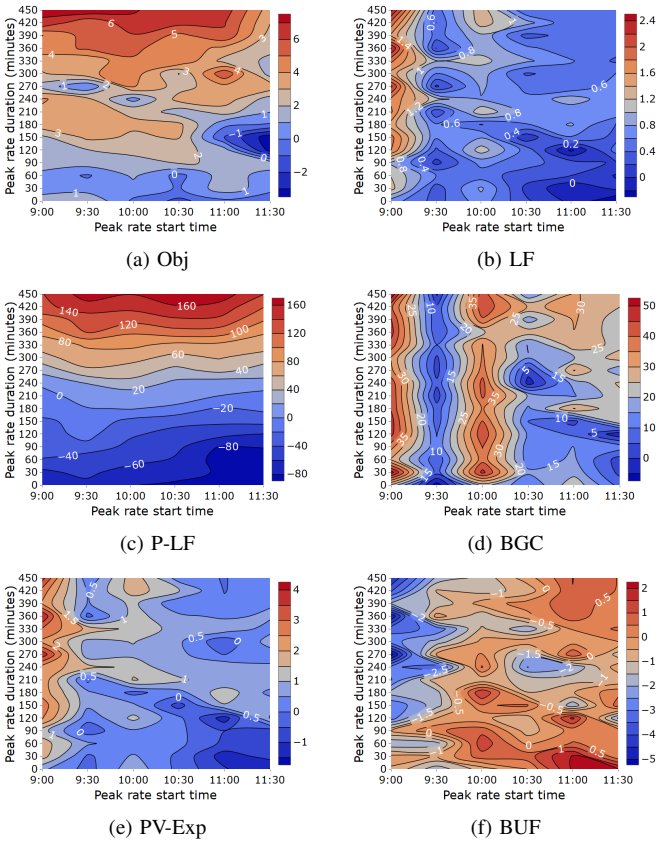

(a) Obj (b) LF

(c) P-LF (d) BGC

(e) PV-Exp (f) BUF

Fig. 2. System sensitivity to variation in peak rate start time and duration.

Real-Time Topology Detection in Unbalanced Distribution System Using Micro-PMU And Smart Meter Data: A MIQP Approach

Zahra Soltani, *Student Member, IEEE*, and Mojdeh Khorsand, *Member, IEEE*
School of Electrical, Computer, and Energy Engineering, Arizona State University, Tempe, AZ 85287, USA
Email: zsoltani@asu.edu and mojdeh.khorsand@asu.edu

The information of distribution network topology is crucial for the real-time (RT) operation and control studies such as state estimation, volt/var control, distribution power flow study, and control of distributed energy resources (DERs). However, the communication links between switch devices and distribution management system and the number of RT measurements are limited in the distribution network, which makes the knowledge of system operator from the distribution system very restricted. Also, reconfiguration and switching actions may occur more frequently with integration of DERs in distribution system. Therefore, an efficient distribution system topology processor is critical for success of distribution management systems. However, topology processor in the unbalanced distribution system is challenging due to single-phase switches, switch cabinets, capacitor switches, mutual impendences between phases in a line, and various phase configurations (i.e., single-phase, two-phase, and three-phase) of feeders and laterals. This paper proposes a mixed-integer quadratic programming formulation based on linearized rectangular IV formulation to determine the topology of the unbalanced primary distribution system. In the proposed formulation, untransposed distribution lines, single-phase switches, and shunt elements of distribution lines are modeled. The power injection formulations are linearized using iterative first-order approximation of Taylor series. In order to eliminate nonlinearity due to inclusion of binary variables associated with status of single-phase switches, the big M technique is utilized. The proposed model includes linear constraints and convex objective function, which results in a global optimal solution. The proposed model can handle identifying multiple three-phase and single-phase switching actions at each time instant without information of switch statuses in the prior time intervals. The proposed model only requires measurement information at each time snapshot to identify the topology of the system correctly. Furthermore, the proposed topology detection problem can estimate system states simultaneously. Figure 1 shows the flowchart of the simulation procedure for the proposed primary topology processor in the unbalanced distribution system.

The model is simulated using a modified unbalanced IEEE 13-bus distribution system [1]. Measurement data includes two μPMUs measurements, smart meter data on load buses, and substation measurements. In order to show the performance of the proposed topology processor, two case studies are investigated. In the case 1, 108 scenarios including all possible topologies of the system are considered. In each scenario, status of 12 single-phase switches and measurement noise are randomly chosen. The accuracy of the proposed iterative primary topology processor among all scenarios is 100%. Since, the proposed model is able to estimate power system states in the primary distribution system, the obtained voltage magnitude and angle values from case 1 are shown in Figures 2 and 3 using absolute error index. The figures confirm that the errors in estimating system states are small. In the case 2, real world residential load data from Pecan Street Project with a time resolution of 15 minutes for smart meter data is used [2]. The simulations are conducted for 100 scenarios of various topologies and measurement noise. Monte Carlo simulation is conducted to generate these 100 scenarios which each of them includes 96 time intervals (one day every 15 minutes). In each time interval of each scenario, status of 12 single-phase switches and measurement noise are randomly chosen. The accuracy of the proposed topology processor among all scenarios is 99.95%.

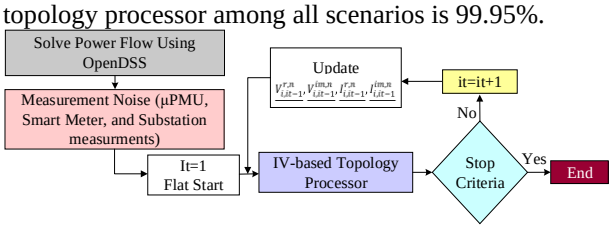

Figure 1: Topology Processor for Unbalanced Distribution Systems.

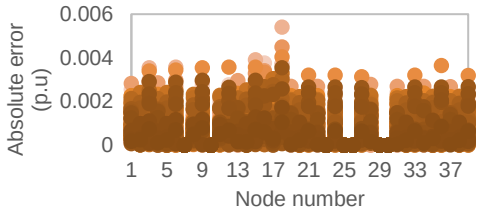

Figure 2: Absolute Error for Voltage Magnitude Estimation.

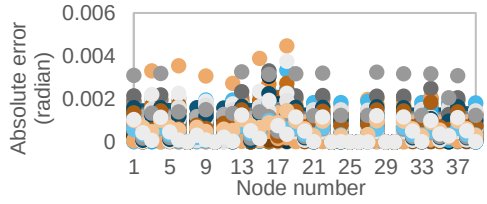

Figure 3: Absolute Error for Voltage Angle Estimation.

REFERENCES

[1] Distribution System Analysis Subcommittee Report, "Radial distribution test feeders." [Online]. Available: http://www.ewh.ieee.org/soc/pes/dsacom/testfeeders/index.html.
[2] "Pecan Street Inc. Dataport," 2019. [Online]. Available: https://dataport.pecanstreet.org/.

Comparison of Principal Component Analysis Techniques for PMU Data Event Detection

L. Souto, J. Meléndez, S. Herraiz
Intelligent Systems and Control Engineering group
Universitat de Girona, Girona, Spain
laiz.souto, joaquim.melendez, sergio.herraiz AT udg.edu

***Abstract*—Principal component analysis (PCA) is a dimensionality reduction technique often applied to detect events in large amounts of data collected by phasor measurement units (PMU) at transmission and distribution level. This article considers five different approaches to select an appropriate number of principal components and evaluates the accuracy of correct event detections with use of two statistical tests in a $1-$hour data file from the UT-Austin Independent Texas Synchrophasor Network with voltage magnitudes collected at different PMU substations.**

I. Selection of principal components

Five different methods to select an appropriate number of principal components with dimensionality reduction are introduced as follows.

a) Kaiser criterion: This criterion retains all r principal components containing at least as many information as a single original variable in terms of variance.

$$r := \{\max\ j \in \{1, \cdots, m\} \mid \lambda_j \geq \frac{1}{m}\sum_{i=1}^{m}\lambda_i\} \tag{1}$$

b) Automatic scree plot: In this method, the eigenvalues are plotted decreasingly such that r corresponds to the eigenvalue whose distance to the origin of the coordinate system is the shortest, as the idea is to search for an elbow in the plot.

$$r := \{i \in \{1, \cdots, m\} \mid \min_{i} \sqrt{\lambda_i^2 + i^2}\} \tag{2}$$

c) Explained variance: In this method, a minimum percentage of the total variance is defined and r is taken as the smallest integer satisfying it.

$$r := \frac{1}{m}\sum_{i=1}^{r}\lambda_i \times 100 \geq Var\,(\%) \tag{3}$$

d) Variance reconstruction error: In this method, the optimal value of r is given by the minimum variance reconstruction error, considering a faulty observation as a unitary vector $\xi_\mathbf{i}$ multiplied by a fault magnitude f and the correlation matrix of reconstruction error $\mathbf{R}$.

$$r := \{j \in \{1, \cdots, m\} \mid \min_{j}\ {\xi_\mathbf{i}}^T \mathbf{R} \xi_\mathbf{i}\} \tag{4}$$

TABLE I
Event detection results (Yes/No) over a $10-$s window

	Kaiser			Scree plot			Variance			VRE			Detectability			
#	r	T2	Q	r	T2	Q	r	T2	Q	r	T2	Q	r	T2	r	Q
1	3	Y	Y	4	Y	Y	3	Y	Y	3	Y	Y	2	Y	2	Y
2	2	N	Y	3	N	Y	3	N	Y	1	N	Y	4	Y	1	Y
3	2	Y	Y	2	Y	Y	3	N	Y	2	Y	Y	4	Y	1	Y
4	2	Y	Y	2	Y	Y	3	Y	Y	1	Y	Y	2	Y	2	Y
5	3	Y	N	3	Y	N	3	Y	N	2	Y	Y	3	Y	1	Y
6	2	Y	Y	2	Y	Y	3	Y	Y	1	N	Y	2	N	2	Y
7	2	N	Y	3	N	Y	3	N	Y	2	N	Y	2	N	2	Y
8	2	N	Y	3	Y	N	2	N	Y	2	N	Y	3	Y	3	N
9	3	Y	Y	2	N	Y	3	Y	Y	1	N	Y	3	Y	1	Y
10	2	Y	Y	2	Y	Y	2	Y	Y	1	N	Y	2	Y	2	Y
11	2	Y	Y	5	Y	Y	3	Y	Y	1	N	Y	2	Y	2	Y
12	2	Y	Y	2	Y	Y	3	Y	Y	1	N	Y	2	Y	2	Y
13	2	Y	Y	3	Y	N	3	Y	N	2	Y	Y	3	Y	1	Y
14	2	Y	Y	2	Y	Y	3	Y	Y	1	Y	Y	2	Y	2	Y
15	2	Y	Y	2	Y	Y	3	Y	Y	1	N	Y	2	Y	2	Y
16	2	Y	Y	2	Y	Y	2	Y	Y	1	N	Y	2	Y	2	Y

e) Statistical detectability: In this criterion, r is chosen such that the smallest detectable events can be detected statistically in the projection subspace and residual subspace, such that (5) holds with a single PCA model or (6) holds with two PCA models built separately for T^2 and SPE statistics.

$$r := \{\min\ i \in \{1, \cdots, m\} \mid T_{x_f}^2 \geq T_{lim}^2\ and\ Q_{x_f} \geq Q_{lim}\} \tag{5}$$

$$r := \begin{cases} r_{T^2} := \{\min\ i \in \{1, \cdots, m\} \mid T_{x_f}^2 \geq T_{lim}^2\} \\ r_Q := \{\min\ i \in \{1, \cdots, m\} \mid Q_{x_f} \geq Q_{lim}\} \end{cases} \tag{6}$$

II. Case study

The procedures aforementioned have been tested with PMU data from the UT-Austin Independent Texas Synchrophasor Network. For illustration, Table I displays the detection results and the corresponding r of each selection method, considering a $10-$second sliding window to build the PCA models.

III. Conclusion

The results indicate that the PCA methodology is able to identify different types of events, regardless of the approach used to select the number of principal components. Nonetheless, the statistical detectability criterion is the most accurate with both T^2 and SPE statistics. The results calculated with T^2 and SPE statistics are complementary in some cases, whereas the time window also contributes to the task.

N-*k* Security Assessment and Screening for Large-Scale Random Equipment Faults in Bulk Power Grid under Extreme Weather

Tingkai Sun, Xue Li, Tao Jiang

Department of Electrical Engineering, Northeast Electric Power University, Jilin 132012, Jilin Province, China;

Email: suntingkai@aliyun.com

***ABSTRACT*: Under extreme weather conditions such as typhoon, ice disaster and rainstorm, the grid equipment faults probability and the number of high-order contingency states will be greatly increased. Therefore, it seriously affects the calculation accuracy of the traditional *N-k* contingency analysis methods based on probability and the computational efficiency of calculating the impact of *N-k* contingency states. This work proposes an *N-k* contingency analysis method based on impact increments, and this method can use limited low order contingency states of grid analysis results, and calculates impact of the corresponding high order contingency states by using the impact increments of low order contingency states, and use the independent relationship between equipment to further reduce the amount of calculation of contingency analysis so that a large number of high order *N-k* contingency states can be quickly analyzed and screened. The IEEE RTS 79 test case are employed to evaluate the performance of the proposed methods. The results show that the *N-k* contingency analysis method proposed in this work can rapidly and accurately calculate the impact of *N-k* contingency states and accurately screen the high-impact *N-k* contingency states.**

Key equations:

$$I_s = \sum_{k=1}^{N_{CTG}} \sum_{u \in \Omega_s^k} \Delta I_u$$

$$\Delta I_s = \sum_{k=0}^{n_s} (-1)^{n_s - k} \sum_{u \in \Omega_s^k} I_u$$

$$\Omega_s^k = \{u \mid u \subset s, Card(u) = k\}$$

Key figure:

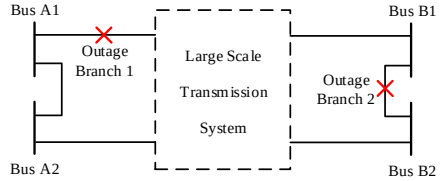

Fig. 1 *N-k* contingency analysis method based on impact increments

Key results:

Figure 2 and Figure 3 take the IEEE RTS79 system as an example to verify the accuracy of the proposed method.

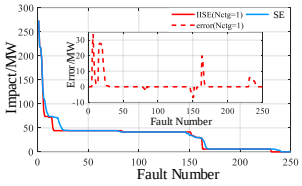

(a) *N*-2 contingency states

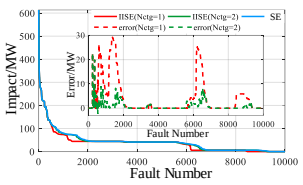

(b) *N*-3 contingency states

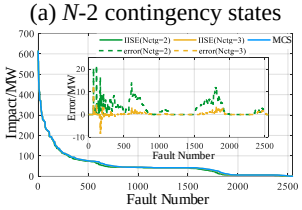

(c) *N*-4 contingency states

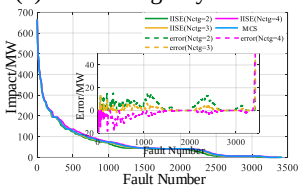

(d) *N*-5 contingency states

Fig. 2 Precision analysis of IEEE RTS 79 test system

Tab.1 Comparison of efficiency between State Enumeration method and Impact Increments method

Example	SE	IISE	
		N_{CTG}=1	N_{CTG}=2
	Time(s)	Time(s)	Time(s)
N-1	7.822	7.822	-
N-2	191	7.834	-
N-3	6809	7.909	199

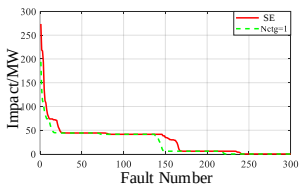

(a) *N*-2 contingency states

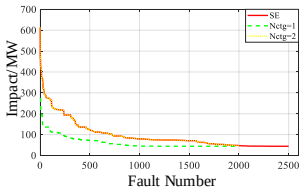

(b) *N*-3 contingency states

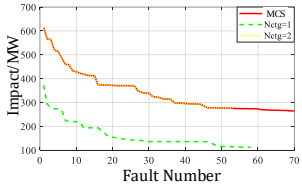

(c) *N*-4 contingency states

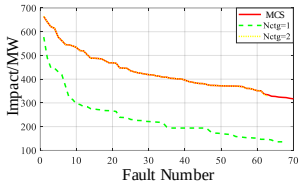

(d) *N*-5 contingency states

Fig. 3 Precision analysis of screening high-impact *N-k* contingency states

Quantum-Secure Microgrid

Zefan Tang, Yanyuan Qin, Zimin Jiang, Walter O. Krawec, Peng Zhang

***Abstract*—Existing microgrid communication relies on classical public key systems, which are vulnerable to attacks by means of quantum computers. In this paper, we present a potent solution to the quantum era microgrid challenges by using quantum key distribution (QKD) for information-theoretically secure authentication. Specifically, three contributions have been made: 1) a novel QKD-based communication architecture is established for microgrid, 2) a quantum-secure microgrid testbed is built in RTDS environment using the practical decoy-state QKD algorithm, and 3) different critical issues are analyzed based on the testbed and the QKD algorithm. The test results provide valuable resources for building a quantum-secure microgrid.**

***Index Terms*—Quantum secure, microgrid, quantum key distribution, algorithm, cyber security, resilience**

I. Preliminary Results

In this paper, we investigate the feasibility of using QKD for building a quantum-secure microgrid. Specifically, a novel QKD-based communication architecture is established for microgrid. A quantum-secure microgrid testbed is built in RTDS environment for evaluation and validation.

Based on the testbed and the QKD algorithm, the following critical issues are further addressed: 1) the effect of the distance (between two communication parties) on the QKD-based microgrid's performance is evaluated; 2) the speed of data transmission is analyzed, such that it will be clear which levels of service the QKD system can provide for microgrid; and 3) the impacts of different attack levels on the QKD-based microgrid system under various conditions (e.g., different distances and data transmission speeds) are evaluated.

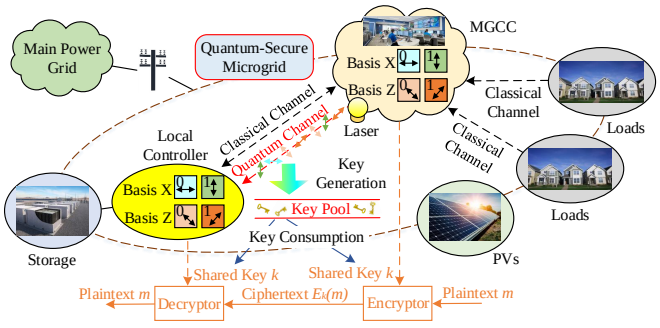

Fig. 1. QKD-based microgrid communication architecture. It contains two types of communication: classical communication and quantum communication. Key bits are generated continuously via QKD, and stored in a key pool.

This work was supported by the National Science Foundation under Grant ECCS-1831811.

Z. Tang, Z. Jiang and P. Zhang are with the Department of Electrical and Computer Engineering, Stony Brook University, Stony Brook, NY 11794, USA (e-mail: p.zhang@stonybrook.edu).

Y. Qin and W. O. Krawec are with the Department of Computer Science and Engineering, University of Connecticut, Storrs, CT 06269, USA.

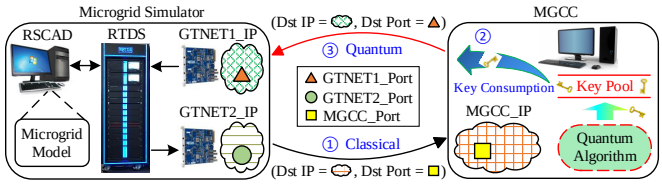

Fig. 2. Network topology for the quantum-secure microgrid testbed. Two GTNET cards are used for the classical and quantum communications between RTDS and the microgrid control center (MGCC). Once the MGCC needs to send data to RTDS, it extracts a given number of key bits from the key pool. If the key generation is faster than the key consumption, there will be enough key bits; and otherwise, the key bits will be used up.

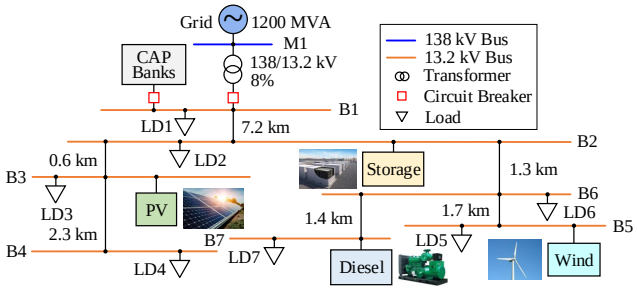

Fig. 3. One-line diagram of the microgrid model. The distributed energy resources include a diesel generator, a photovoltaic system, and a doubly-fed induction generator wind turbine system. A battery storage is also added. It uses P-Q control, and requires communication with the MGCC.

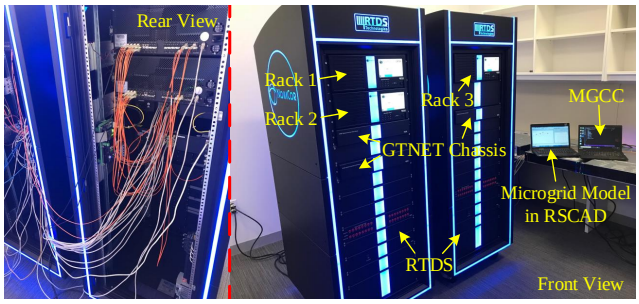

Fig. 4. Testbed setup for quantum-secure microgrid in RTDS environment. The microgrid model is developed in RSCAD. The MGCC runs on a dedicated computer, which receives data from and sends data back to RTDS.

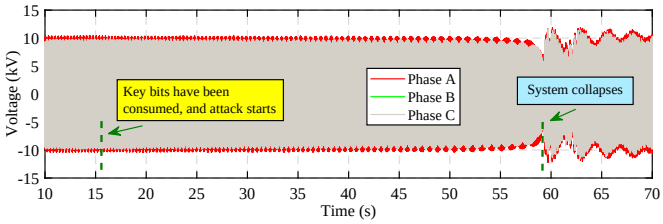

Fig. 5. Voltage response of bus 1 before and after the key bits are used up. At $t = 16$ s, the key bits are used up, making the system vulnerable to attacks. The magnitude of the voltage gradually decreases. The frequency also decreases. At $t = 59$ s, the system collapses. It is therefore of great importance to have enough key bits in the key pool.

Enhancing Situational Awareness: Prediction of Protection Relay Operations After a Contingency

Ramin Vakili, *Student Member*, IEEE, and Mojdeh Khorsand, *Member*, IEEE
School of Electrical, Computer and Energy Engineering, Arizona State University, Tempe, AZ, USA
rvakili@asu.edu and mojdeh.khorsand@asu.edu

Situational awareness plays a critical role in resilient smart electric grids due to the increase in uncertain and unforeseen events, e.g., the stochastic nature of renewable and distributed energy resources (DERs) as well as cyber-attack threats. The operation of modern electric grids near their security limit has resulted in a reduced stability margin, making these grids vulnerable to severe disturbances. Therefore, online monitoring of the static/dynamic stability of modern power systems is known to be one of the most important tasks to enhance situational awareness in the system and prevent blackouts [1].

Wide Area Measurements (WAMS) using synchronized phasor measurement units (PMUs) are being widely used in the Western Electricity Coordinating Council (WECC) system to provide a wide range of applications such as situational awareness for operational decision making. Eastern Interconnection Phasor Project (EIPP) provides new opportunities to deploy the measurements from PMUs in real-time analysis to evaluate the system dynamic performance [2]. Using the online information provided by PMUs, many research works have developed different online Dynamic Security Assessments (DSA) methods which can provide the operator with an early prediction of system rotor angle or voltage stability following various contingencies. As shown in [3], different protection systems that exist in a power grid play a significant role in defining the behavior of the system during disturbances. Distance relays as well as Under Voltage Load Shedding (UVLS) and Under Frequency Load Shedding (UFLS) relays are among the most important protection relays in the system. However, in the DSA methods developed in previous research works, the behavior of these protection relays has not been assessed during disturbances.

The proposed machine-learning-based algorithm equips the operators with an online tool to predict the behavior of distance relays as well as UFLS and UVLS relays in the system for several seconds after a disturbance, using the real-time data obtained from the PMU units. This gives the operators (or automatic control systems) enough time to initiate proper control actions and enlightens the operators of how a disturbance spreads in the grid and what areas are affected.

Besides its application as an online DSA method, the developed algorithm can be used as a fast offline tool which uses the results of early-terminated transient stability studies (e.g. simulation results captured for one cycle after the disturbance) to identify the critical protection relays which are essential to be modeled in the transient stability studies, thereby addressing the current challenges in modeling all the protection relays in transient stability studies.

The dataset needed for training and testing the proposed machine learning (ML) algorithm is created by conducting extensive offline transient stability studies considering different types of contingencies and operating conditions. The problem of predicting the operation of protection relays is a classification problem. Different ML algorithms can be used for training a classifier for predicting protection relay operations, among which, the decision tree is used in this paper. Voltages of the 10 electrically closest high-voltage buses (i.e. the buses with the voltage level of 345 kV and above, which are usually equipped with PMU units) to the relay locations are captured for one cycle after the disturbance and is used as the features of the algorithm.

I. RESULTS

Three decision trees for predicting distance relay as well as UFLS and UVLS relay operations are trained and tested on the WECC system representing the 2018 summer peak load case considering different types of contingencies and operating conditions. The performances of the algorithms are evaluated using four metrics of accuracy, the accuracy of predicting no operation cases (ANO), recall, and precision. ANO and precision show that what portion of no-operation and operation predictions of the algorithm is correct, respectively. The recall show that what portion of the total operation cases are correctly identified as operation. The results are provided in Table. I.

Table I. Performance of the trained decision trees

The trained algorithm	Accuracy (%)	ANO (%)	Recall	Precision
Distance relays	97.31	98.17	0.943	0.945
UFLS relays	99.11	99.85	0.949	0.991
UVLS relays	97.82	98.71	0.929	0.929

The results show that the trained algorithms can predict the operation or no-operation of the relays with high accuracy. The precision values for all the algorithms are more than 0.9, which indicates that when the algorithms predict the operation of a relay, the prediction is accurate in more than 90% of the time. Also, the recall value is more than 0.9 for all the algorithms, which shows that the trained algorithms can identify more than 90% of the operation cases. This makes the trained algorithms a great planning tool for identifying the critical protection relays in different contingencies, as well. The proposed algorithm predicts operation of distance relay, UFLS relay, and UVLS in only 0.2746, 0.2718, and 0.3932 ms, respectively, which shows that the trained algorithms are fast enough to satisfy the need of an online DSA method to provide an early alert of the pending relay operations in the system.

REFERENCES

[1] Y. Xu, Z. Y. Dong, K. Meng, R. Zhang, and K. P. Wong, "Real-time transient stability assessment model using extreme learning machine," in *IET Generation, Transmission & Distribution*, vol. 5, no. 3, pp. 314-322, Mar. 2011.

[2] K. Sun, S. Likhate, V. Vittal, S. Kolluri, and S. Mandal, "An online dynamic security assessment scheme using phasor measurements and decision trees," *IEEE Power and Energy Society General Meeting - Conversion and Delivery of Electrical Energy in the 21st Century*, Pittsburgh, PA, 2008.

[3] M. Abdi-Khorsand, and V. Vittal, "Identification of Critical Protection Functions for Transient Stability Studies," *IEEE Transactions on Power Systems*, vol. 33, no. 3, pp. 2940-2948, May 2018.

MPC Based Battery and Thermostat set-point Scheduling for Demand Response Applications in a University Campus Building

Divya T. Vedullapalli, *Student Member, IEEE*
Ramtin Hadidi, *Member, IEEE*
The Department of Electrical and Computer Engineering
Clemson University
Clemson, USA
dvedull, rhadidi @ clemson.edu

Abstract – In this work, we develop a demand management controller in a building with a battery energy storage system (BESS) and Heating Ventilation and Air Conditioning (HVAC) set-point scheduling using the Model Predictive Control (MPC). The outcome is the automation of the battery allocation and thermostat settings of the HVAC for a given set of building parameters, utility rate structure and battery specifications. Battery operation is optimized with mixed integer linear programming (MILP) and model predictive control (MPC). It is observed that the grid limit changes adaptively avoiding unnecessary peak reduction with MPC. HVAC operation is modeled mathematically to optimize the power bill. The platform has been simulated on a campus university building modeled in EnergyPlus.

***Index Terms*— Battery energy storage system (BESS), Demand charge management, HAVC Scheduling, Model Predictive Control (MPC), Optimization.**

I. INTRODUCTION

Peak power demand causes problems to the utilities, such as the need of added capacity only for a fraction of 24 hrs., and strain on the grid leading to blackouts. Utilities encourage consumers through demand response programs to change their power usage habits and maintain a flat energy consumption profile. In response to such programs, commercial consumers can make use of batteries to shift the load partially from peak to off-peak time and reduce the electricity cost. A building's thermal mass can also be used as a virtual battery to store the heat energy by pre-cooling or pre-heating during off-peak hours and reducing the power consumption during peak hours.

This project involves the development of a demand management controller for a commercial building. An accurate forecast of the load consumption profile is necessary to find the optimal operation schedule since forecast errors often lead to sub-optimal or infeasible solutions. The following are the major contributions of this work:

1. A forecaster that predicts the power from the facility for the next 24 hours which will be the main input to the optimizing algorithm.
2. Modeling of the university building in EnergyPlus and comparison of the simulated building power with actual power consumption of the building
3. An optimizer for the HVAC operation that will calculate setpoints to minimize the electricity bill for the power consumed by HVAC by utilizing the thermal mass of the building to store heat/cool energy without sacrificing the comfort or productivity of building occupants or the performance of devices and equipment in the building.
4. A Novel mathematical modeling of the HVAC for use in optimization model has been developed to schedule the thermostat set-points subjected to time-of-use electricity pricing.
5. An optimizer for the BESS operation that will schedule the battery to satisfy the predicted load of the building in step (1) with its HVAC power determined in step (3). The objective of this optimizer is to minimize the monthly electricity bill subjected to time-of-use electricity pricing with demand charges.

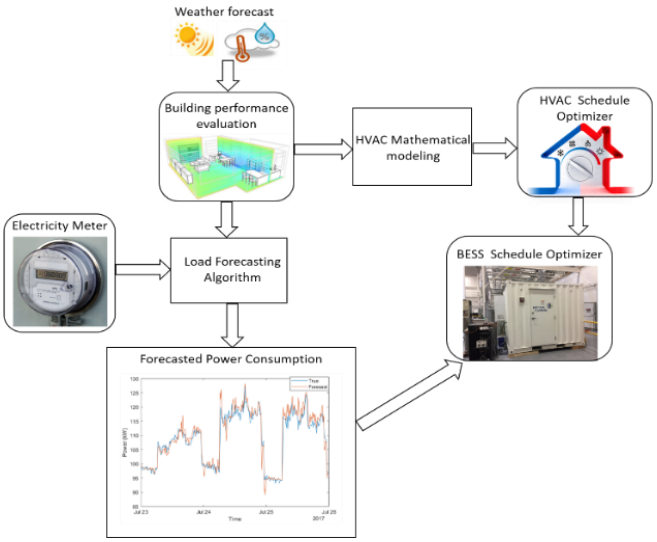

Fig 1. Schematic of the proposed algorithm

This algorithm is implemented on a single storied building with an area of 52,000 square foot and 45 conditioned zones located in Clemson University. Its power consumption is highly dynamic, and its power prediction is exigent for developing a demand response algorithm.

Verification of Physics-Informed Neural Networks: Formal Guarantees for Power System Applications

Andreas Venzke and Spyros Chatzivasileiadis
Department of Electrical Engineering
Technical University of Denmark
Lyngby, Denmark
{andven, spchatz}@elektro.dtu.dk

***Abstract*—This work presents a framework for verifying physics-informed neural network behavior in power system applications. Machine learning approaches including neural networks have shown significant promise, e.g., by performing power system security assessment at a fraction of the time required by conventional approaches. Neural networks are, however, treated so far as black-box tools and trained physics-agnostic, i.e., without knowledge of the underlying physical equations and constraints. This represents a major obstacle towards their adoption in practice. For power system applications and leveraging mixed integer linear reformulations of trained neural networks, this works introduces a rigorous framework to provide formal guarantees of neural network behaviour and to train physics-informed neural networks. We demonstrate our methodology on a range of IEEE test cases, illustrating that physics-agnostic training can lead to substantial worst-case physical constraint violations.**

I. Motivation

The increase of uncertainty in both generation and load presents challenges for secure power system operation. Machine learning, such as decision trees and neural networks, has demonstrated significant potential for highly complex classification tasks including the security assessment of power systems. However, the inability to anticipate the behavior of neural networks, which have been usually treated as a black box, has been posing a major barrier in the application of such methods in safety-critical systems, such as power systems. In this work, we develop provable formal guarantees of the behavior of neural networks for power system application, building on [1]. Our methods allow to evaluate the robustness and improve the interpretability of neural networks and have the potential to build the missing trust of system operators in neural networks, enabling their application in practice.

II. Summary

Leveraging a mixed-integer reformulation of trained neural networks from [2], we develop a rigorous framework to provide formal guarantees for both classification and regression neural networks for power system applications.

For classification neural networks, we verify continuous input regions for which we can guarantee the same classification, i.e. operating regions for which the classifiers predicts 'safe' operation with respect to defined security criteria. At the same time, we can use this framework to identify so-called adversarial examples. These are small changes to the neural network input which lead to a false change in classification, i.e. from 'unsafe' to 'safe'. By systematically including adversarial examples in the training procedure we increase the robustness of classification neural networks. We demonstrate our methods on the IEEE 9-bus, 14-bus, and 162-bus systems, treating both N-1 security and small-signal stability.

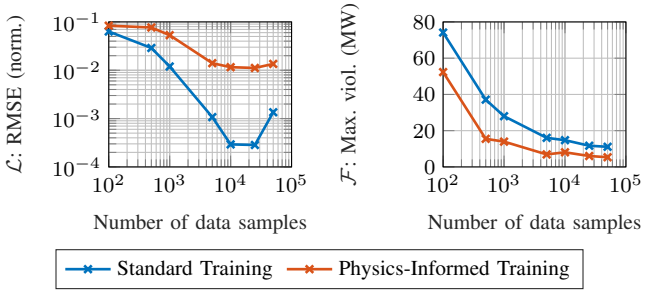

Fig. 1. We compare standard and physics-informed training of a neural network for predicting the solution to the DC-OPF problem for an IEEE 30 bus system as a function of the system loading. We show the accuracy in terms of root mean square error (RMSE) and the worst-case bound on the maximum physical constraint violation for the defined input domain $\mathcal{D}$ as a function of the number of data samples used in training.

For regression neural networks, we train neural networks to predict the solution to DC optimal power flow (DC-OPF) problems with the system loading as input. We provide exact worst-case guarantees on the violation of physical constraints $\mathcal{F}$ for a defined neural network input domain $\mathcal{D}$. To tighten these guarantees, we train physics-informed neural networks. To this end, we modify the objective function of neural network training to $\mathcal{L} + \gamma\mathcal{F}$, where $\mathcal{L}$ is the loss function associated with the accuracy, γ is a weighting term and the term $\mathcal{F}$ penalizes the constraint violation. We demonstrate our methodology on range of PGLib OPF cases up to 300 buses, illustrating that physics-agnostic training can lead to large worst-case physical constraint violations, whereas physics-informed training can reduce these substantially. Fig. 1 shows the obtained results for the IEEE 30 bus test system.

References

[1] A. Venzke and S. Chatzivasileiadis, "Verification of neural network behaviour: Formal guarantees for power system applications," *arXiv preprint arXiv:1910.01624*, 2019.

[2] V. Tjeng, K. Xiao, and R. Tedrake, "Evaluating robustness of neural networks with mixed integer programming," *arXiv preprint arXiv:1711.07356*, 2017.

An Online Energy Flow Control Strategy for Regional Integrated Energy System

Guofeng Wang†, Chongbo Xu†, Chengpeng Hu†, Xiaodong Yang‡,Youbing Zhang*†
† Zhejiang University of Technology, Hangzhou 310023, China
‡ Huazhong University of Science and Technology, Wuhan 430074, China

***Abstract*—In this paper, we propose an online strategy for optimal energy flow control based on Lyapunov method in regional integrated energy system. First, consider the changes in specific events. e.g., basic load, electricity price, queue length of controllable load, an event triggering mechanism is established to automatically execute the scheduling signals. Without relying on a priori knowledge, Lyapunov optimization method is then used to control virtual energy queue of active load and the system stability in real time. Finally, the remaining renewable energy resources are allocated in a pre-defined priority. The theoretical deduction and numerical results prove the feasibility of the proposed online algorithm.**

I. Energy Flow Control Framework

A. Construction of the RIES System

We establish a typical architecture for regional integrated energy system (RIES) in this paper (Fig. 1).

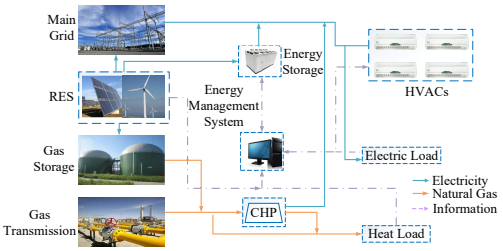

Fig. 1. Architecture for regional integrated energy system.

B. Problem Formulation

A stochastic programming problem is formulated as:

$$\textbf{(P0)} \triangleq \min \lim_{T\to\infty} \sup \frac{1}{T}\sum_{t=0}^{T-1} \mathbb{E}\{C(t)\} \tag{1}$$

Transform the original problem [1] **(P0)** into:

$$\begin{aligned}\textbf{(P1)} \triangleq \min(\Theta + \sum_{i=1}^{N}[Q_i(t)L_i(t) + X_i(t) \\ (V_i R(t)\frac{X_i(t) - S_i(t)}{P_i} - Q_i(t))])\end{aligned} \tag{2}$$

The solution of minimizing objective function can be simplified to the following auxiliary theorems to determine the value of $X_i(t)$,

$$X_i(t) = \begin{cases} 0\ , & V_i R_t \frac{X_i(t)-S_i(t)}{P_i} > Q_i(t) \\ P_i, & V_i R_t \frac{X_i(t)-S_i(t)}{P_i} \leq\ Q_i(t) \end{cases} \tag{3}$$

This work was supported by National Natural Science Foundation of China (No. 51777193) and National Postdoctoral Program for Innovative Talents of China under Grants No. BX20190126.

It is obvious that the computational complexity will not increase exponentially with the system dimension increase. The proposed online algorithm can ensure that the scheduling of $X_i(t)$ is applicable in the case of high-order system.

C. Comparison Analysis of Optimization Results

Through simulation, results under three different schemes e.g. OALO (Online Algorithm with Lyapunov Optimization), Online Algorithm OACI (Online Algorithm with Current Information), OALO+P2G are shown in Table I.

TABLE I
Simulation Results In Three Cases

Cases	Cost (¥)	RES Utilization (%)	Comfort Level (%)
A.OACI	631.74	54.46	79.76
B.OALO	520.66	55.38	67.38
C.OALO+P2G	457.90	98.08	67.38

According to the comparison figure of running time shown in Fig. 2, the opening/closing frequency of HVAC in OACI is obviously higher than that in OALO, which will substantially worsen the hardware of HVAC.

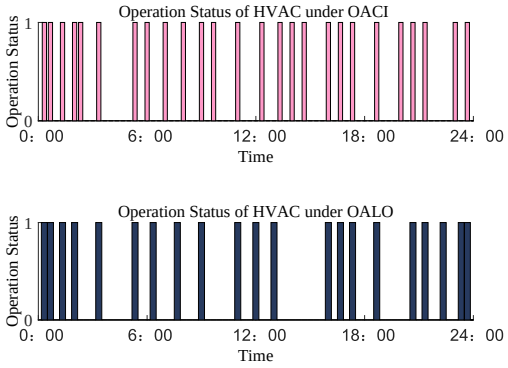

Fig. 2. Comparison of the HVAC operation status

II. Conclusion

We propose an event-driven online energy optimization algorithm for the regional integrated energy system incorporating P2G and CHP technology. The introduction of P2G and CHP technology enhances the coupling degree between the electrical network of the RIES, effectively reduces the gas cost of users and significantly improves the utilization of RES.

References

[1] M. J. Neely, "Stochastic network optimization with application to communication and queueing systems," *Synthesis Lectures on Communication Networks*, vol. 3, no. 1, pp. 1–211, 2010.

Diversity Factor Prediction for Distribution Feeders with Interpretable Machine Learning Algorithms

Wenyu Wang, Nanpeng Yu, Jie Shi
Department of Electrical and Computer Engineering
University of California, Riverside
Riverside, USA

Nery Navarro
Grid Modernization
Southern California Edison
Pomona, USA

***Abstract*—The maximum diversified demand is an important factor to consider when utilities design new distribution systems. To estimate the maximum diversified demand, engineers need to make an estimate of the diversity factor (DF). In practice, electricity utility companies usually estimate the DF using DF tables, in which the DF changes with the number of customers. However, besides the number of customers, DF also depends on many other factors, such as customer type, weather, demographics, and socioeconomic conditions. Ignoring these factors, DF tables have limited accuracy. In addition, engineers cannot interpret or understand how various factors affect the DF. In this paper, by leveraging supervised machine learning algorithms, we build comprehensive DF prediction models that take a variety of factors into account. These models show high prediction accuracy and interpretabilty when applied to real-world distribution feeders. Using the interpretation method called SHapley Additive exPlanations, we quantify the importance of different features in determining DFs. Finally, we offer more insights into how various factors affect DFs.**

***Index Terms*—Distribution circuit planning, diversity factor, interpretable machine learning, SHapley Additive exPlanations, supervised machine learning.**

Over Frequency Curtailment of PV Generation in Low Inertia, Islanded Microgrids

Jan Westman
The Department of Electrical and Computer Engineering
Clemson University
Clemson, USA
jwestma@clemson.edu

Ramtin Hadidi
The Department of Electrical and Computer Engineering
Clemson University
Clemson, USA
rhadidi@clemson.edu

Curtiss Fox
The Department of Electrical and Computer Engineering
Clemson University
Clemson, USA
fox8@clemson.edu

Jesse Leonard
The Department of Electrical and Computer Engineering
Clemson University
Clemson, USA
jpleona@clemson.edu

***Abstract*— The use of FREQ/WATT droop control of solar photovoltaic (PV) inverters has been demonstrated to provide effective mitigation of over frequency events in power systems with high penetrations of distributed PV resources. These investigations have often been conducted in the context of distribution and transmission systems with hundreds of MW of rotating generation. In the case of islanded microgrids with rotating generation capacity on the order of tens of MW, the system inertia will be much lower and the generator dynamics more tightly coupled to the PV inverter dynamics, leading to relatively less stable system frequency. This investigation proposes to test the use of the FREQ/WATT function on the operation and control of a small industrial, island microgrid grid with over 50% penetration of PV resources by utilizing real-time digital simulation with controller-hardware-in-the-loop (CHIL) testing of commercially available generator control systems. The results will illustrate the dynamic response of the test system frequency to several load rejection events as well as the sensitivity of the system frequency to the FREQ/WATT function parameters. The objective of the investigation is to determine the suitability of the FREQ/WATT function to provide decentralized over frequency curtailment of the microgrid test model PV system.**

Keywords—controller-hardware-in-the-loop, droop control, inverters, island microgrids, PV, real-time digital simulation

I. Test Set-up

The test model represents a three phase, 4160 V microgrid composed of four 2.5 MW, 4160 V, synchronous generators, a 6.6 MW, 480 V solar photovoltaic (PV) system with a step up transformer and an average value model (AVM) of the inverter, and five 1.65 MW induction motors driving compressor loads. The test model is simulated using RTDS Technologies' PB5 processor cards and a one line diagram of the test model is provided in Fig. 1. The PV inverter controls with the implementation of the FREQ/WATT function are included in the simulated test system.

The generator model voltage and speed control is performed by four Woodward easYgen 3400XT-P2 genset control systems. The easYgens are interfaced to the RTDS simulation via the gigabit transceiver I/O (GTIO) cards. A diagram of the controller-hardware-in-the-loop (CHIL) test set-up is shown in Fig. 2.

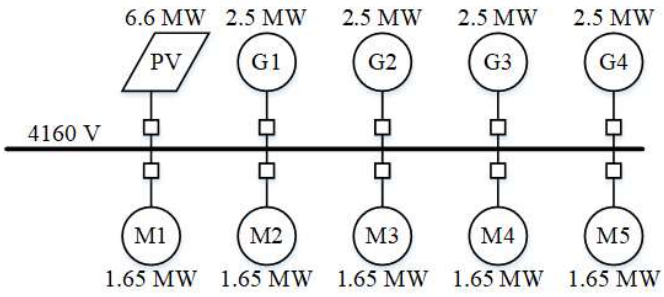

Fig. 1. Microgrid test model implemented in the RTDS simulator.

II. Test Procedure

Sensitivity analysis of the system frequency response to a single, full load induction motor load rejection event is performed for the PV system FREQ/WATT function over frequency deadband d_{of} and droop slope K_{of} parameters. For the analysis of each parameter, the microgrid is simulated for multiple pre-event system operating conditions determined by the number of induction motor loads connected to the microgrid. For each test, the microgrid energy management system (EMS) dispatches the PV system output and the number of synchronous generators based on the maximum loading of the induction motors and the maximum expected solar irradiance (i.e. availability of full PV system output). As a result, each parameter set is tested for varying amounts of system inertia due to the differing numbers of generators dispatched by the EMS with the maximum allowed contribution of the PV system.

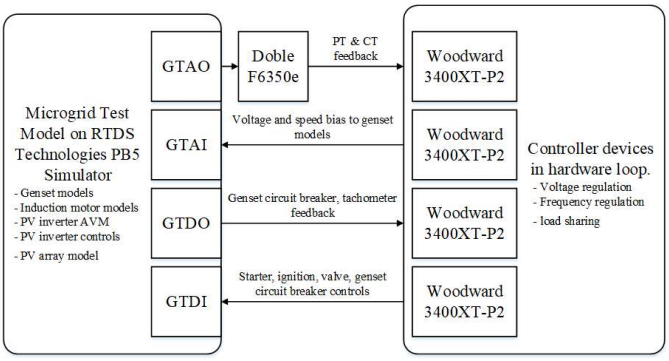

Fig. 2. The genset controller hardware connections to the RTDS simulator.

Nonparametric Joint Chance Constraint for Spinning Reserve Requirements

Chutian Wu, *Student Member, IEEE*, Amin Kargarian, *Member, IEEE*

***Abstract*—Probabilistic decision-making tools are needed for power systems management as the penetration level of uncertain renewable generation increases. These decisions-making tools should be nonparametric, which meant agnostic to probability density functions of renewable generation since probability density functions of renewables may or may nor belong to any known classes of probability distributions. This poster presents data-driven nonparametric joint chance constraints (JCCs) for economic dispatch. Solar generation uncertainty is considered as a random parameter with an unknown probability density function that may not belong to any parametric class of probability function. Since reserve provided by generators is dependent on their ramp up/down capabilities that are time-dependent, reserve up and down constraints at consecutive time intervals are dependent. Thus, we propose to formulate reserve up and down constraints as nonparametric JCCs that are joint over the considered scheduling horizon. Univariate and multivariate kernel density estimators are used to estimate nonparametric probability distributions of solar generation from historical data and then convert line flow and reserve JCCs into their closed-form solvable by standard solvers. Using joint chance constraints enhances system reliability significantly as compared to using individual chance constraints.**

I. Key Equations

1. The objective function is to minimize the operational costs, including generation and reserve costs, of thermal units and battery storage.

$$\min \sum_{\forall t}\sum_{\forall u} c_{1u} + c_{2u}p_{u,t} + c_{3u}p_{u,t}^2 + a_u ru_{u,t} + \sum_{\forall b} \beta_b\left(p_{b,t}^c + p_{b,t}^d\right) + \gamma_b\left(ru_{b,t} + rd_{b,t}\right) \quad (1)$$

2. Reserve up chance constraint:

$$\mathbb{P}\left\{\sum_{\forall u}\left(p_{u,t} + ru_{u,t}\right) + \sum_{\forall b}\left(p_{b,t}^d - p_{b,t}^c + ru_{b,t}\right) + \sum_{\forall r}\widetilde{PR}_{r,t} \geq P_{d,t} \quad \forall t\right\} \geq 1 - \alpha^{JCC} \quad (2)$$

3. Reserve down chance constraint:

$$\mathbb{P}\left\{\sum_{\forall u}\left(p_{u,t} - rd_{u,t}\right) + \sum_{\forall b}\left(p_{b,t}^d - p_{b,t}^c - rd_{b,t}\right) + \sum_{\forall r}\widetilde{PR}_{r,t} \leq P_{d,t} \quad \forall t\right\} \geq 1 - \alpha^{JCC} \quad (3)$$

The authors are with the Department of Electrical and Computer Engineering, Louisiana State University, Baton Rouge, LA 70803 USA (e-mail: cwu17@lsu.edu, kargarian@lsu.edu).

4. Introduce two auxiliary variables to reformulate (2) and (3):

$$P_{d,t} - \sum_{g}\left(p_{g,t} + ru_{g,t}\right) - \sum_{b}\left(p_{b,t}^d - p_{c,t}^c + ru_{b,t}\right) = g_{ju,t} \quad \forall t \quad (4)$$

$$P_{d,t} - \sum_{g}\left(p_{g,t} - rd_{g,t}\right) - \sum_{b}\left(p_{b,t}^d - p_{b,t}^c - rd_{b,t}\right) = g_{jd,t} \quad \forall t \quad (5)$$

5. Reformulated (2) and (3) as follows:

$$\frac{1}{n}\sum_{i=1}^{n}\prod_{j=1}^{m}\left[1 - \kappa_j\left(\frac{g_{ju,t}(x) - X_{j,i}}{h_j}\right)\right] \geq 1 - \alpha' \quad \forall t \quad (6)$$

$$\frac{1}{n}\sum_{i=1}^{n}\prod_{j=1}^{m}\kappa_j\left(\frac{g_{jd,t}(x) - X_{j,i}}{h_j}\right) \geq 1 - \alpha' \quad \forall t \quad (7)$$

II. Key Results

A six-bus system is used, and three cases are considered as follows:

- Case 1: Applying parametric chance constraint considering known density functions (Gaussian) for solar generation
- Case 2: considering reserved constraints as individual chance constraints and applying nonparametric individual chance constraints
- Case 3: Applying the proposed nonparametric joint chance constraints

Although the third case has the highest operation cost and solution time, applying nonparametric JCCs results in the procurement of adequate reserve that ensures system security.

TABLE I
COMPARISON OF APPLYING PARAMETRIC, ICCS, AND 6 HOURS JCCS

	Case 1	Case 2	Case 3
Total Cost ($)	9.3161×10^4	9.3167×10^4	9.3197×10^4
Time (sec)	Less than 1	Less than 1	64

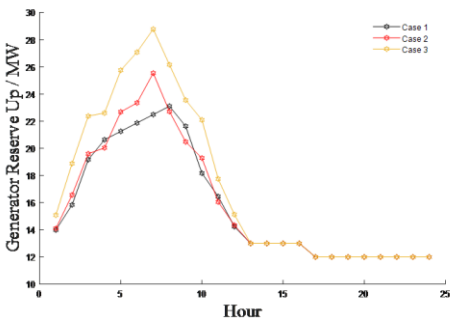

Fig.1. Hourly generation reserve up comparison between three cases.

Distributed Optimal Scheduling of Multi-region Intergrated Energy Systems Considering Regional Heating Network

Mingchao Xia, Zhihao Hua, Qifang Chen
School of Electrical Engineering
Beijing Jiaotong University
Beijing, China

Meijing Lv
Smart Campus Construction Center
University of Finance and Economics
Beijing, China

***Abstract*—This paper focuses on the joint optimization scheduling of multi-region integrated energy systems (IES) and the influence of regional heating networks on joint scheduling. The IES model is firstly established, including the heating network model and the internal equipment model. Then, in order to ensure the independence of each IES, a bi-level model of multi-region IESs joint scheduling considering regional heating network is established, which is solved by distributed algorithm - analysis target cascading method (ATC). Finally, the simulation results show that the proposed model can effectively optimize the energy scheduling between IESs while ensuring the independence of each IES. The regional heating network can be used as heat storage equipment to participate in the joint scheduling, and absorbs the excess heat energy in IES that cannot be transferred to other IESs.**

***Index Terms*-- integrated energy system; heating network; distributed optimal scheduling; distributed algorithm**

I. INTRODUCTION

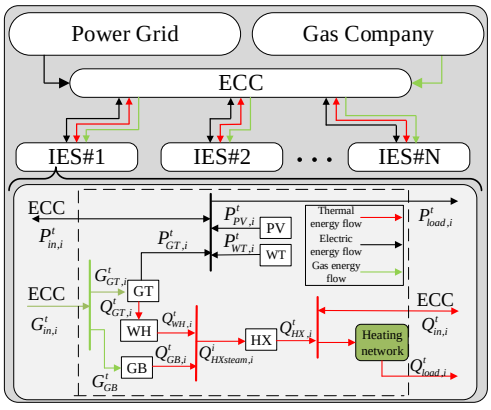

Figure 1. Joint scheduling framework of Multi-region IESs.

The upper layer is the energy coordination center (ECC), and the lower layer is the multi-region IESs. ECC coordinates the distribution of various energy sources and transfers the surplus electric or thermal energy delivered by IES$_i$ to other IES$_i$ with insufficient capacity.

II. KEY EQUATIONS

According to ATC, the original objective functions (f_1, f_2, ⋯, f_N for IESs; F for ECC) are transformed into:

$$\begin{cases} \min \quad f_i\left(y_i,\zeta_i\right)+\lambda\left\|\left(\eta_i^*-\mu_i\right)\right\|_2^2 \\ \min \quad F\left(x,\zeta_1,\zeta_2,\cdots,\zeta_N\right)+\lambda\sum_{i=1}^{N}\left\|\left(\eta_i-\mu_i^*\right)\right\|_2^2 \end{cases} \tag{1}$$

where y_i is the local specific variable of IES$_i$; x is the local specific variable of ECC; ζ_i is the shared variable between ECC and IES$_i$; μ_i^* is the reference value of the penalty term of ECC, equal to the result value of the lower IES$_i$ optimization; η_i^* is the reference value of the penalty term of IES$_i$, equal to the result value of the ECC; λ is the penalty coefficient; η_i and μ_i are shared variables of ECC and IES$_i$.

III. KEY RESULTS

When the objective function of ECC and IES$_i$ is to minimize the cost, the optimized cost is:

TABLE I. COMPARISON BETWEEN CENTRALIZED MODEL AND DISTRIBUTED MODEL

Categories	f_1 ($)	f_2 ($)	f_3 ($)	F ($)
Centralized	35767.31	52031.81	48913.36	100261.83
Distributed	39090.50	49449.41	47997.61	100423.01

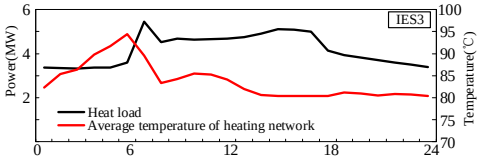

Figure 2. Heat load and average temperature of heating network of IES$_3$.

Under the distributed modeling, different subjects can achieve respectively their optimality. The heating network can provide a way for IES to absorb excess heat energy which cannot be transmitted to other IESs, and reduce the impact of load fluctuation on IES.

This work was supported by the National Science Foundation of China (Grant No. 51677003); this work was supported by the Project funded by China Postdoctoral Science Foundation (Grant No. 2018M631326).

Analysis of Radial Constraint Representation Methods for Distribution Networks

Chengsi Xu, Shufeng Dong
College of Electrical Engineering, Zhejiang University, Hangzhou, China

***Abstract*—In distribution network optimization problems, radial topology is an important constraint to be considered. The review of existing radial constraint representation methods (RCRMs) has not been reported yet, while appropriate method should be selected according to specific network to improve solving efficiency. This paper is devoted to a new RCRM and a summary of the existing RCRMs. Firstly, based on the idea of loop disconnection, a sufficient and necessary condition for distribution network topology to be radial is proposed, and an algorithm for searching all loops in a network is introduced. Then, the differences and characteristics of various RCRMs are analyzed. Finally, the introduced RCRMs are applied to the problem of service restoration reconfiguration. Simulation result on an actual distribution network in Fuzhou, China compares the computing performance of different methods.**

Keywords—radial constraint, distribution network, loop disconnection, service restoration reconfiguration

I. KEY METHODS

A. Existing RCRMs

The following two conditions are usually adopted to ensure that the distribution network topology is radial.

- Condition 1: There are N-N_s closed branches in the distribution network.
- Condition 2: The distribution network is connected.

Where N is the total number of nodes in the network; N_s is the number of substation nodes in the network.

The formula for condition 1 is as follows:

$$\sum_{b=1}^{B} x_b = N - N_s \tag{1}$$

Where B is the total number of branches in the distribution network; b is the branch number; x_b is the state of the bth branch, whose value is 1 when the bth branch is closed and 0 when the bth branch is disconnected.

Many researchers have established the model of condition 2, including the spanning-tree model, the virtual demand model and the path-based model. However, condition 2 involves network connectivity, which is a property related to the whole network, so its corresponding model is complex.

B. A new RCRM based on loop disconnection

Different from the existing methods, this paper takes condition 3 as one of the conditions that radial topology should satisfy, and proposes proposition 1, as follows:

- Condition 3: All loops in the network are disconnected.
- Proposition 1: condition 1 and condition 3 are necessary and sufficient conditions to ensure distribution network topology to be radial.

The formula for condition 1 is as follows:

$$\sum_{m=1}^{M_l} x_{lm} \le M_l - 1, \quad l = 1, 2, \cdots, L \tag{10}$$

This work is supported by National Key R&D Program of China (No. 2016YFB0901300).

Where L is the number of loops in the distribution network; M_l is the number of branches in the lth loop; x_{lm} is the state of the mth branch in the lth loop.

II. CASE STUDY AND RESULTS

We take the service restoration reconfiguration problem as an example to compare the computing performance of different RCRMs. The distribution network is shown in Fig. 1.

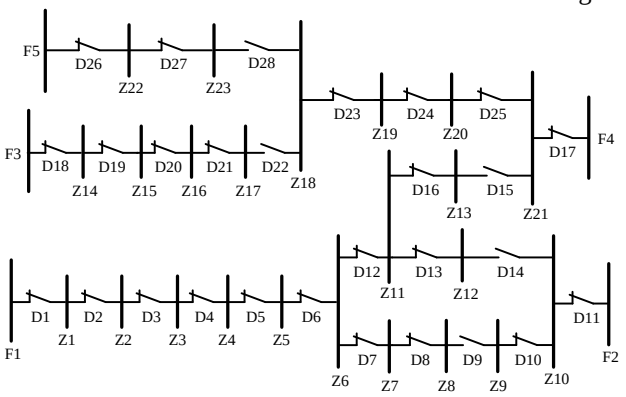

Fig. 1. Diagram of an actual distribution network in Fuzhou, China

In the service restoration reconfiguration problem, using different RCRMs to represent radial constraints. The variable numbers of the spanning-tree model, the virtual demand model, the path-based model and the model proposed in this paper are 112, 84, 187, 56 respectively. And the constraint equation numbers are 140, 164, 238, 103 respectively.

Assume that the substations F1−F5 fault successively, and solve the service restoration reconfiguration models based on different RCRMs respectively. The computing time of different models is shown in TABLE I.

TABLE I. COMPUTING TIME OF DIFFERENT MODELS

Faulty Substation	**Computing Time (ms)**			
	Model in This Paper	***Spanning-tree Model***	***Virtual Demand Model***	***Path-based Model***
F1	12.5	14.7	16.7	26.6
F2	12.3	15.6	17.8	22.5
F3	7.2	8.2	10.6	18.6
F4	10.1	11.3	16.3	21.4
F5	7.4	8.7	9.8	16.6

The comparison result shows that the RCRM based on loop disconnection is applicable to the case where the number of loops in the distribution network is not too large as the one shown in Fig. 1. When the number of loops is large, the spanning tree model or virtual demand model should be selected, among which the spanning tree model is a better choice. When the problem to be analyzed is closely related to the power supply path and the number of loops in the network is small, the power supply path model can be adopted.

Fast Transient Stability Batch Assessment using Cascaded Convolutional Neural Networks

Rong Yan, Guangchao Geng, Quanyuan Jiang, and Yanglin Li

***Abstract*—Stability assessment is a regular routine in both power system planning and operation. It is computationally demanding using state-of-the-art approaches like time-domain simulation (TDS), as numerous scenarios (e.g., N-1 contingencies) have to be assessed for a large batch of contingencies. The purpose of this work is to determine stability conclusion before the simulator reaches the end of simulating time windows. Therefore, TDS can be terminated early so as to reduce the average simulation time for batch assessment without losses of accuracy. The idea is to develop a data-driven methodology to "learn" from existing TDS results in the batch and "infer" stability conclusions using current available TDS output. To achieve this goal, cascaded convolutional neural networks (CNNs) are designed to capture data from different TDS time intervals, extract features, predict stability probability and determine TDS termination. While accumulating more knowledge in batch processing, early termination criterion is refreshed continuously via feedback learning to terminate TDS increasingly earlier, with the increase of existing TDS results in the batch. Case studies in IEEE 39-bus and Polish 2383-bus system illustrate effectiveness of the proposed method.**

***Index Terms*—Convolutional neural networks, data driven, machine learning, time-domain simulation, transient stability assessment.**

I. Proposed Method

In this paper, a novel fast transient stability batch assessment framework using cascaded CNNs is proposed, in order to determine stability conclusion using partial TDS output and early terminate TDS to shorten the average simulation time for a large batch of contingencies without losses of accuracy. Considering the assessment time of training samples, we proposed a model refreshing mechanism by the lights of semi-supervised learning, so that early termination criterion can be refreshed continuously during batch assessment. In general, this paper is highlighted with the following three contributions:

1) Cascaded CNNs are designed to capture data from different TDS time intervals, extract features automatically, predict stability probability and determine TDS termination. It is a novel framework to accelerate the process of security check and enhancement in grid planning and day-ahead dispatch.

2) Early termination criterion refreshing mechanism via feedback learning is proposed in this work. While accumulating more knowledge in batch processing, criterion can be refreshed continuously to terminate TDS increasingly earlier, with the increase of existing TDS results in the batch. Moreover, mechanism also enhances the adaptability to changed operating condition.

3) The proposed framework together with some algorithmic enhancements (e.g., misjudgment scenarios based loss function) demonstrates accurate assessment results with lower computational burden, compared with existing methods.

R. Yan, G. Geng (Corresponding author), Q. Jiang and Y. Li are with the College of Electrical Engineering, Zhejiang University, China (email: {yanrong052,ggc,jqy,21610189}@zju.edu.cn,). This work was supported by National Natural Science Foundation of China (51677164), Fundamental Research Funds for the Central Universities (2018QNA4018).

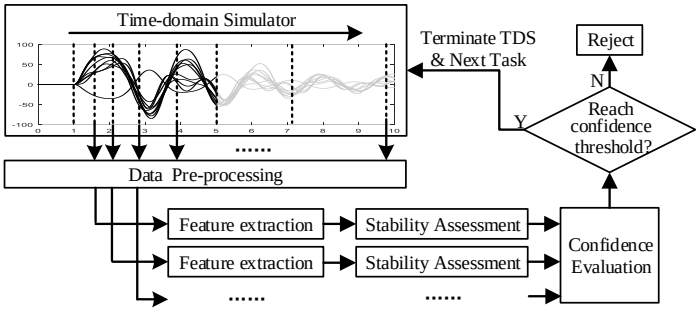

Fig. 1. The application framework of fast transient stability batch assessment.

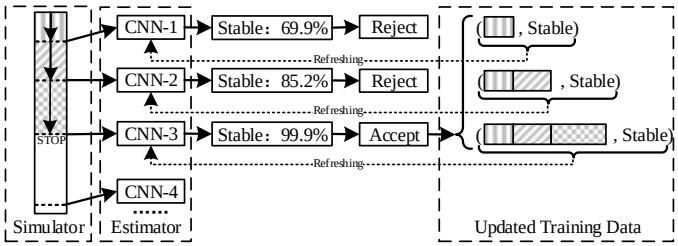

Fig. 2. Model refreshing mechanism.

II. Case Studies

Two typical systems with different scales are investigated: IEEE 39-bus test system and Polish 2383-bus power system. The following table illustrated the comparison test result of Polish 2383-bus system.

TABLE I
Indices Comparison between the Proposed and Existing Method using Polish 2383-bus System

Method	AC(%)	FD(%)	FA(%)	RJ(%)	AEST(s)	MST(s)
EEM	96.07	3.93	0	0	5.407	5.502
TCC	99.10	0.88	0.02	0	2.047	2.030
SVM	91.01	0.09	0	0	4.057	≈ 0
DT	98.26	0.94	0.84	0	2.566	≈ 0
CNN	98.26	0.32	1.42	0	2.279	0.400
RNN	98.31	0.33	0.27	1.09	2.072	0.069
Proposed	99.82	0.11	0.07	0	1.118	0.697

* The accuracy requirement of online TSA frameworks is set to 98% (except SVM), and training samples SVM: 15,000, DT: 9,500, single CNN and RNN: 7,500.

Paper Id: 20PESGM1191

1191

PESGM 2020

Virtual Synchronous Generator Control of Variable Speed Pumped Storage Hydropower with Full-size Converter

Zhengwen Yang, Fen Tang, Xuezhi Wu, Wei Wang, Jingya Jiang
National Active Distribution Network Technology Research Center
Beijing Jiaotong University of Beijing, P.R. China

Abstract

To allow power electronics interfaced variable speed pumped storage hydropower (PSH) providing adjustable inertia as well as frequency and voltage support, a virtual synchronous generator (VSG) control scheme of variable speed PSH with the full-size converter is proposed. First, the mathematical models of reversible pump-turbine are given. On this basis, the proposed VSG control strategy is presented, where the machine-side converter aims to provide a steady DC-link voltage and meet the reversible pump-turbine requirements while the grid-side converter conducts the VSG control. In this way, the original fixed inertia of reversible pump-turbine, which is wasted by the conventional control, and the equivalent inertia of intermedia capacitor could be controllable integrated into the adjustable system inertia to grid. Finally, the simulation study of a 5MW VSPSH is carried out on Matlab/Simulink to verify the effectiveness of the proposed control method. The comparative results of fixed speed PSH, variable speed PSH with conventional control and the proposed control demonstrate that the proposed control strategy has good reference tracking and presents adjustable inertia to grid, which is meaningful to facilitate frequency and voltage support of the power system.

Keywords—variable speed pumped storage hydropower (VSPSH); full-size converter (FSC); virtual synchronous generator (VSG)；rotor inertia and virtual inertia

A. The basic structure of variable speed pumped storage hydropower with full-size converter

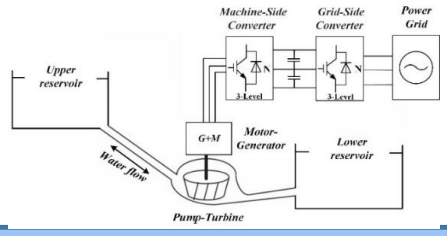

The typical variable speed pumped storage hydropower with full-size grid-connected converter consists of a reversible pump-turbine, a motor-generator i.e. electrically excited synchronous generator (EESG), and a three-level full-size converter (FSC) which is composed of the machine-side converter (MSC) and grid-side converter (GSC). The GSC is connected to the grid and is usually controlled to provide a steady DC-link voltage and meet the power quality requirements, while the MSC is connected to EESG and control the active and reactive power injected into the grid.

B. The model of reversible pump-turbine

The available hydraulic mechanical power P_{PT} can be expressed as formula (1),where η is the hydraulic turbine efficiency, ρ is the volume density of water, g is the acceleration due to gravity, Q is the water flow rate passing through the turbine, and H is the effective water head.For a fixed water head, the pump-turbine hydrodynamic torque depends mainly on the water flow rate and on the rotational speed, which is given as formula (2). Neglecting the mechanical friction effects, the pump-turbine motion equation is expressed as formula (3). where J is the total inertia of the pump-turbine and motor-generator and T_{em} is the electromagnetic torque of EESG.

$$P_{PT}=\eta P_h=\eta\rho gHQ_w \quad (1)$$

$$T_{PT}(Q_w,\Omega)=P_{PT}/\Omega \quad (2)$$

$$T_{PT}(Q_w,\Omega)-T_{em}=J(d\Omega/dt) \quad (3)$$

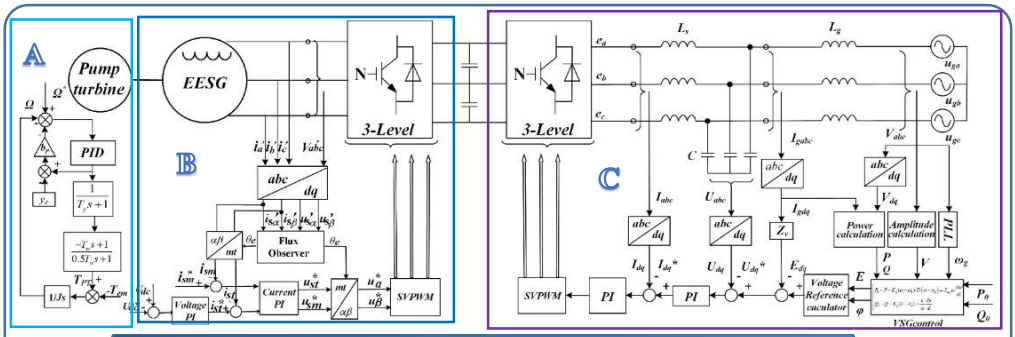

C. The proposed virtual synchronous generator control schematic diagram

The pump-turbine side adopts the closed-loop speed control as shown in Fig A, thus PSH could operate at optimal target speed Ω* under a certain head. The machine-side converter control strategy is mainly composed of a DC-link voltage outer loop and a torque current inner loop to control the intermediate DC-link voltage as shown in Fig B. The VSG-based three-phase converter control method includes the outer loop VSG control and the inner loop control as shown in Fig C, which can not only quickly respond to superior power scheduling commands but also participate in power regulation when the grid frequency or voltage fluctuates.

D. Simulation result

TABLE I MAIN PARAMETERS

	S_N (MVA)	V_{dc} (V)	V_{ac} (V)	N (r/min)	J (kgm²)
C-PSH	5	-	3300	1000	6800
FSC-VSPSH1	5	5200	3300	1000	6800
FSC-VSPSH2	5	5200	3300	1000	6800

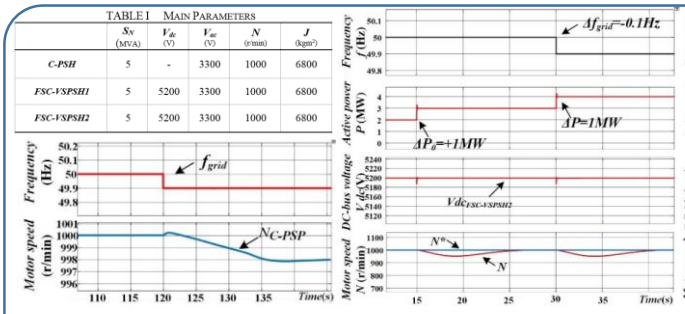

Fig.1. Simulation results of C-PSH when Δf_{grid}=-0.1Hz

Fig.2.Simulation results of ***FSC-VSPSH2,*** J_{VSG}=2 when $\triangle P_0$=+1MW at 15s and Δf_{grid}=-0.1Hz at 30s.

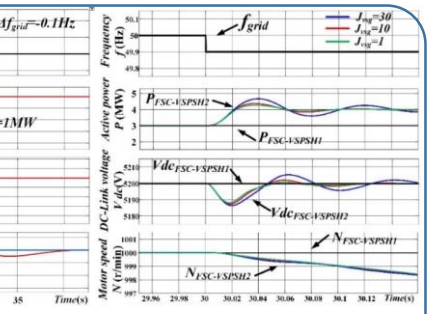

Fig.3. Simulation results of ***FSC-VSPSH*** when $\triangle f_{grid}$=-0.1Hz.

Based on MATLAB/Simulink，the proposed control strategies are validated. C-PSH: Fixed speed PSH ; FSC-VSPSH1:variable speed PSH with conventional control; FSC-VSPSH2:variable speed PSH with the VSG control . The main waveforms of VSPSH2 with J_{vsg} = 2 when power command steps up and grid frequency steps down are presented in Fig.2. At 15s, the power command P_0 is changed from 2MW to 3MW. At 30s, the grid frequency is reduced by 0.1Hz. It can be seen that VSPSH2 achieves good reference tracking and presents inertia support to grid frequency changes, which proves the effectiveness of the VSG control strategy. The comparative results of three cases when grid frequency steps down are shown in Fig.1 and Fig.3. It can be seen from Fig.1 that the C-PSH can respond to the grid frequency changes at 3MW power generation. However, the adjustment range of the rotational speed is limited, and the kinetic energy released on the rotor is small.

The simulation results of FSC-VSPSH1 and FSC-VSPSH2 when the grid frequency changes by 0.1Hz at 30s are shown in Fig. 3. FSC-VSPSH2 under the VSG control strategy, with different J_{vsg} (J_{vsg}=30, 10, 1), the entire FSC-VSPSH2 can respond to the frequency changes of the grid, while the FSC-VSPSH1 does not change. When the grid frequency drops by 0.1 Hz, FSC-VSPSH2 can automatically reduce the rotor speed to release the inertia to support output energy and the DC-link capacitance releases the energy on it as well. As the governor controls the opening output of guide vane to increase, the influent flow is larger and the speed rises, and the turbine continues to provide energy to grid. Under different J_{vsg}, the active power and DC-link side voltages vary in different magnitudes. Compared with VSPSH1, since the FSC completely decouples the pump-turbine from the grid, in the face of grid frequency changes, there is no change in VSPSH1 under the traditional control strategy, and the active power is still maintained at 3MW, and the speed and DC-link voltage do not change.

E、Conclusion

The comparative results of fixed speed HSP, variable speed HSP with conventional control and the proposed control demonstrate that the application of the VSG control strategy in VSPSH is meaningful to facilitate frequency and voltage support of the power system. The method is coordinated by the pump-turbine, the synchronous motor, the machine-side converter, and the grid-side converter, and can not only respond to the superior power dispatching command but also provide the necessary active power and reactive power for the grid. In addition, it is also possible to make full use of the pumping unit own inertia and DC capacitor inertia to provide the adjustable virtual inertia by the virtual synchronous generator, which is conducive to grid stability.

ACKNOWLEDGMENT

This work was funded by the National Key R&D Program of China (2018YFB0905200).

Estimating the Flexibility Benefit of Concentrating Solar Plants in Electricity Markets

Yanghao Yu, Ershun Du, Ning Zhang
State Key Lab. of Power System, Dept. of Electrical Engineering, Tsinghua University, Beijing, China
ningzhang@tsinghua.edu.cn

Siwei Liu, Zhidong Wang
State Grid Economic and Technological Research Institute, Beijing, China

***Abstract*—When equipped with thermal energy storage (TES), concentrating solar power (CSP) plants can provide both energy benefit and flexibility benefit for power systems. It is capable of shifting generation to periods with insufficient solar irradiation, providing ancillary services, and supplying firm capacity at peak load periods. In this paper, we focus on the operation behavior of CSP when simultaneously participating in three types of electricity market—energy market, ancillary service (AS) market, and capacity market. The results of case study show the quantified flexibility benefit of CSP in electricity markets. The optimal configuration of CSP in terms of TES and solar multiple (SM) is also analyzed.**

***Index Terms*—Concentrating solar power, thermal energy storage, flexibility benefit, electricity market.**

I. Introduction

The controllability of CSP brings the opportunity for CSP to provide both electricity energy and operation flexibility. From the view of power system planning and operation, the potential benefits provided by CSP can be divided into three main parts as energy value, ancillary services value and capacity value.

In this paper, we evaluate the flexibility benefit of CSP through considering it to participate in energy market, ancillary service market, and capacity market. The flexibility of CSP is reflected by the strategic generation curve and adjustable output interval. The benefit model of CSP in joint electricity markets is formulated as a mixed integer programming (MILP) problem.

II. Case Study

The case study analyzes how the CSP plant optimally operates in three types of markets and how much benefit is obtained when equipped with TES. The benefit results are summarized in Table I. The average daily revenues are compared for the base case participating in all the three markets, the case without capacity market, the case participating in energy market only, and the case without TES.

TABLE I
Benefits of CSP cases participating in different markets

Daily Revenue(k$)	Base Case	No Capacity	Energy-Only	No TES
Energy	31.92	31.40	34.39	19.37
Reserve	2.71	3.21	0	0
Regulation	3.67	4.46	0	0
Capacity	17.33	0	0	0
Total Revenue	55.63	39.07	34.39	19.37
Flexibility Benefit	36.26 (65.2%)	19.70 (50.4%)	15.02 (43.7%)	-

Fig. 1 compares the operation of CSP in the four cases. Typically, the optimal CSP output and solar power curve in the summer week scenario are presented.

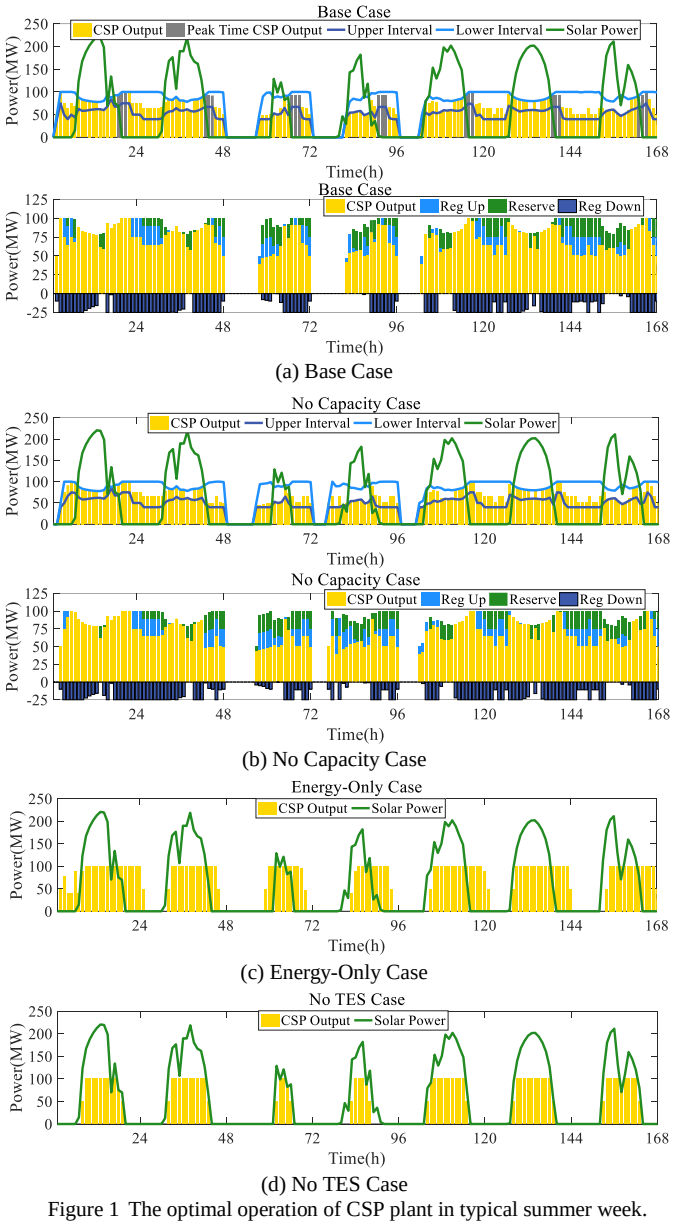

(a) Base Case

(b) No Capacity Case

(c) Energy-Only Case

(d) No TES Case

Figure 1 The optimal operation of CSP plant in typical summer week.

III. Conclusion

Equipped with TES, CSP has the flexibility to shift generation and address the uncertainty of solar energy. Besides energy market, participating AS market and capacity market can significantly improve the flexibility benefit of CSP. Moreover, after sensitive analysis, the optimal configuration of CSP is reached at an 8-hour-TES and a 2.3 SM.